NUREG/IA-0148

International Agreement Report

Assessment of RELAP5/MOD3.1 Using LSTF Ten-Percent Main Steam-Line-Break Test Run SB-SL-01

Prepared by
J. G. Oh, H. D. Lee, K. K. Jee, S. K. Kang/KOPEC
Y. S. Bang, K. W. Seul/KINS
H. Kumamaru, Y. Anoda/JAERI

Korea Power Engineering Company
150 Duckjin-Dong, Yusong-Ku
Taejon, Korea 305–353

Korea Institute of Nuclear Safety
P.O. Box 114
Yusong, Taejon
Korea 305–600

Japan Atomic Energy Research Institute
Tokai-Mura, Naka-Gun
Ibaraki-Ken 319–1195, Japan

Office of Nuclear Regulatory Research
U.S. Nuclear Regulatory Commission
Washington, DC 20555–0001

September 1998

Prepared as part of
The Agreement on Research Participation and Technical Exchange under the
International Thermal-Hydraulic Code Assessment and Maintenance Program (CAMP)

Published by
U.S. Nuclear Regulatory Commission

AVAILABILITY NOTICE

Availability of Reference Materials Cited in NRC Publications

NRC publications in the NUREG series, NRC regulations, and *Title 10, Energy,* of the *Code of Federal Regulations,* may be purchased from one of the following sources:

1. The Superintendent of Documents
   U.S. Government Printing Office
   P.O. Box 37082
   Washington, DC 20402–9328
   <http://www.access.gpo.gov/su_docs>
   202–512–1800

2. The National Technical Information Service
   Springfield, VA 22161–0002
   <http://www.ntis.gov/ordernow>
   703–487–4650

The NUREG series comprises (1) technical and administrative reports, including those prepared for international agreements, (2) brochures, (3) proceedings of conferences and workshops, (4) adjudications and other issuances of the Commission and Atomic Safety and Licensing Boards, and (5) books.

A single copy of each NRC draft report is available free, to the extent of supply, upon written request as follows:

Address: Office of the Chief Information Officer
Reproduction and Distribution
Services Section
U.S. Nuclear Regulatory Commission
Washington, DC 20555–0001
E–mail: <GRW1@NRC.GOV>
Facsimile: 301–415–2289

A portion of NRC regulatory and technical information is available at NRC's World Wide Web site:

<http://www.nrc.gov>

All NRC documents released to the public are available for inspection or copying for a fee, in paper, microfiche, or, in some cases, diskette, from the Public Document Room (PDR):

NRC Public Document Room
2121 L Street, N.W., Lower Level
Washington, DC 20555–0001
<http://www.nrc.gov/NRC/PDR/pdr1.htm>
1–800–397–4209 or locally 202–634–3273

Microfiche of most NRC documents made publicly available since January 1981 may be found in the Local Public Document Rooms (LPDRs) located in the vicinity of nuclear power plants. The locations of the LPDRs may be obtained from the PDR (see previous paragraph) or through:

<http://www.nrc.gov/NRC/NUREGS/SR1350/V9/lpdr/html>

Publicly released documents include, to name a few, NUREG-series reports; *Federal Register* notices; applicant, licensee, and vendor documents and correspondence; NRC correspondence and internal memoranda; bulletins and information notices; inspection and investigation reports; licensee event reports; and Commission papers and their attachments.

Documents available from public and special technical libraries include all open literature items, such as books, journal articles, and transactions, *Federal Register* notices, Federal and State legislation, and congressional reports. Such documents as theses, dissertations, foreign reports and translations, and non-NRC conference proceedings may be purchased from their sponsoring organization.

Copies of industry codes and standards used in a substantive manner in the NRC regulatory process are maintained at the NRC Library, Two White Flint North, 11545 Rockville Pike, Rockville, MD 20852–2738. These standards are available in the library for reference use by the public. Codes and standards are usually copyrighted and may be purchased from the originating organization or, if they are American National Standards, from—

American National Standards Institute
11 West 42nd Street
New York, NY 10036–8002
<http://www.ansi.org>
212–642–4900

DISCLAIMER

This report was prepared under an international cooperative agreement for the exchange of technical information. Neither the United States Government nor any agency thereof, nor any of their employees, makes any warranty, expressed or implied, or assumes any legal liability or responsibility for any third party's use, or the results of such use, of any information, apparatus, product, or process disclosed in this report, or represents that its use by such third party would not infringe privately owned rights.

NUREG/IA-0148

International Agreement Report

Assessment of RELAP5/MOD3.1 Using LSTF Ten-Percent Main Steam-Line-Break Test Run SB-SL-01

Prepared by
J. G. Oh, H. D. Lee, K. K. Jee, S. K. Kang/KOPEC
Y. S. Bang, K. W. Seul/KINS
H. Kumamaru, Y. Anoda/JAERI

Korea Power Engineering Company
150 Duckjin-Dong, Yusong-Ku
Taejon, Korea 305–353

Korea Institute of Nuclear Safety
P.O. Box 114
Yusong, Taejon
Korea 305–600

Japan Atomic Energy Research Institute
Tokai-Mura, Naka-Gun
Ibaraki-Ken 319–1195, Japan

Office of Nuclear Regulatory Research
U.S. Nuclear Regulatory Commission
Washington, DC 20555–0001

September 1998

Prepared as part of
The Agreement on Research Participation and Technical Exchange under the
International Thermal-Hydraulic Code Assessment and Maintenance Program (CAMP)

Published by
U.S. Nuclear Regulatory Commission

NUREG/IA-0148 has been reproduced from the best copy available.

ASSESSMENT OF RELAP5/MOD3.1 USING LSTF 10% MAIN STEAM LINE BREAK TEST RUN SB-SL-01

Abstract

Results produced by the RELAP5/MOD3.1 computer code were compared with the experimental data from JAERI's LSTF Test Run SB-SL-01 for a 10% main steam line break transient in a pressurized water reactor. The code simulation for the base case included a total of 189 fluid control volumes and 199 flow junctions to model the transient two-phase flow phenomena. Also, a total of 180 heat slabs were used to model the system heat transfer. The code predictions of the experimental results are generally satisfactory for the trends of key parameters.

Sensitivity studies performed for the break discharge coefficient, the separator drain line loss coefficient, and the number of steam generator nodes did not reveal any strong dependencies. Nevertheless, optimal values of these parameters that led to the lowest overall statistical error were obtained, and these values were subsequently used in the "Base Case" analysis.

Table of Contents

Abstract i
Table of Contents ii
List of Tables iii
List of Figures iii
Summary of Study vi
1. Introduction 1
2. Experimental Facility Description
(Large Scale Test Facility ; LSTF) 5
3. Test Description (Experiment SB-SL-01) 7
4. Description of Code Version and Input Deck 9
4.1 Input Modelling 9
4.2 Initial and Boundary Conditions 11
5. Results from Base Calculation 12
5.1 Break Junction Flow Behavior 12
5.2 Vessel Upperhead Voiding 13
5.3 RCS and Secondary Pressure Response 14
5.4 Thermal Response 15
5.5 Water Level Behavior 16
5.6 Loop Mass Flow Behavior 17
6. Discussion of Statistical Results 19
7. Sensitivity Studies 22
7.1 Break Junction Discharge Coefficient (Cd) 23
7.2 Separator drain line loss coefficient (K) 23
7.3 Steam Generator Nodalization 24
8. Run Statistics 26
9. Conclusion and Recommendation 27
References 29
Tables 30
Figures 40

List of Tables

3.1 Sequence of Events for Experiment SB-SL-01 30

3.2 Initial and Boundary Conditions for Experiment SB-SL-01 31

5.1 List of Assessment Parameters (LSTF SB-SL-01) 32

6.1 The Mean Errors (ε) for the Base Calculation (Cd=0.85, K=10.0, n=5) ... 33

6.2 The Root-Mean-Square Errors (ε_{RMS}) for the Base Calculation (Cd=0.85, K=10.0, n=5) 34

6.3 The Standard Deviations of the Errors (σ_{ε}) for the Base Calculation (Cd=0.85, K=10.0, n=5) 35

7.1 The Root-Mean-Square Errors (ε_{RMS}) for the Sensitivity Study on the Discharge Coefficient (Cd) 36

7.2 The Root-Mean-Square Errors (ε_{RMS}) for the Sensitivity Study on the S/G Drain Line Loss Coefficient (K) 37

7.3 The Root-Mean-Square Errors (ε_{RMS}) for the Sensitivity Study on the Number of Steam Generator Nodes (n) 38

8.1 Run Statistics Data in Base Calculation 39

List of Figures

2.1 Schematic View of ROSA-VI LSTF 40

3.1 Three Core Power Control Curves for LSTF 41

4.1 RELAP5/MOD3.1 Nodalization of LSTF for MSLB Transient Assessment 42

5.1 Break Flow Rate 43

5.2 Break Void Fraction 44

5.3 Break Density 45

5.4 Vessel Upperhead Void Fraction 46

5.5 Pressurizer Pressure 47

5.6 Volume Averaged Void Fraction of Three Upperhead Nodes 48

5.7 Downcomer Flow Rate of Intact Loop 49

5.8 Secondary Pressure of Broken Loop 50

5.9 Secondary Pressure of Intact Loop 51

5.10 Cold leg Temperature of Intact Loop 52

5.11 Cold leg Temperature of Broken Loop 53
5.12 Hot leg Temperature of Intact Loop 54
5.13 Hot leg Temperature of Broken Loop 55
5.14 SG Steam Dome Temperature of Intact Loop 56
5.15 SG Downcomer Temperature of Intact Loop 57
5.16 SG Downcomer Temperature of Intact Loop (4 loops) 58
5.17 SG Steam Dome Temperature of Broken Loop 59
5.18 SG Downcomer Temperature of Broken Loop 60
5.19 SG Downcomer Temperature of Broken Loop (4 loops) 61
5.20 SG Boiler Bottom Temperature of Broken Loop 62
5.21 SG Boiler Middle Temperature of Broken Loop 63
5.22 SG Boiler Top Temperature of Broken Loop 64
5.23 SG Boiler Bottom Temperature of Intact Loop 65
5.24 SG Boiler Middle Temperature of Intact Loop 66
5.25 SG Boiler Top Temperature of Intact Loop 67
5.26 Average Temperature of RCS Broken Loop 68
5.27 Collapsed Liquid Level of Pressurizer 69
5.28 Narrow Range of Liquid Level of S/G Intact Loop 70
5.29 Narrow Range of Liquid Level of S/G Broken Loop 71
5.30 Liquid Level of S/G Intact Loop 72
5.31 Liquid Level of S/G Broken Loop 73
5.32 Pump Suction Flow Rate of Broken Loop 74
5.33 Pump Suction Flow Rate of Intact Loop 75
5.34 Downcomer Flow Rate of Broken Loop 76
5.35 Separator Flow Rate of Intact Loop 77
5.36 Separator Flow Rate of Broken Loop 78
7.1 Comparison of Break Flow Rate (Cd Value Sensitivity) 79
7.2 Comparison of Pressurizer Pressure (Cd Value Sensitivity) 80
7.3 Comparison of Secondary Pressure of Broken Loop (Cd Value Sensitivity) 81
7.4 Comparison of Secondary Temperature of Broken Loop (Cd Value Sensitivity)..... 82
7.5 Comparison of Break Void Fraction (Cd Value Sensitivity) 83
7.6 Comparison of Secondary Pressure of Intact Loop (Cd Value Sensitivity) 84
7.7 Comparison of Secondary Temperature of Intact Loop

(Cd Value Sensitivity) 85
7.8 Collapsed Liquid Level of Pressurizer (Cd Value Sensitivity) 86
7.9 Downcomer Flow Rate of Intact Loop (Cd Value Sensitivity) 87
7.10 Downcomer Flow Rate of Broken Loop (Cd Value Sensitivity) 88
7.11 Comparison of Break Flow Rate (K Value Sensitivity) 89
7.12 Comparison of Pressurizer Pressure (K Value Sensitivity) 90
7.13 Comparison of Secondary Pressure of Broken Loop (K Value Sensitivity).. 91
7.14 Comparison of Secondary Temperature of Broken Loop
(K Value Sensitivity) 92
7.15 Comparison of Break Void Fraction (K Value Sensitivity) 93
7.16 Comparison of Secondary Pressure of Intact Loop (K Value Sensitivity) ... 94
7.17 Comparison of Secondary Temperature of Intact Loop
(K Value Sensitivity) 95
7.18 Collapsed Liquid Level of Pressurizer (K Value Sensitivity) 96
7.19 Downcomer Flow Rate of Intact Loop (K Value Sensitivity) 97
7.20 Downcomer Flow Rate of Broken Loop (K Value Sensitivity) 98
7.21 Comparison of Break Flow Rate (S/G Nodes Sensitivity) 99
7.22 Comparison of Pressurizer Pressure (S/G Nodes Sensitivity) 100
7.23 Comparison of Secondary Pressure of Broken Loop
(S/G Nodes Sensitivity) 101
7.24 Comparison of Secondary Temperature of Broken Loop
(S/G Nodes Sensitivity) 102
7.25 Comparison of Break Void Fraction (S/G Nodes Sensitivity) 103
7.26 Comparison of Secondary Pressure of Intact Loop
(S/G Nodes Sensitivity) 104
7.27 Comparison of Secondary Temperature of Intact Loop
(S/G Nodes Sensitivity) 105
7.28 Collapsed Liquid Level of Pressurizer (S/G Nodes Sensitivity) 106
7.29 Downcomer Flow Rate of Intact Loop (S/G Nodes Sensitivity) 107
7.30 Downcomer Flow Rate of Broken Loop (S/G Nodes Sensitivity) 108
7.31 Steam Generator Nodalization Diagram for The Nodes Sensitivity Study .. 109
7.32 The Required CPU Time for Calculation (S/G Nodes Sensitivity) 110
8.1 The Required CPU Time in The Base Calculation 111

Summary of Study

This report presents a comparison of RELAP5/MOD3.1 computer code results to the experimental data from the Japan Atomic Energy Research Institute Large Scale Test Facility(JAERI LSTF) Test Run SB-SL-01 for simulating a 10% main steam line break (MSLB) transient in a pressurized water reactor (PWR). The LSTF volumes are scaled at 1/48 of a typical 3423 MWt Westinghouse 4-loop PWR, however the height and relative elevations of each component are full scale. The LSTF core consists of 1104 full length electrical heater rods, which are used to simulate PWR nuclear fuel rods. Greater details about the LSTF design and the scaling used therein are provided in Section 2, "Experimental Facility Description", and the procedures used are given in Section 3, "Test Description".

The RELAP5/MOD3.1 nodalization for benchmarking the LSTF Test Run SB-SL-01 included a total of 189 fluid control volumes and 199 flow junctions to simulate the thermal-hydraulic phenomena. A total of 180 heat slabs were used to model the system heat transfer phenomena through the heater rods, the steam generator tubes, the internal structural components, and the vessel shell. Further details pertaining to the input modeling can be found in Section 4, "Description of Code Version and Input Deck". The code initialization via a steady state simulation is described therein as well.

Sensitivity studies were performed with the RELAP5/MOD3.1 computer code to investigate the effect of the break flow discharge coefficient (Cd), the steam separator drain line loss coefficient (K), and the number of steam generator nodes (n) upon the thermal hydraulic performance of the code. This sensitivity study revealed only a marginal dependence of the predictive capabilities of RELAP5/MOD3.1 on these three parameters. Nevertheless, the following optimal values of these parameters were selected based on minimum overall statistical error: Cd = 0.85; K = 10.0; n = 5. A more detailed account of the sensitivity analysis is given in Section 7, "Sensitivity Studies".

The "Base Calculation" investigation of the 10% MSLB transient uses the values Cd = 0.85, K = 10.0, and n = 5 for the code simulation. Comparison between the RELAP5/MOD3.1 code predictions and the LSTF Test Run SB-SL-01 experimental data are described in Section 5, "Results from the Base Calculation". The quantification of these comparisons via statistical error evaluations are given in Section 6, "Discussion of Statistical Results". Salient features of the results of these comparisons are provided below.

On the whole, the code-data comparisons based on gross features are reasonably good. The code, however, appears to have difficulty in accounting for finer details which leads to significant deviations from the experimental results in certain important cases. As an example, the RELAP5/MOD3.1 code cannot predict steep variable changes or sharp gradients. A manifestation of this occurs at the time of High Pressure Safety Injection(HPSI), as outlined in the following summary description.

The break flow rate is predicted well by the code, except toward the end of the transient. The hot leg temperature of the intact and broken loops, the cold leg temperature of the broken loop, the steam generator (SG) downcomer temperature of the intact loop, and the average temperature of the reactor coolant system (RCS) broken loop are all predicted reasonably well by the RELAP5/MOD3.1 computer code as compared to the SB-SL-01 experimental data for a MSLB transient.

The code prediction of the cold leg temperature of the intact loop is in reasonable agreement with the experimental data until the initiation of HPSI. Subsequently, the code predictions and the experimental data show considerable divergence because the RELAP5/MOD3.1 code cannot track the steep decrease in temperature with time which occurs HPSI. A similar divergence occurs for the time variation of the pressurizer pressure, secondary pressure of the intact loop, and the volume-averaged void fraction of the three upperhead nodes, with respect to the initiation of HPSI. The code predictions of the broken loop SG temperature diverge from the experimental values

essentially from the very beginning of the transient. At the end of the transient, the temperature discrepancy is about 11%. The collapsed liquid level of the pressurizer is predicted rather poorly by the code following initiation of HPSI.

The computer code substantially underpredicts the time rate of change of the liquid level, leading to an underprediction of the collapsed liquid level by about 27% at the end of the transient. The RELAP5/MOD3.1 output relating to the intact loop downcomer and separator flow rates also deviates considerably from the SB-SL-01 experimental data.

1. Introduction

The objective of the investigation reported here was to evaluate the accuracy of the thermal hydraulic computer code RELAP5/MOD3.1 in simulating a design basis MSLB PWR transient. The output from this computer code was compared to the experimental data from Test Run SB-SL-01 of the ROSA-IV Large Scale Test Facility (LSTF) operated by Japan Atomic Energy Research Institute(JAERI). The experiment Test Run SB-SL-01 was the simulation of the 10% main steam line break (MSLB)

Simulation of a postulated main steam line break (MSLB) is important from the perspective of potential plant damage and related environmental consequences, although the probability of occurrence of such an event is considered to be small. The closure of the main steam isolation valves (MSIVs) following a MSLB will prevent blowdown of the secondary plant system for all breaks except those for which the break is located between the steam generator (SG) outlets and the MSIVs. As a result, only the broken loop SG secondary side will blowdown during such an accident. This SG secondary side acts as a heat sink owing to the decreasing pressure.

This may lead to excessive cooling and subsequent re-pressurization and "pressurized thermal shock" of the reactor coolant system (RCS), which poses a potential threat to the integrity of the reactor vessel (RV). Other potential damage stems from the possibility of a "reactivity power excursion", that is, return to power via aqddition of reactivity, as a consequence of the excessive cooling of the reactor coolant system (RCS). Finally, the possibility of SG tube failure arises because lowering the SG shell side pressure causes a greater pressure difference across these tubes. Computer code simulations and calculations are needed for an examination and understanding of these phenomena and the potential severity of the consequences of an accident since it is

not generally feasible to perform full scale tests. And for assessment and verification of code calculations, it is imperative that the code calculations be compared against integral system data. From the viewpoint of reactor safety, it is very important to verify the predictive capability of thermal-hydraulic safety analysis codes for transient accidents.

The LSTF was designed as a 1/48 scale, integral test/experimental facility for simulating the response of a PWR to design basis loss-of-coolant-accidents (LOCAs) and plant transients. The Test Run SB-SL-01, conducted during 1990 at the LSTF, simulated experimentally a 10% MSLB transient in a PWR.

In modeling the 10% MSLB transient Test Run SB-SL-01 with RELAP5/MOD3.1, it was recognized at the outset that the following variable parameters might affect the code-data comparisons: the break discharge coefficient (Cd), the steam separator drain line loss coefficient (K), and the number of S/G nodes (n). Hence, sensitivity studies were performed with the RELAP5/MOD3.1 computer code using the following set of values for the three sensitivity parameters:

$$Cd = \{0.75, 0.80, 0.85, 0.90\}; K = \{0.0, 10.0, 50.0, 100.0\}; n = \{3, 5, 7, 9\}.$$

The results of these studies did not indicate a pronounced dependence of the code output on the sensitivity parameters. Nevertheless, based on certain statistical error criteria or indices used, it was concluded that the following values of the sensitivity parameters produced the minimum overall discrepancy between the computer code predictions and the experimental data values: $Cd = 0.85$; $K = 10.0$; and, $n = 5$.

The "Base Calculation" investigation of the 10% MSLB transient used these optimal values of Cd, K, and n. On the whole, the code-data comparisons from this

investigation are reasonably satisfactory. The code, however, has difficulty in predicting the finer details of the physical phenomena involved in a MSLB transient. In turn, this leads to significant deviations between the code output and the experimental data in some important cases.

The break flows are predicted accurately by the code, except towards the end of the transient. Also predicted reasonably well by the RELAP5/MOD3.1 computer code are the following time variations: the hot leg temperature of the intact and broken loops, the cold leg temperature of the broken loop, the SG downcomer temperature of the intact loop, and the average temperature of the RCS broken loop.

The code prediction of the intact loop cold leg temperature is in reasonable agreement with the experimental data until the initiation of high pressure safety injection (HPSI). Subsequently, the code output and the experimental data diverge significantly, as the RELAP5 computer code cannot model steep variable change or sharp gradients associated with the initiation of HPSI. A similar situation, with respect to initiation of HPSI, exists with the time variations of the pressurizer pressure, secondary pressure of the intact loop, and the volume averaged void fraction of the three reactor vessel (RV) upperhead nodes. The code predictions of the broken loop SG temperature diverge from the experimental values from the very beginning of the transient, culminating in a difference of 11% between the code output and the test data values at the end of the transient. The pressurizer collapsed liquid level is underpredicted by the code following HPSI, and at the end of the transient this underprediction amounts to 27% of the experimental value. The intact loop downcomer and separator flow rates produced by the code also deviate significantly from the test values.

The LSTF experimental facility is described in Section 2, while the Test Run SB-SL-01 is discussed in Section 3. The input deck modeling and initialization of the code are discussed in Section 4. The results of the "Base Calculation" are provided in Section 5. The evaluation of statistical errors, based on difference between the code and experimental data for various time values, is given in Section 6. A discussion of the sensitivity studies regarding the optimal values of Cd, K and n can be found in Section 7. The run statistics are given in Section 8.

2. Experimental Facility Description
(Large Scale Test Facility ; LSTF)

The Rig Of Safety Assessment (ROSA)-IV Program's Large Scale Test Facility (LSTF) is a test facility for integral simulation of thermal-hydraulic response of a pressurized water reactor (PWR) during small break loss-of-coolant accidents (SBLOCAs) and plant transients. The PWR core nuclear fuel rods are simulated by using electrical heater rods in the LSTF.

A brief outline of the ROSA-IV program's LSTF is given below, with special emphasis on its suitability for simulating the main steam line break transient.

The LSTF experimental facility was designed to model the thermal-hydraulic phenomena in a PWR during postulated small break LOCAs and plant transients. The general facility view is shown in Figure 2.1 [1].

The LSTF volumes are scaled at 1/48 of a typical 3423 MWt Westinghouse 4-loop PWR reference plant. The height of each component and the relative elevations are full scale, (i.e., they are equal to the corresponding components and elevations of the reference plant) in order to correctly simulate the coolant flow under natural circulation conditions. The flow areas are also scaled by 1/48 in the pressure vessel, and by 1/24 in the two steam generators. However, the hot and cold legs are scaled so as to conserve the ratio of the length to the square root of pipe diameter for the reference PWR. Such an approach was used in order to simulate the flow regime transitions in the primary loops. The core power is scaled by 1/48 at power equal to 14% of the reference four loop PWR. The LSTF core consists of 1104 full length (3.66m) electrical heater rods (including 1008 powered rods and 96 unpowered rods) placed in a 17×17 array, as in the nuclear reactor core of the reference plant. Geometric parameters such as diameter, rod-to-rod pitch, and rod heated length in the test core are equal to the corresponding values in the reactor core, so as to preserve the heat transfer characteristics of the core.

The test core has a rated thermal output of 10 MW.

Generation of non-condensible gases in the core such as hydrogen is simulated by injection of nitrogen gas into the core. The broken loop in which the steam line break occurs, represents a single loop of the reference plant, while the other three loops are represented by a single intact loop. The steam generators and secondary coolant systems are designed to simulate both steady state and transient responses of the 2/48 scaled steam and feedwater flows, as well as the scaled primary-to-secondary heat transfer in the reference PWR. The 141 U-tubes in each steam generator are arranged in a square array, and they consist of nine groups of U-tubes with different heights.

The inner diameter and wall thickness of each U-tube are 19.6 mm and 2.9 mm, respectively. The pressurizer is located on the hot leg connected to the intact steam generator. It is scaled in accordance with the facility volume scaling requirements. Also, the height to diameter ratio of the pressurizer is conserved in relation to the reference PWR.

The system break in the reference PWR is simulated in the LSTF by using a break unit. The break unit consists of a venturi flow meter, a spool piece to measure the two-phase break flow rate and density, a break orifice and a break valve. The break valve is designed to open in less than 0.1 second.

3. Test Description (Experiment SB-SL-01)

Experimental run SB-SL-01 was conducted during 1990 in the LSTF, located at the Japan Atomic Energy Research Institute (JAERI). This experiment simulated a 10% main steam line break transient in a pressurized water reactor (PWR), and it was initiated by manual operation at the beginning of the break.

The break was located in the main steam line of steam generator B. The break diameter was 31.9 mm, which corresponds to 10% of the cold leg flow area. The experiment SB-SL-01 was carried out at full power. Three core power control curves were used for the LSTF experiments, as shown in Figure 3.1 [2]. The JAERI core power curve, in which the delayed neutron fission power is estimated conservatively, was used for the test run SB-SL-01.

The reactor trip was initiated by manual operation at the beginning of the break, rather than by reactor trip signal generation following the break. Automatic protective actions taken during the early period of the main steam line break included closure of MSIVs, steam generator auxiliary feedwater injection, and safety injection. The MSIVs closure was initiated by manual operation at the time of the break, rather than by safety injection signal (SIS) generated on a low pressure of 4.24 MPa in the broken loop secondary side. The auxiliary feedwater flow, delayed by the loss of off-site power, started refilling the intact loop steam generator at 28 seconds after the break. The HPSI was designed so as to change the injection location during the test. This system included two pumps : a high pressure injection pump (PH) and a charging pump (PJ). The safety injection flow was initiated manually at 1156 seconds, rather than by automatic SIS. The sequence of main events for the test run SB-SL-01 is summarized in Table 3.1 [3].

Prior to the initiation of the experiment, LSTF facility was set to have a primary system pressure of 15.52 MPa, a primary system hot leg and cold leg temperature of 598.1K and 562.4K, respectively, and a primary coolant flow rate of 24.3 kg/sec. The

steam generator secondary side pressure and temperature were set to 7.3 MPa and 495.2K, respectively, and the feedwater flow rate was 2.74 kg/s. The initial test core power level was 10 MW. Table 3.2 summarizes the initial conditions used for test run SB-SL-01.

4. Description of Code Version and Input Deck

The RELAP5 code is based on a non-homogeneous and non-equilibrium model for one dimensional, two-phase system. Recently, the RELAP5/MOD3 code development program has been initiated to develop a code version suitable for the analysis of all transient and postulated accidents in PWR systems. In this code assessment on the MSLB, the unmodified released code version, RELAP5/MOD3.1 is used.

A RELAP5/MOD3.1 input deck specific to experimental run SB-SL-01 was created from the reference input deck of LSTF. This was accomplished via an iterative process of modifications and updates, using input values and options appropriate to the experimental data and analyses

4.1 Input Modelling

The RELAP5/MOD3.1 model of the LSTF facility for experimental run SB-SL-01 included 189 fluid control volumes and 199 flow junctions. The system nodalization is illustrated schematically in Figure 4.1. A total of 180 heat slabs (shown as shaded areas in Figure 4.1) were used in the model to represent heat transfer in the steam generator, reactor, primary system piping, and pressurizer.

The volumes in the reactor vessel numbered 100 to 156. Flow enters from the cold legs into the vessel downcomer annulus in branch 104. The primary reactor vessel flow path is downward through the downcomer (annulus 108) to the lower plenum (volumes 112 and 116). A portion of the inlet flow is bypassed directly to the hot legs through the slip-fit between the core barrel assembly and reactor vessel wall at the hot leg nozzles. Another portion of the inlet flow is diverted upward through volumes 101 and 100 to the upper head (volumes 148 and 152). The upper plenum is represented by volumes 128 to 140. Volume 156 represents the guide tubes that route a portion of the core exit

flow from the upper plenum to the upper head. The reactor core hot channel (volume 124) is subdivided into nine equally spaced volumes. Heat structures were used to represent the fuel pins, the major internal structures (thermal shield, core barrel wall, guide tube walls, etc.), and the reactor vessel cylindrical shell and spherical heads. The use of these heat structures allows simulation of inter-region heat transfer, such as heat transfer between the core and bypass regions.

The steam generators are represented by nine volumes in the primary system and thirteen volumes in the secondary system. Heat is exchanged between the primary and secondary sides of the steam generator via the U-tubes, which are modelled as heat structures. The multi-volume model for the steam generators is quite important for simulating the heat transfer phenomena accurately.

The main and auxiliary feed water systems are modelled by time dependent volumes (volumes 360 and 350 in the broken loop and volumes 560 and 550 in the intact loop, respectively). The feed water and steam flow rates are regulated by 'control logic' in order to maintain the required secondary pressure and liquid level.

The pressurizer is modelled by surge line (volume 600) and by pressurizer vessel (volume 610). The pressurizer vessel is divided into eight subvolumes.

The hot leg is modelled by seven volumes (volumes 202 to 216 in the broken loop and volumes 402 to 416 in the intact loop, respectively), while the cold leg is modelled by three volumes (volumes 244 to 252 in the broken loop and volumes 444 to 452 in the intact loop, respectively). The pumps in each loop are represented by volumes 240 and 440 respectively.

The HPSI, LPSI and charging tank are modelled by time dependent volumes numbered 760 to 780 in the broken loop and 720 to 750 in the intact loop, respectively. The accumulator (volume 700) is connected to the cold legs of both loops via the distributor (volume 710). The control valve in the accumulator line (valve 711 and 712) serves to isolate the accumulator when the accumulator is empty.

On the secondary side of steam generator B, the 10 % main steam line break was simulated by opening a valve (junction 915) at break time. The break diameter was 31.9 mm, and the discharge coefficient was adjusted to a value of 0.85 to match the break flow rate, via results obtained from the sensitivity studies. In view of the importance of the primary system pressure calculation, pressure control systems associated with the pressurizer (such as heaters, sprays, PORVs, and SRVs) were included in the model.

The input deck for the base case calculation listed in Appendix A is based on the RELAP5/MOD3 code manual [4].

4.2 Initial and Boundary Conditions

A RELAP5/MOD3.1 steady state simulation was performed in order to obtain appropriate steady state system conditions prior to the initiation of a steam line break. A comparison between the simulated initial test conditions thus obtained (from the code run) and the corresponding measured initial test conditions are given in Table 3.2. In general, the agreement between the simulated and the measured initial test conditions is satisfactory. However, the primary coolant pump speed is an exception. The RELAP5/MOD3.1 prediction of the pump speed is lower than that measured in the test. The reasons for the underpredicted coolant pump speed are not clear. However, this discrepancy is believed to have negligible effect on the overall system transient. All relevant information pertaining to the initial and boundary conditions was incorporated in the steady-state and transient input decks for the RELAP5/MOD3.1 computer code.

5. Results from Base Calculation

The RELAP5/MOD3.1 computer code calculations were compared against the experimental data from JAERI's LSTF test run SB-SL-01. The initial and boundary conditions used in the computer code simulations were obtained from a steady state run. The sequence of thermal-hydraulic events during the transient calculation are summarized in Table 3.1. The corresponding experimental data values are also summarized in this table for comparison. Also, the computer code simulations used a break discharge coefficient value of 0.85, and a separator drain line loss coefficient value of 10.0, for the base calculation.

The assessment of the RELAP5/MOD3.1 computer code against the experimental data is described below in relation to several important physical parameters such as break flow rate, pressurizer pressure and steam generator secondary side temperature. Table 5.1 summarizes the list of assessment parameters. For each listed assessment parameters, the identification numbers for the RELAP5/MOD3.1 calculation and the corresponding LSTF SB-SL-01 measurement are provided in the first two columns, respectively. The uncertainty in measurement associated with each assessed parameter is given in column 3. The last column identifies the figure which shows a comparison between the code calculation and the corresponding experimental data for each assessed parameter.

5.1 Break Junction Flow Behavior

Figure 5.1 ~ Figure 5.3 show a comparison between the experimental data and the calculated results for the steamline break junction. The computer code-test data comparisons are generally good, except for about 50 seconds following initiation of the transient. During the initial 50 seconds, the calculated break flow was overpredicted by

0.3 ~ 1.1 kg/sec, which is equivalent to an overprediction of 5 ~ 16% in relation to the experimental data. The code predicts a constant void fraction value of 1.0 at the break junction, while the small deviation of the experimental data from this value could be attributed to uncertainties associated with experiments and the processing of test data. The code predictions of the mass flow rate (Figure 5.1) and appropriately scaled mass density variation (Figure 5.3) are essentially identical. This attests to the validity of the results in Figure 5.2, namely that the break flow void fraction is essentially constant throughout the transient.

5.2 Vessel Upperhead Voiding

For severe cooldown events such as MSLB, reactor vessel upperhead should be modeled carefully such that any voiding in the upperhead is monitored. The vessel upperhead modeling affects the system pressure significantly due to voiding effect [5, 6, 7]. Following the initial rapid depressurization, the process slows down as the vessel upperhead reaches saturation and begins to flash.

Figure 5.4 shows RELAP5/MOD3.1 code output pertaining to void fraction variation with time in the three vessel upperhead nodes. The bottom node is full of water at all times, while the same holds for the middle node except between 1089 seconds and 1361 seconds (following the initiation of the transient) when the void fraction varies between 0.0 and 0.14. The void fraction for the top node in the vessel upperhead varies between 0.0 and 1.0 for times between 721 seconds and 3241 seconds, reaching the peak value between 1097 seconds and 1265 seconds. During other times, the top node in the vessel upperhead is full of water.

The volume averaged void fraction in the three vessel upperhead nodes is shown in Figure 5.6. An examination of the code output and the experimental data from the plots indicates significant differences between RELAP5/MOD3.1 predictions and the test

results. The experimental data always indicate presence of steam in a two-phase mixture, while the code output cannot confirm the presence of any steam at all for the first 750 seconds of the transient. During this initial time frame (of 750 seconds), the experimental data indicate a void fraction of about 0.05 (or 5%). Conversely, while the experimental data indicate an essentially linear variation of the void fraction with time, with values between about 0.025 and 0.04 for times between around 1350 seconds and 3500 seconds, the code predicts an essentially linear variation with values varying between 0.24 and 0.0 for practically the same time interval. Again, the experimental void fraction variation around 1350 seconds is very steep, while the predicted code variation is very gradual.

5.3 RCS and Secondary Pressure Response

The RELAP5/MOD3.1 code prediction regarding the primary side pressure agrees reasonably well with the experimental data for the initial 800 to 1000 seconds of the transient as can be seen from Figure 5.5. Thereafter, while the rate of increase of pressure is approximately the same for the code calculation and the experimental data, the code overpredicts the pressure by about 1 MPa. According to Figure 5.5, a similarly favorable comparison between code predictions and experimental data holds for the secondary side pressure variation with time for the intact loop during the initial 800 seconds. Subsequently, however, the pressure for this case is underpredicted by about 0.4 MPa after about 1000 seconds. This underprediction of pressure by the code after about 800 seconds appears to be related to the code overprediction of primary side pressure after about 800 seconds (Figure 5.5), and the overprediction of intact loop downcomer flow rate around this time (Figure 5.7).

On the other hand, the secondary side depressurization transients for the both broken loop and intact loop are predicted quite well by the RELAP5/MOD3.1 computer

code in relation to the experimental variation (Figure 5.8 and 5.9, respectively). This transient involves a monotonically decreasing variation of pressure with time, on account of flow of steam through the pipe break.

5.4 Thermal Response

Following the closure of the main steam isolation valves (or MSIVs), the main steam line break transient involves blowdown of the two-phase fluid mixture only on the broken loop steam generator secondary side. Thus, the steam generator tubes in the broken loop are cooled at a fast rate, thereby causing rapid cooling of the primary system.

The intact loop cold leg temperature variation with time is shown in Figure 5.10. The code predictions show excellent agreement with the experimental data until the time of HPSI injection at around 1170 seconds into the transient. These comparisons are significantly less satisfactory as the time rate of change of temperature for the code prediction and the experimental data are substantially different. The code successively overpredicts and underpredicts the experimental temperature values, leading to an underprediction of about 45℃ at 3500 seconds. The colder HPSI liquid causes a nearly instantaneous steep change in the observed temperature, leading to lowering of the cold leg temperature by about 54℃. The RELAP5/MOD3.1 code underpredicts this temperature drop by a substantial amount.

The broken loop cold leg temperatures involve a uniformly-decreasing monotonic variation with time, as can be seen from Figure 5.11, on account of the blowdown of the secondary side of the isolated, broken loop steam generator. For this case, the RELAP5/MOD3.1 predictions show excellent agreement with the experimental data. The hot leg temperature variation of the intact and broken loops is shown in Figures 5.12 and 5.13, respectively. For both of these cases, the RELAP5/MOD3.1 predictions

show very good agreement with the test data, and the two transients are virtual facsimiles of one another.

The intact loop steam generator steam dome temperature is shown in Figure 5.14. The code output shows excellent agreement with the test data for the initial 800 seconds approximately. Thereafter, the code output underpredicts the measured temperatures by about 15℃. The code predictions of the intact loop steam generator downcomer temperatures are in reasonable agreement with the experimental data, as shown in Figures 5.15 and 5.16, which indicate steady-state conditions around 1600 seconds.

The broken loop steam generator steam dome temperature comparisons are shown in Figure 5.17, and these are not satisfactory. The code underpredicts the experimental data, and the discrepancy gets progressively worse with time, culminating in an underprediction of around 50℃ at the end of the transient. The broken loop steam generator downcomer temperature comparisons are shown in Figures 5.18 and 5.19. The code again underpredicts the data, but the discrepancy here is small.

The steam generator boiler temperature-time variations for the broken loop are shown in Figures 5.20～5.22 and those for the intact loop are shown in Figures 5.23～5.25. The overall comparisons are satisfactory, but the RELAP5/MOD3.1 temperature predictions are generally lower than the corresponding experimental data. The discrepancy typically ranges between 5℃ and 10℃, but for the top and middle of the broken loop boiler, it is as large as 20℃. The average temperature comparisons for the RCS broken loop are shown in Figure 5.26, and these are quite satisfactory.

5.5 Water Level Behavior

The code-data comparisons for the collapsed liquid level of the pressurizer are shown in Figure 5.27. The comparisons are excellent for the initial 1300 seconds of the transient with respect to (i) the collapsed liquid level, (ii) the time when the pressurizer

becomes empty, and (iii) the time when the pressurizer starts to refill. However, beyond the HPSI injection time when the refill process gets initiated, the comparisons are less satisfactory as the code underpredicts the rate of refill significantly. Towards the end of the transient, the code underpredicts the collapsed liquid level by about 1.8m.

Figures 5.28～5.31 show the steam generator collapsed liquid level of the intact and broken loops. The RELAP5/MOD3.1 comparisons with the experimental data are reasonably satisfactory, although the code prediction typically underestimates the experimental values.

5.6 Loop Mass Flow Behavior

Figure 5.32 and 5.33 show the flow rate variation on the primary side of the intact and broken loops. Here, the RELAP5/MOD3.1 flow rate predictions compare very well with the test data. The large difference in the steady-state values of the flow rate for the broken and intact loops are caused by insufficient mixing of primary side coolant by natural circulation after the reactor coolant pumps are shut down.

The downcomer flow rate of the broken loop is shown in Figures 5.34. The computer code flow rate predictions compare favorably with those of the experimental data, including the time of attainment of quasi-steady state conditions (～200 seconds). During the early stage of the transient, the computer code-test data comparisons are good. However, following the rapidly changing depressurization prediction of the code around 800 seconds and the start of HPSI injection (at 1156 seconds), the code overpredicts the experimental data for the downcomer mass flow rate very substantially (by an average of about 200%) for nearly 900 seconds. Subsequently, the code-data comparisons are reasonably satisfactory, but the code underpredicts the flow rate by about 1 kg/sec. A similar situation is observed for the code prediction of separator flow rate in the intact loop, Figures 5.35, especially for the inlet flow and liquid discharge

flow. The code prediction of broken loop separator flow is shown in Figure 5.36, indicating that a quasi-steady state flow rate of about 1 kg/sec is attained in about 500 seconds after the initiation of the transient.

6. Discussion of Statistical Results

For an objective evaluation and judgement of the agreement between the values calculated by RELAP5/MOD3.1 and the experimental data values, it is necessary to define quantitative parameters that can be used as a measure of the accuracy of the code predictions. The most important parameter used to evaluate the relative accuracy of the code prediction in the present work is the fractional error, which is defined as the ratio of the error of the calculated variable to the experimental value of the variables.

$$\varepsilon_i = \frac{(X_i)_{code} - (X_i)_{\exp}}{(X_i)_{\exp}} \tag{1}$$

In equation (1), ε_i is the fractional error of the predicted value by the code, $(X_i)_{code}$ is the value of the dimensional variable calculated by the code at time $t = t_i$ and $(X_i)_{exp}$ is the value of the corresponding variable obtained from the experimental data, which is assumed to be the true value.

In order to compare the accuracy of the predicted values, the mean error (ε), the root-mean-square (RMS) error (ε_{RMS}), and the standard deviation of the error, (σ_ε) were also computed using the following equations :

$$\bar{\varepsilon} = \sum_{i=1}^{N} \frac{\varepsilon_i}{N} \tag{2}$$

$$\varepsilon_{RMS} = \left[\sum_{i=1}^{N} \frac{\varepsilon_i^{\,2}}{N} \right]^{1/2} \tag{3}$$

$$\sigma_\varepsilon = \left[\frac{1}{N} \sum_{i=1}^{N} \left(\varepsilon_i - \bar{\varepsilon}\right)^2 \right]^{1/2} = \left[\left(\varepsilon_{RMS}\right)^2 - \varepsilon^2 \right]^{1/2} \tag{4}$$

Roughly speaking, the predicted values that lead to low estimates of ε, ε_{RMS},

and σ_ε may be considered to be a good fit to the experimental data.

Tables 6.1 ~ 6.3 give values for ε, ε_{RMS}, and σ_ε, respectively, for the 'Base Calculation' (Cd=0.85 and K=10.0) as described in Figures 5.1 ~ 5.36. The section on 'Discussion of Results' compares the RELAP5/MOD3.1 computer code output against the relevant experimental data.

The entire transient was sub-divided into three sub-intervals, and corresponding data values for various variables were accordingly categorized into three sub-sets. A total of 125 time points were used in each of the two time intervals (0 sec, 1000 sec) and (1000 sec, 2000 sec), and a total of 188 time points were used in the third time interval (2000 sec, 3500 sec). Statistical characterization of the differences between the code predictions and the corresponding experimental data were performed over each of the three time sub-intervals as well as over the entire transient (consisting of a total of 438 points). All 'statistical' evaluations considered here involve only one time-dependent sample function (for each variable), and the statistical error characterization is based on time averages.

These statistical evaluations over the three sub-intervals as well as over the entire transient are summarized in Table 6.1 ~ 6.3. These three tables for the 'Base Calculation' show, respectively, the mean error, the root-mean-square error, and the standard deviation of the errors between the code and data values for 28 different variables which characterize the MSLB transient.

The results in Tables 6.1 ~ 6.3 quantify the 'Discussion of Result' approximately. As can be seen from Tables 6.1 ~ 6.3, the statistical error values for most cases are generally reasonably low. However, there are several cases wherein the values obtained for the statistical parameters are rather misleading. As indicated earlier, the main reason

for this lies in the division by small (close to zero) values of $(X_i)_{exp}$ for obtaining ε_i It can be concluded that these statistical error values reflect or quantify the characteristics of the corresponding code-data comparisons for the majority of the cases reasonably well.

7. Sensitivity Studies

The sensitivity studies described here are related to any investigation into the effect of certain parameters on code predictions. Optimal results of these parameters are selected so that the differences between the code calculations and the experimental data are minimized. The statistical error values are used as a guide in assessing the optimal values of the sensitivity parameters. For the investigation reported here, the break flow discharge coefficient (Cd), the separator drain line loss coefficient (K), and the number of steam generator nodalization (n) are selected as the sensitivity parameters which have a significant impact on the computer code predictions.

The sensitivity studies for these parameters are shown plotted in Figures 7.1 ~ 7.30. The values of ε_{RMS} (i.e., the RMS or root-mean-square value) for the three classes of sensitivity studies are presented in Tables 7.1 ~ 7.3. This statistical summary of the sensitivity studies was discussed in the preceding section. For each of the three classes of sensitivity studies, ten cases are considered for the purpose of statistical error evaluation. The error evaluations for the sensitivity studies were performed over the time interval 0.0 to 1000.0 seconds for all variables.

For each of the ten cases considered, the statistical error values are of the same order of magnitude for the three classes of sensitivity studies. As was the situation for the base calculation, the majority of the cases in Table 7.1 ~ 7.3 reflect acceptable error values. Table 7.1 for the discharge coefficient sensitivity study is based on the Cd values of 0.75, 0.80, 0.85, and 0.90. Table 7.2 for the separator drain line loss coefficients sensitivity study uses K values of 0.0, 10.0, 50.0 and 100.0. Table 7.3 for the nodalization sensitivity study is based on 3,5,7 and 9 steam generator nodes.

In summary, the sensitivity studies do not indicate a pronounced dependence on the break flow discharge coefficient (Cd), the separator drain line loss coefficient (K), or the number of steam generator nodes (n). Nevertheless, Cd=0.85, K=10.0, and n=5

are considered the optimal values for the three parameters investigated here.

7.1 Break Junction Discharge Coefficient (Cd)

Break junction discharge coefficient (Cd) values of 0.75, 0.80, 0.85, and 0.90 were chosen for this sensitivity study. A lowering of the Cd value led to a decrease in the break junction flow, as is to be expected from the basic definition of this variables. Since different mass and energy blowdown rates result in different system depressurization rates, the steam generator shell side temperatures and associated heat removal rates are expected to be different for the four different discharge coefficient cases.

For the important time variations of break flow rate and pressurizer pressure, the value Cd=0.85 leads to the lowest RMS error value, as can be seen from Table 7.1. For most of the remaining time variations of important physical parameters, such as the break void fraction, there is very little to choose between the four values of Cd.

7.2 Separator drain line loss coefficient (K)

The steam separator provides practically 100% dry steam during normal operation. During an accident scenario, such as the main steam line break (MSLB) transient, the flow rates through the separator could be several times larger than the design basis value. The separator performance under conditions that exist in a MSLB transient is very important because it can change water inventory in the secondary system. This is the principal factor that affects the heat transfer from the primary to the secondary side. A separator component was used to simulate the steam generator separator and an annulus component was used to simulate the steam generator downcomer, such that an internal recirculation flow is maintained.

The separator drain lines were modeled as a junction flowing into the downcomer from the separator to avoid frothing conditions in the downcomer during steady state initialization. However, this introduced an undesirable side effect during steam generator inventory depletion transients. When steam was carried under from the separator via the drain lines, the liquid was forced up the downcomer to the steam dome via the separator by-pass.

This non-physical phenomenon could be suppressed by using a large loss coefficient in the separator drain line. This is the approach historically undertaken with RELAP5/MOD2 [8, 9]. In order to study the effect of internal recirculation flow on the void fraction and water inventory in the secondary side, steam separator drain line loss coefficients of 0.0, 10.0, 50.0 and 100.0 were chosen in conjunction with a break junction discharge coefficient of 0.85.

For the two physical variables of break flow rate and pressurizer pressure, the loss coefficient values K=0.0 and K=10.0 lead to nearly the same statistical error, as can be seen from Table 7.2. For most of the remaining variations, it is again a toss-up between these two K values with regard to optimality for minimum error. However, when considering the time variations of break void fraction, secondary pressure and temperature of intact loop, collapsed liquid level of pressurizer, and downcomer flow rates of intact and broken loops, the value K=10.0 leads to a smaller error level than K=0.0 with respect to the data-code comparisons.

7.3 Steam Generator Nodalization

It is seen from Table 7.3 that, with regard to the number of steam generator nodes (n), the value n=5 leads to the lowest overall RMS error for variations of break flow rate, pressurizer pressure, break void fraction, secondary pressure and temperature of intact loop, and the downcomer flow rates of intact and broken loops. The data-code

comparisons for the four different nodalizations are almost the same in relation to the variations of secondary pressure and temperature of broken loop.

Figure 7.31 shows the steam generator nodalization diagram for the nodalization sensitivity study. The four different cases of nodalization show 3, 5, 7 and 9 nodes in the steam generator, while the nodalization for other components remains unchanged.

Figure 7.32 shows a plot of CPU time vs transient (or real) time. For a given nodalization parameter n, this curve represents a linear relationship between the transient (or real) time and CPU time. However, for a fixed value of the transient time, the CPU time is a monotonically-increasing or convex function of the number of nodes n. (In other words, the CPU time increase with n at a faster rate than that indicated by a linear relationship).

8. Run Statistics

The SUN SPARC/station 20 workstation (at KOPEC) with OS Version 5.4 was used as the main frame computer for the calculations described here.

Figure 8.1 presents a plot of the required CPU time vs transient time for the base calculation. The user-specified maximum time step was 0.003906 second (in real time) for the entire transient calculation. The run statistics from the major edit are summarized in Table 8.1. The grind time can be calculated as follows:

CPU time(sec),	$CPU = 232736.40 - 28.15 = 232708.25$
Number of time steps,	$DT = 895880 - 0 = 895880$
Number of volumes,	$C = 189$
Transient real time,	$RT = 3500$ (sec)

$$Grind\ time = CPU \times 1000 / (C \times DT) = 1.3744\ CPU\ msec/vol/step$$

9. Conclusion and Recommendation

The overall comparisons between the RELAP5/MOD3.1 computer code predictions and the LSTF Test Run SB-SL-01 experimental data for a MSLB transient are reasonably satisfactory. This code provides approximate, but useful, predictions with regard to the variations of mass flow rate, void fraction, pressure, collapsed liquid level, temperature, and system flow rate for such a transient. Some of the results of comparison between the code output and the experimental data are quite good. However, certain shortcomings of this code are also apparent, when the code-data comparisons are examined more closely.

Sensitivity investigations with respect to the effects of the break discharge coefficient (Cd), the separator drain line loss coefficient (K), and the number of nodes in the steam generator (n) on code-data comparisons did not reveal a pronounced and straightforward dependence. The parameter values Cd=0.85, K=10.0, and n=5 were nevertheless selected as optimal values, based upon the lowest overall statistical error for the code-data comparisons.

The following suggestions are recommended for improving the performance of RELAP5/MOD3.1 in relation to the experimental results obtained for simulations of the MSLB phenomena :

(1) The RELAP5/MOD3.1 computer code (and previous versions of this code) cannot properly account for short wavelength or high frequency physical phenomena. This can be noted in the time variations of volume averaged void fraction of upperhead nodes (Figure 5.6), and in the substantial underprediction of the refill rate (for the collapsed liquid level) of the pressurizer (Figure 5.27). A related case involves the underprediction of variable changes occurring over a small time interval, as can be seen in Figure 5.10 ('cold leg temperature of intact loop'), and in Figures 5.28, 5.30. The

inability of RELAP5 to predict high frequency phenomena can be also seen in Figure 5.34 ('downcomer flow rate of broken loop'), where the code output displays instability in the form of highly oscillatory output, due to insufficient 'damping' of the mathematical or numerical models.

Although a more comprehensive description of this modeling deficiency in RELAP5 is beyond the scope of this investigation, it is suggested here that the inter-phase drag sub-model in the two-phase models of RELAP5 should be investigated further for a practical implementation of problem dependent, optimal numerical 'damping'. Suitable modeling of the inter-phase drag in this code is expected to mitigate the deficiencies noted above.

(2) The improvement of the void fraction and conservation of mass modeling in RELAP5 would lead to a significant improvement in the predictive capabilities of this code.

Although the prediction of break void fraction by the code (Figure 5.2) is reasonable, the calculated values of void fraction for the three upperhead nodes (Figure 5.6) involve significant discrepancy for the entire transient. These shortcomings affect, in turn, predictions of pressure variation (Figure 5.5 and 5.9), collapsed liquid level variation (Figures 5.27～5.31), and mass flow rates (Figures 5.32～5.36).

References

[1] The ROSA-IV Group, 1990 b, "ROSA-IV Large Scale Test Facility (LSTF) System Descriptions, JAERI-M 90-176, Japan Atomic Energy Research Institute.

[2] The ROSA-IV Group, 1989, "Supplemental Description of ROSA-IV LSTF with No. 1 Simulated Fuel Rod Assembly", JAERI-M 89-113, Japan Atomic Energy Research Institute.

[3] The ROSA-IV Group, 1990 a, "Quick Look Report for LSTF Test SB-SL-01", Japan Atomic Energy Research Institute.

[4] The RELAP5 Development Team, 1995, "RELAP5/MOD3 Code Manual", NUREG/CR-5535.

[5] Lin, C. L., Chao. J., Chiu, C., 1984, "A Boron Model for the Main Steam Line Break Transient", Proceedings of International Nuclear Power Plant Thermal Hydraulic And Operations Topical Meeting (China), pp 22-24.

[6] Tang, Jan-Ru, Wang, Song-Feng, Yuann, Ruey-Ying, 1986, "An Analysis of Steam Line Break Accident for Maanshan Units 1 & 2 Using RETRAN-02/MOD3 Code", Proceedings of Second International Nuclear Power Plant Thermal Hydraulics And Operations, pp 15-17.

[7] Liang, Kuo-Shing, Wang, Song-Feng, 1986, "Systematic Evaluation of the Main Steam Line Break Accident for a Typical Westinghouse Three Loop Plant Using RELAP5/MOD2 Code", Proceedings of Second International Nuclear Power Plant Thermal Hydraulics And Operations, pp 15-17.

[8] Rogers, J. M., 1989 a, "An Analysis of MB-2 100 % Steam Line Break Test T-2013 Using RELAP5/MOD2", AEEW-R2476, UKAEA Atomic Energy Establishment, WINFRITH Reactor Systems Analysis Division.

[9] Rogers, J. M., 1989 b, "An Analysis of Semiscale Mod-2C S-FS-1 Steam Line Break Test Using RELAP5/MOD2", UKAEA Atomic Energy Establishment, WINFRITH Reactor Systems Analysis Division.

Table 3.1 Sequence of Events for Experiment SB-SL-01

Event	Measured Data (seconds)	Calculated Data (seconds)
Transient initiations	0	0
Reactor scram	0	0
MSIV closure	2	2
Steam generator feedwater valve closure	2	2
Turbine throttle valve closure	0	2
Auxiliary feedwater injection	28	58
High pressure safety injectionsteam	1156	1156
PORV open	3312	2905

Table 3.2 Initial and Boundary Conditions for Experiment SB-SL-01

Parameters	Units	LSTF (Measured)	RELAP5/MOD3.1 (Calculated)
Core power	MW	10.000±0.044	10.000
Pressurizer pressure	MPa	15.520±0.080	15.590
Hot leg fluid temperature	K	598.100±4.396	599.400
Cold leg fluid temperature	K	562.400±4.134	564.100
Primary coolant flow rate	kg/sec	24.3000±0.2668	24.6000
Pressurizer liquid level	m	2.7000±0.0086	2.6400
Primary coolant pump speed	rpm	800±4	768
Primary coolant flow control valves	-	fully open	fully open
SG secondary pressure	MPa	7.3000±0.0393	7.3000
SG secondary liquid level	m	10.3000±0.0329	11.8165
SG feedwater temperature	K	495.2000±3.8477	495.4000
SG feedwater and main steam flow rates	kg/sec	2.7400±0.0442	2.7500

Table 5.1 List of Assessment Parameters (LSTF SB-SL-01)

Description	Calculation	Measurement	Uncertainty	Figure
Break Flow Rate	mflowj 91500	FE560A-BU	0.7686 kg/sec	5.1
Break Void Fraction	voidg 32801	SP-VOLUME	Not Found	5.2
Break Density	rho 32801	N/A	N/A	5.3
Pressurizer Pressure	p 61004	PE300A-PR	0.1078 MPa	5.4
Vessel Upperhead Void Fraction	voidg 14401 voidg 14801 voidg 15201	N/A	N/A	5.5
Volume Averaged Void Fraction of Three Upperhead Nodes	rho 14401 rho 14801 rho 15201	SB-SL-01	Not Found	5.6
Secondary Pressure of Broken Loop	p 31601	PE450-SGB	0.0539 MPa	5.7
Secondary Pressure of Intact Loop	p 51601	PE430-SGA	0.0539 MPa	5.8
Hotleg Temperature of Intact Loop	tempf 40001	TE020D-HLA	3.3070 K	5.9
Coldleg Temperature of Intact Loop	tempf 45201	TE080D-CLA	3.3070 K	5.10
SG Steam Dome Temperature of Intact Loop	tempf 51601	TE-245C-SGA	3.1080 K	5.11
SG Downcomer Temperature of Intact Loop	tempf 50005	TE432-SGA	3.1080 K	5.12
SG Downcomer Temperature of Intact Loop (4 loops)	tempf 50005	TE431-SGA TE432-SGA TE433-SGA TE434-SGA	3.1080 K	5.13
Hotleg Temperature of Broken Loop	tempf 20001	TE170D-HLB	3.3070 K	5.14
Coldleg Temperature of Broken Loop	tempf 25201	TE220D-CLB	3.3070 K	5.15
SG Steam Dome Temperature of Broken Loop	tempf 31601	TE-245C-SGB	3.1080 K	5.16
SG Downcomer Temperature of Broken Loop	tempf 30005	TE472-SGB	3.1080 K	5.17
SG Downcomer Temperature of Broken Loop (4 loops)	temp 30005	TE471-SGB TE472-SGB TE473-SGB TE474-SGB	3.1080 K	5.18
SG Boiler Bottom Temperature of Broken Loop	tempf 30401	TE-099C-SGB	3.1080 K	5.19
SG Boiler Middle Temperature of Broken Loop	tempf 30403	TE-150C-SGB	3.1080 K	5.20
SG Boiler Top Temperature of Broken Loop	tempf 30405	TE-192F-SGB	3.1080 K	5.21
SG Boiler Bottom Temperature of Intac Loop	tempf 50401	TE-099C-SGA	3.1080 K	5.22
SG Boiler Middle Temperature of Broken Loop	tempf 50403	TE-150C-SGA	3.1080 K	5.23
SG Boiler Top Temperature of Broken Loop	tempf 50405	TE-178C-SGA	3.1080 K	5.24
Average Temperature of RCS Broken Loop	tempf 20001 tempf 25201	TE240-HLB	3.3070 K	5.25
Collapsed Liquid Level of Pressurizer	cntrvar 610	LE280-PR	0.0544 m	5.26
Narrow Range of Liquid Level of S/G Intact Loop	cntrvar 508	LE440-SGA	0.0192 m	5.27
Narrow Range of Liquid Level of S/G Broken Loop	cntrvar 308	LE460-SGB	0.0192 m	5.28
Liquid Level of S/G Intact Loop	cntrvar 512	LE441-SGA LE442-SGA LE430-SGA	0.0352 m	5.29
Liquid Level of S/G Broken Loop	cntrvar 312	LE461-SGB LE462-SGB LE450-SGB	0.0352 m	5.30
Pump Suction Flow Rate of Broken Loop	mflowj 24001	FE160B-LSB FE160A-LSB	0.0174 kg/s 1.0710 kg/s	5.31
Pump Suction Flow Rate of Intact Loop	mflowj 44001	FE020B-LSA FE020A-LSA	0.0174 kg/s 1.0710 kg/s	5.32
Downcomer Flow Rate of Broken Loop	mflowj 30100	FE471-SGB FE472-SGB FE473-SGB FE474-SGB	0.1169 kg/s	5.33
Downcomer Flow Rate of Intact Loop	mflowj 50100	FE431-SGA FE432-SGA FE433-SGA FE434-SGA	0.1129 kg/s	5.35
Separator Flow Rate of Broken Loop	mflowj 30801 mflowj 30802 mflowj 30803	N/A	N/A	5.37
Separator Flow Rate of Intact Loop	mflowj 50801 mflowj 50802 mflowj 50803	N/A	N/A	5.38

Table 6.1 The Mean Errors ($\bar{\varepsilon}$) for the Base Calculation (Cd=85, K=10.0, n=5)

No.	Figure No.	Parameters	Time Range (sec)			
			0≤t<1000	1000≤t<2000	2000≤t<3500	0≤t<3500 (full range)
1	5.1	Break Flow Rate	-0.0107	0.0080	0.1175	0.0474
2	5.2	Break Void Fraction	-0.0024	0.0106	0.0113	0.0723
3	5.4	Pressurizer Pressure	-0.0028	0.0763	0.0709	0.0499
4	5.6	Volume Averaged Void Fraction of Three Upperhead Nodes	-0.6236	5.2755	1.5681	1.9991
5	5.7	Secondary Pressure of Broken Loop	-0.1553	-0.1733	-0.2463	-0.1994
6	5.8	Secondary Pressure of Intact Loop	-0.0009	-0.1165	-0.1196	-0.0848
7	5.9	Hotleg Temperature of Intact Loop	-0.0000	-0.0092	-0.0070	-0.0056
8	5.10	Coldleg Temperature of Intact Loop	0.0021	0.0163	-0.0422	-0.0128
9	5.11	SG Steam Dome Temperature of Intact Loop	-0.0021	-0.0239	-0.0283	-0.0196
10	5.12	SG Downcomer Temperature of Intact Loop	-0.0103	0.0038	0.0029	-0.0006
11	5.14	Hotleg Temperature of Broken Loop	-0.0001	-0.0124	-0.0178	-0.0112
12	5.15	Coldleg Temperature of Broken Loop	-0.0081	-0.0087	-0.0134	-0.0105
13	5.16	SG Steam Dome Temperature of Broken Loop	-0.0395	-0.0861	-0.1091	-0.0826
14	5.17	SG Downcomer Temperature of Broken Loop	-0.0193	-0.0135	-0.0145	-0.0156
15	5.19	SG Boiler Bottom Temperature of Broken Loop	-0.0173	-0.0140	-0.0180	-0.0166
16	5.20	SG Boiler Middle Temperature of Broken Loop	-0.0167	-0.0366	-0.0362	-0.0308
17	5.21	SG Boiler Top Temperature of Broken Loop	-0.0233	-0.0392	-0.0401	-0.0348
18	5.22	SG Boiler Bottom Temperature of Intact Loop	-0.0018	-0.0163	-0.0174	-0.0127
19	5.23	SG Boiler Middle Temperature of Intact Loop	-0.0012	-0.0208	-0.0236	-0.0164
20	5.24	SG Boiler Top Temperature of Intact Loop	-0.0033	-0.0176	-0.0162	-0.0129
21	5.25	Average Temperature of RCS Broken Loop	-0.0034	-0.0117	-0.0170	-0.0116
22	5.26	Collapsed Liquid Level of Pressurizer	-0.5160	-3.0766	-0.2608	-1.1393
23	5.27	Narrow Range of SG Level of Intact Loop	0.2396	-0.3400	-0.2882	-0.1521
24	5.28	Narrow Range of SG Level of Broken Loop	-0.8151	-0.9153	-0.9188	-0.8881
25	5.31	Pump Suction Flow Rate of Broken Loop	0.5014	0.0336	0.0501	0.1806
26	5.32	Pump Suction Flow Rate of Intact Loop	0.5991	0.3029	11.6543	5.0488
27	5.33	Downcomer Flow Rate of Broken Loop	-0.3198	-0.4050	-0.2666	-0.3214
28	5.35	Downcomer Flow Rate of Intact Loop	0.0451	2.5183	-0.8304	0.3779
The number of data points used for evaluation			125	125	188	438

Table 6.2 The Root-Mean-Square Errors (ε_{RMS})
for the Base Calculation (Cd=0.85, K=10.0, n=5)

No.	Figure No.	Parameters	Time Range (sec)			
			0≤t<1000	1000≤t<2000	2000≤t<3500	0≤t<3500 (full range)
1	5.1	Break Flow Rate	0.0270	0.0159	0.1437	0.0939
2	5.2	Break Void Fraction	0.0135	0.0110	0.0117	0.0120
3	5.4	Pressurizer Pressure	0.0173	0.0777	0.0778	0.0655
4	5.6	Volume Averaged Void Fraction of Three Upperhead Nodes	0.9335	6.8087	2.8789	4.1526
5	5.7	Secondary Pressure of Broken Loop	0.1661	0.1751	0.2468	0.2067
6	5.8	Secondary Pressure of Intact Loop	0.0257	0.1173	0.1198	0.1013
7	5.9	Hotleg Temperature of Intact Loop	0.0027	0.0095	0.0074	0.0072
8	5.10	Coldleg Temperature of Intact Loop	0.0032	0.0226	0.0518	0.0360
9	5.11	SG Steam Dome Temperature of Intact Loop	0.0046	0.0241	0.0284	0.0227
10	5.12	SG Downcomer Temperature of Intact Loop	0.0150	0.0052	0.0031	0.0087
11	5.14	Hotleg Temperature of Broken Loop	0.0025	0.0130	0.0179	0.0137
12	5.15	Coldleg Temperature of Broken Loop	0.0090	0.0092	0.0135	0.0112
13	5.16	SG Steam Dome Temperature of Broken Loop	0.0446	0.0868	0.1091	0.0884
14	5.17	SG Downcomer Temperature of Broken Loop	0.0202	0.0135	0.0148	0.0162
15	5.19	SG Boiler Bottom Temperature of Broken Loop	0.0182	0.0141	0.0181	0.0171
16	5.20	SG Boiler Middle Temperature of Broken Loop	0.0177	0.0373	0.0379	0.0332
17	5.21	SG Boiler Top Temperature of Broken Loop	0.0251	0.0394	0.0404	0.0364
18	5.22	SG Boiler Bottom Temperature of Intact Loop	0.0055	0.0168	0.0175	0.0149
19	5.23	SG Boiler Middle Temperature of Intact Loop	0.0034	0.0213	0.0237	0.0193
20	5.24	SG Boiler Top Temperature of Intact Loop	0.0047	0.0178	0.0163	0.0145
21	5.25	Average Temperature of RCS Broken Loop	0.0038	0.0121	0.0170	0.0131
22	5.26	Collapsed Liquid Level of Pressurizer	0.6301	13.9244	0.2712	7.4569
23	5.27	Narrow Range of SG Level of Intact Loop	2.1236	0.3410	0.2887	1.1657
24	5.28	Narrow Range of SG Level of Broken Loop	0.8436	0.9153	0.9188	0.8969
25	5.31	Pump Suction Flow Rate of Broken Loop	2.5046	0.0362	0.0530	1.3714
26	5.32	Pump Suction Flow Rate of Intact Loop	2.4229	20.2147	107.287	69.6087
27	5.33	Downcomer Flow Rate of Broken Loop	0.4001	0.4359	0.8085	0.6163
28	5.35	Downcomer Flow Rate of Intact Loop	2.4101	3.3852	0.8375	2.2890
The number of data points used for evaluation			125	125	188	438

Table 6.3 The Standard Deviations of the Errors (σ_ε) for the Base Calculation (Cd=0.85, K=10.0, n=5)

No.	Figure No.	Parameters	Time Range (sec)			
			0≤t<1000	1000≤t<2000	2000≤t<3500	0≤t<3500 (full range)
1	5.1	Break Flow Rate	0.0248	0.0138	0.0827	0.0811
2	5.2	Break Void Fraction	0.0133	0.0030	0.0029	0.0097
3	5.4	Pressurizer Pressure	0.0171	0.0144	0.0321	0.0425
4	5.6	Volume Averaged Void Fraction of Three Upperhead Nodes	0.6947	4.3043	2.4144	3.6397
5	5.7	Secondary Pressure of Broken Loop	0.0587	0.0244	0.0157	0.0543
6	5.8	Secondary Pressure of Intact Loop	0.0256	0.0142	0.0065	0.0556
7	5.9	Hotleg Temperature of Intact Loop	0.0027	0.0023	0.0024	0.0044
8	5.10	Coldleg Temperature of Intact Loop	0.0024	0.0157	0.0300	0.0337
9	5.11	SG Steam Dome Temperature of Intact Loop	0.0041	0.0029	0.0013	0.0116
10	5.12	SG Downcomer Temperature of Intact Loop	0.0109	0.0036	0.0011	0.0087
11	5.14	Hotleg Temperature of Broken Loop	0.0025	0.0039	0.0012	0.0078
12	5.15	Coldleg Temperature of Broken Loop	0.0039	0.0028	0.0017	0.0037
13	5.16	SG Steam Dome Temperature of Broken Loop	0.0208	0.0108	0.0027	0.0315
14	5.17	SG Downcomer Temperature of Broken Loop	0.0057	0.0015	0.0029	0.0044
15	5.19	SG Boiler Bottom Temperature of Broken Loop	0.0057	0.0016	0.0019	0.0038
16	5.20	SG Boiler Middle Temperature of Broken Loop	0.0058	0.0073	0.0113	0.0126
17	5.21	SG Boiler Top Temperature of Broken Loop	0.0114	0.0039	0.0044	0.0106
18	5.22	SG Boiler Bottom Temperature of Intact Loop	0.0051	0.0042	0.0014	0.0078
19	5.23	SG Boiler Middle Temperature of Intact Loop	0.0032	0.0042	0.0014	0.0101
20	5.24	SG Boiler Top Temperature of Intact Loop	0.0033	0.0024	0.0016	0.0066
21	5.25	Average Temperature of RCS Broken Loop	0.0018	0.0030	0.0011	0.0060
22	5.26	Collapsed Liquid Level of Pressurizer	0.3616	13.5803	0.0744	7.3694
23	5.27	Narrow Range of SG Level of Intact Loop	2.1100	0.0263	0.0161	1.1558
24	5.28	Narrow Range of SG Level of Broken Loop	0.2171	0.0023	0.0022	0.1250
25	5.31	Pump Suction Flow Rate of Broken Loop	2.4539	0.0137	0.0172	1.3594
26	5.32	Pump Suction Flow Rate of Intact Loop	2.3477	20.2124	106.653	69.4254
27	5.33	Downcomer Flow Rate of Broken Loop	0.2404	0.1611	0.7633	0.5259
28	5.35	Downcomer Flow Rate of Intact Loop	2.4097	2.2622	0.1086	2.2576
The number of data points used for evaluation			125	125	188	438

Table 7.1 The Root-Mean-Square Errors (ε_{RMS}) for the Sensitivity Study on the Discharge Coefficient (Cd)

(K=10.0, n=5)

No.	Figure No.	Parameters	Discharge Coefficient			
			Cd=0.75	Cd=0.80	Cd=0.85	Cd=0.90
1	Figure 7.1	Break Flow Rate	0.0435	0.0280	0.0270	0.0394
2	Figure 7.2	Pressurizer Pressure	0.0232	0.0196	0.0173	0.0189
3	Figure 7.3	Secondary Pressure of Broken Loop	0.0751	0.1226	0.1661	0.2048
4	Figure 7.4	Secondary Temperature of Broken Loop	0.0349	0.0400	0.0446	0.0494
5	Figure 7.5	Break Void Fraction	0.0133	0.0134	0.0135	0.0136
6	Figure 7.6	Secondary Pressure of Intact Loop	0.0227	0.0258	0.0246	0.0274
7	Figure 7.7	Secondary Temperature of Intact Loop	0.0043	0.0045	0.0046	0.0051
8	Figure 7.8	Collapsed Liquid Level of Pressurizer	0.5327	0.5778	0.6301	0.6721
9	Figure 7.9	Downcomer Flow Rate of Intact Loop	2.4534	2.4114	2.4101	2.4205
10	Figure 7.10	Downcomer Flow Rate of Broken Loop	0.4333	0.4328	0.4001	0.4405
The number of data points used for evaluation			125	125	125	125

Table 7.2 The Root-Mean-Square Errors (ϵ_{RMS}) for the Sensitivity Study on the S/G Drain Line Loss Coefficient (K)

(Cd=0.85, n=5)

No.	Figure No.	Parameters	Loss Coefficient			
			K=0.00	K=10.0	K=50.0	K=100.0
1	Figure 7.11	Break Flow Rate	0.0259	0.0270	0.0328	0.0338
2	Figure 7.12	Pressurizer Pressure	0.0169	0.0173	0.0174	0.0175
3	Figure 7.13	Secondary Pressure of Broken Loop	0.1657	0.1661	0.1661	0.1672
4	Figure 7.14	Secondary Temperature of Broken Loop	0.0443	0.0443	0.0445	0.0445
5	Figure 7.15	Break Void Fraction	0.0135	0.0135	0.0151	0.0136
6	Figure 7.16	Secondary Pressure of Intact Loop	0.0264	0.0248	0.0232	0.0224
7	Figure 7.17	Secondary Temperature of Intact Loop	0.0046	0.0046	0.0043	0.0043
8	Figure 7.18	Collapsed Liquid Level of Pressurizer	0.6252	0.6262	0.6274	0.6285
9	Figure 7.19	Downcomer Flow Rate of Intact Loop	2.6412	2.4101	2.4705	2.4000
10	Figure 7.20	Downcomer Flow Rate of Broken Loop	0.4377	0.4006	0.4278	0.4400
The number of data points used for evaluation			125	125	125	125

Table 7.3 The Root-Mean-Square Errors (ε_{RMS}) for the Sensitivity Study on the Number of Steam Generator Nodes (n)

(Cd=0.85, K=10.0)

No.	Figure No.	Parameters	Number of S/G Nodes			
			n=3	n=5	n=7	n=9
1	Figure 7.21	Break Flow Rate	0.0511	0.0270	0.0371	0.0389
2	Figure 7.22	Pressurizer Pressure	0.0154	0.0173	0.0179	0.0175
3	Figure 7.23	Secondary Pressure of Broken Loop	0.1404	0.1661	0.1684	0.1676
4	Figure 7.24	Secondary Temperature of Broken Loop	0.0410	0.0443	0.0450	0.0449
5	Figure 7.25	Break Void Fraction	0.0167	0.0135	0.0153	0.0157
6	Figure 7.26	Secondary Pressure of Intact Loop	0.0312	0.0248	0.0253	0.0245
7	Figure 7.27	Secondary Temperature of Intact Loop	0.0054	0.0046	0.0046	0.0043
8	Figure 7.28	Collapsed Liquid Level of Pressurizer	0.6031	0.6262	0.6309	0.6327
9	Figure 7.29	Downcomer Flow Rate of Intact Loop	3.3190	2.4101	2.4527	4.3797
10	Figure 7.30	Downcomer Flow Rate of Broken Loop	0.8223	0.4006	0.4361	0.4376
The number of data points used for evaluation			125	125	125	125

Table 8.1 Run Statistics Data in Base Calculation

Transient time (sec)	CPU time (sec)	Attempted ADV	Repeated ADV	Last DT	Courant DT
0	28.75	0	0	3.125E-2	0
500	33481.12	127880	0	3.906E-3	4.74466E-3
1000	66705.25	255880	0	3.906E-3	4.46076E-3
1500	99842.10	383880	0	3.906E-3	4.49261E-3
2000	132695.70	511880	0	3.906E-3	4.51401E-3
2500	166225.70	639880	0	3.906E-3	4.53266E-3
3000	199659.60	767880	0	3.906E-3	4.54726E-3
3500	232736.40	895880	0	3.906E-3	4.56085E-3

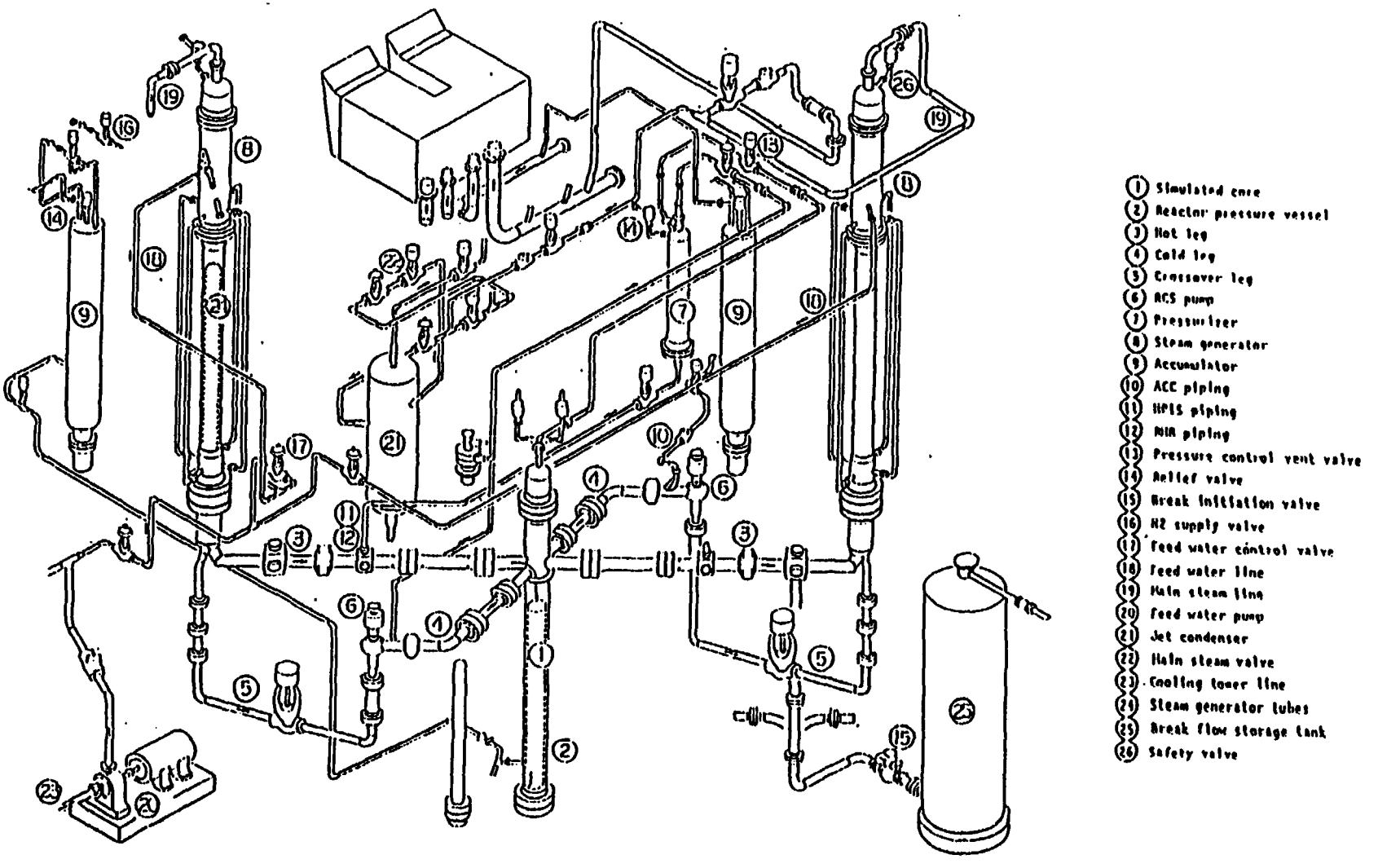

Figure 2.1 Schematic View of ROSA-VI LSTF

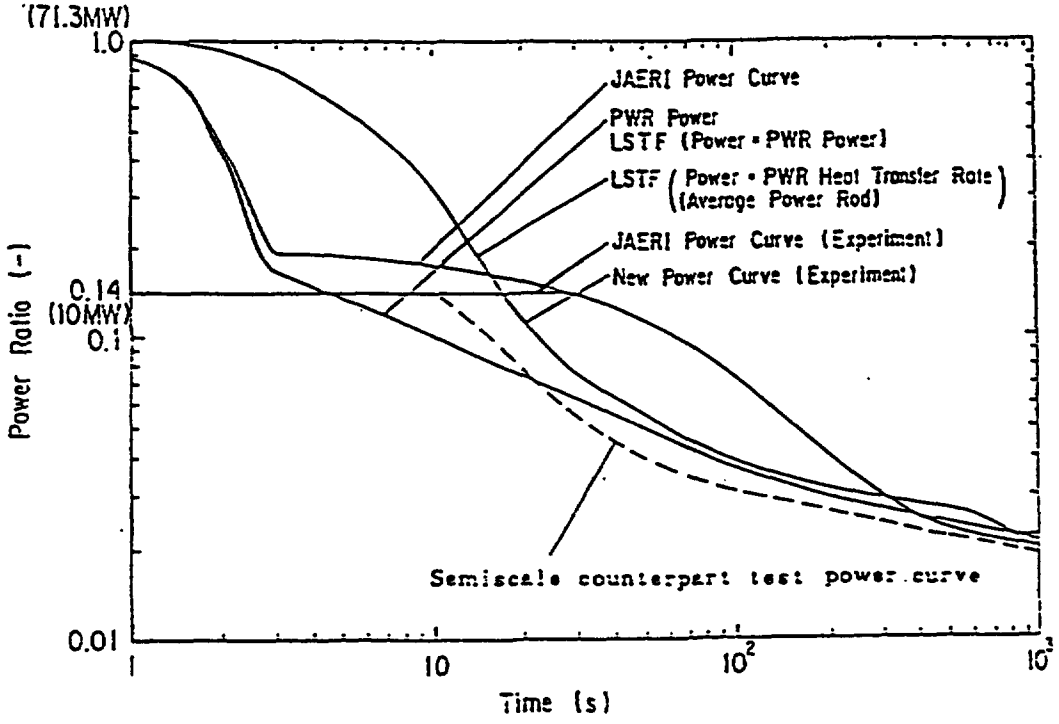

Figure 3.1 Three Core Power Control Curves for LSTF

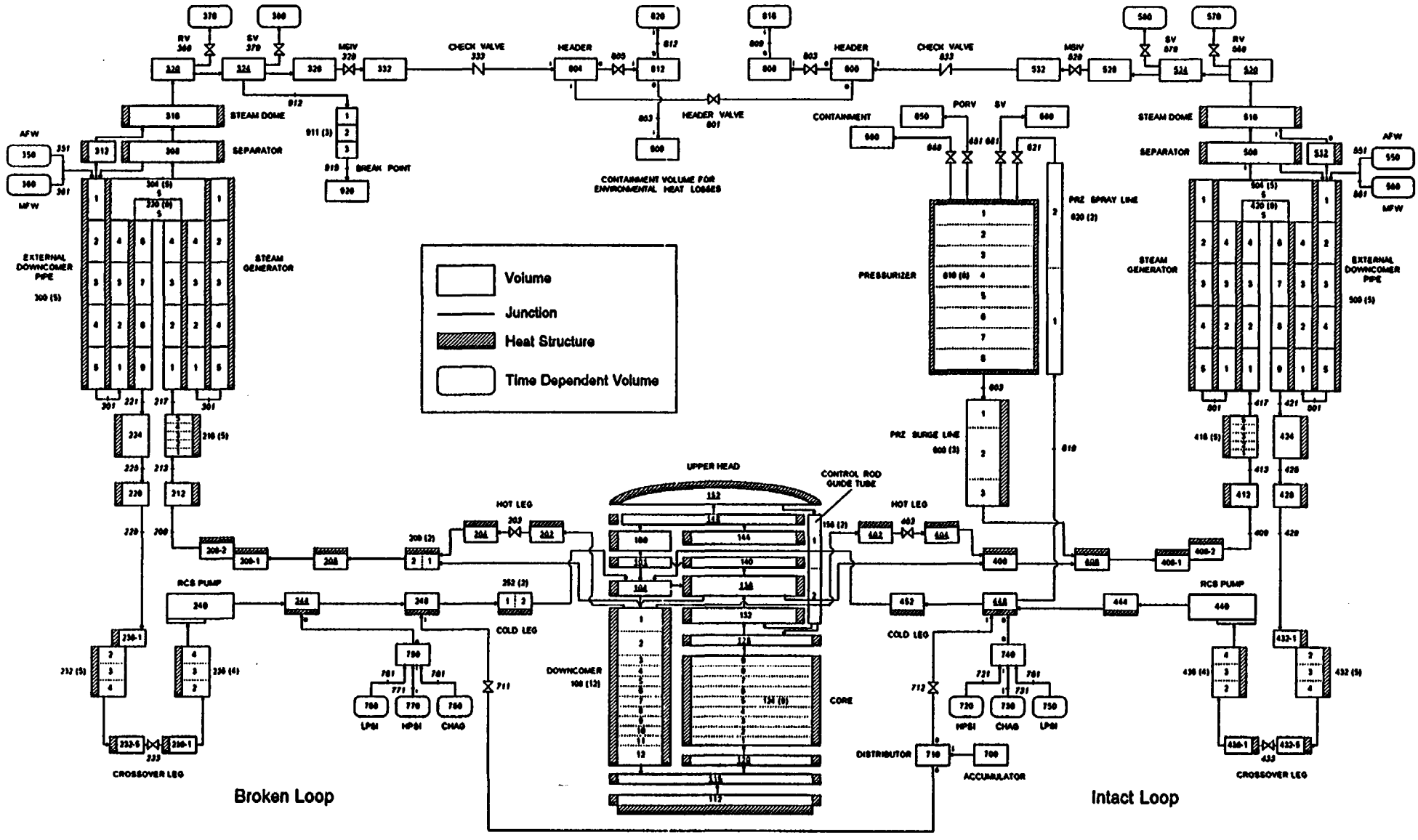

Figure 4.1 RELAP5/MOD3.1 Nodalization of LSTF for MSLB Transient Assessment

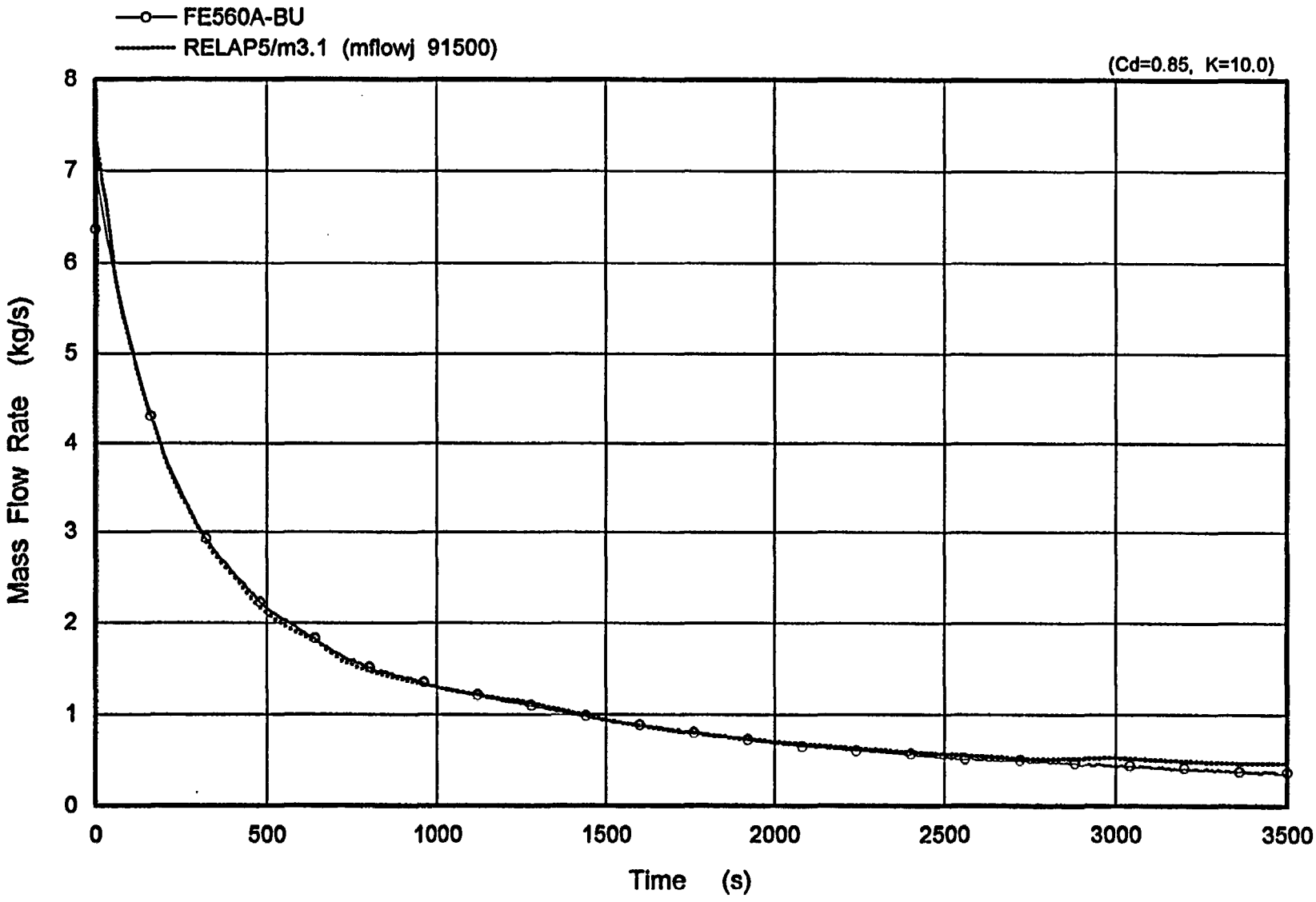

Figure 5.1 Break Flow Rate

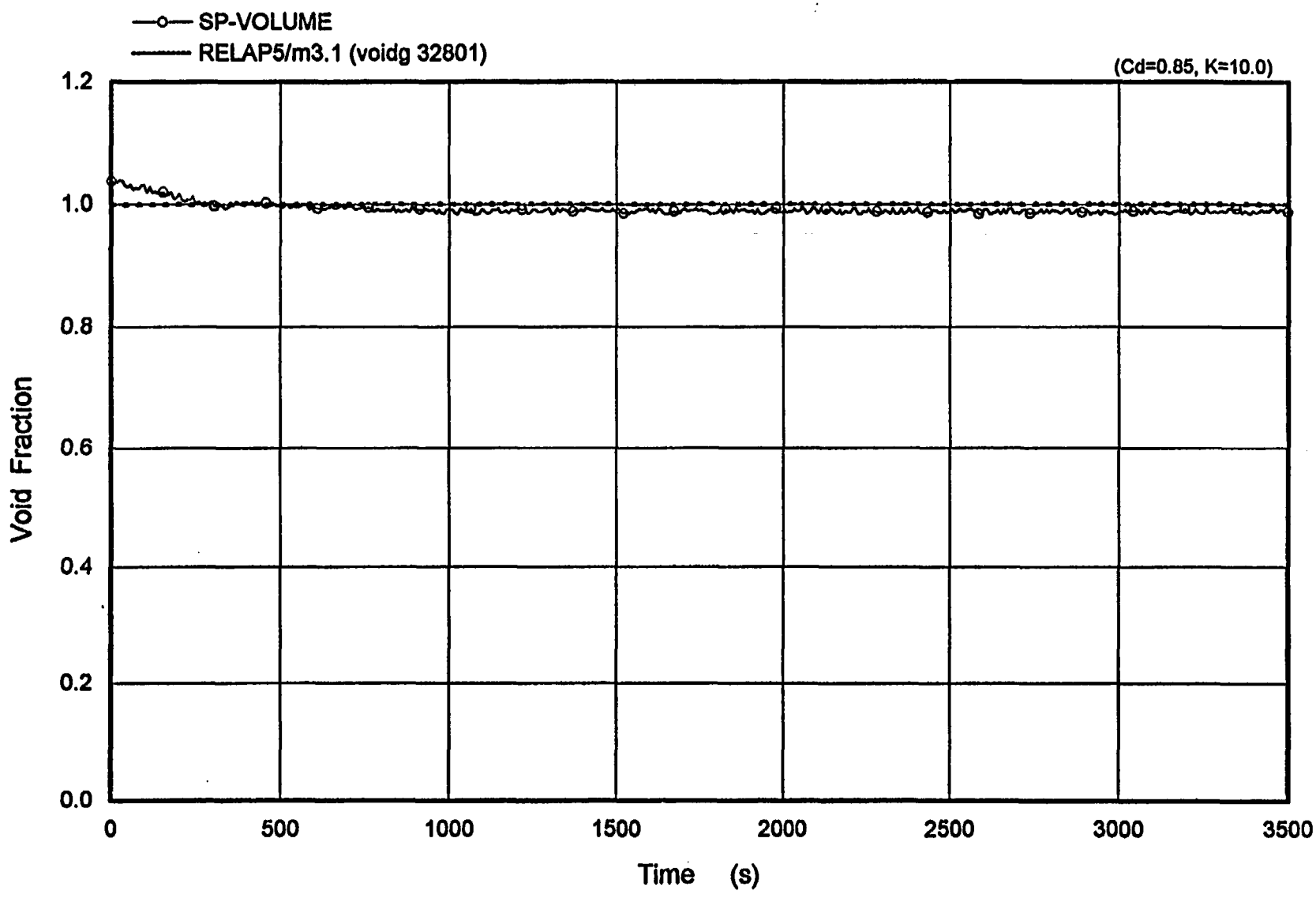

Figure 5.2 Break Void Fraction

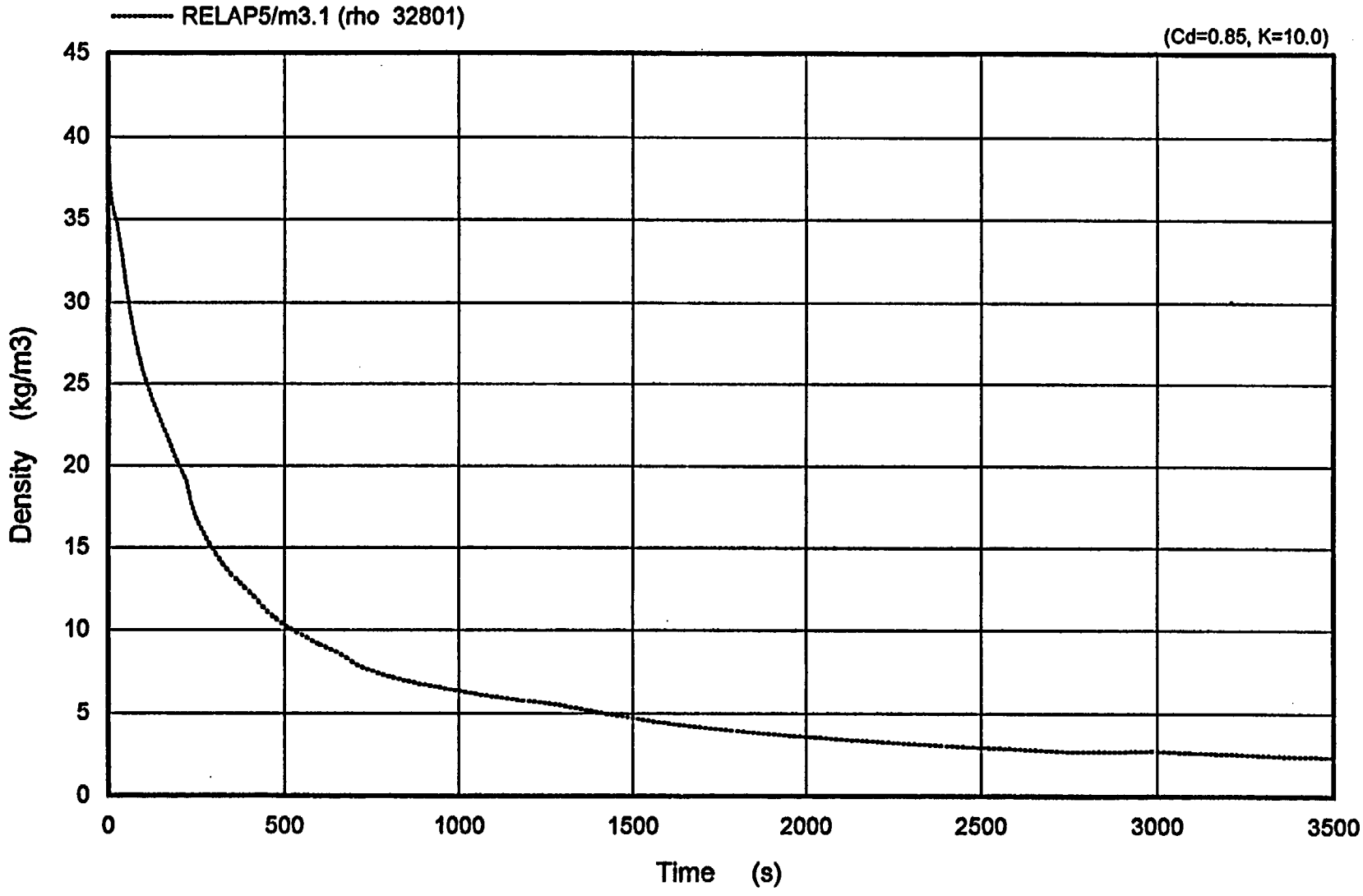

Figure 5.3 Break Density

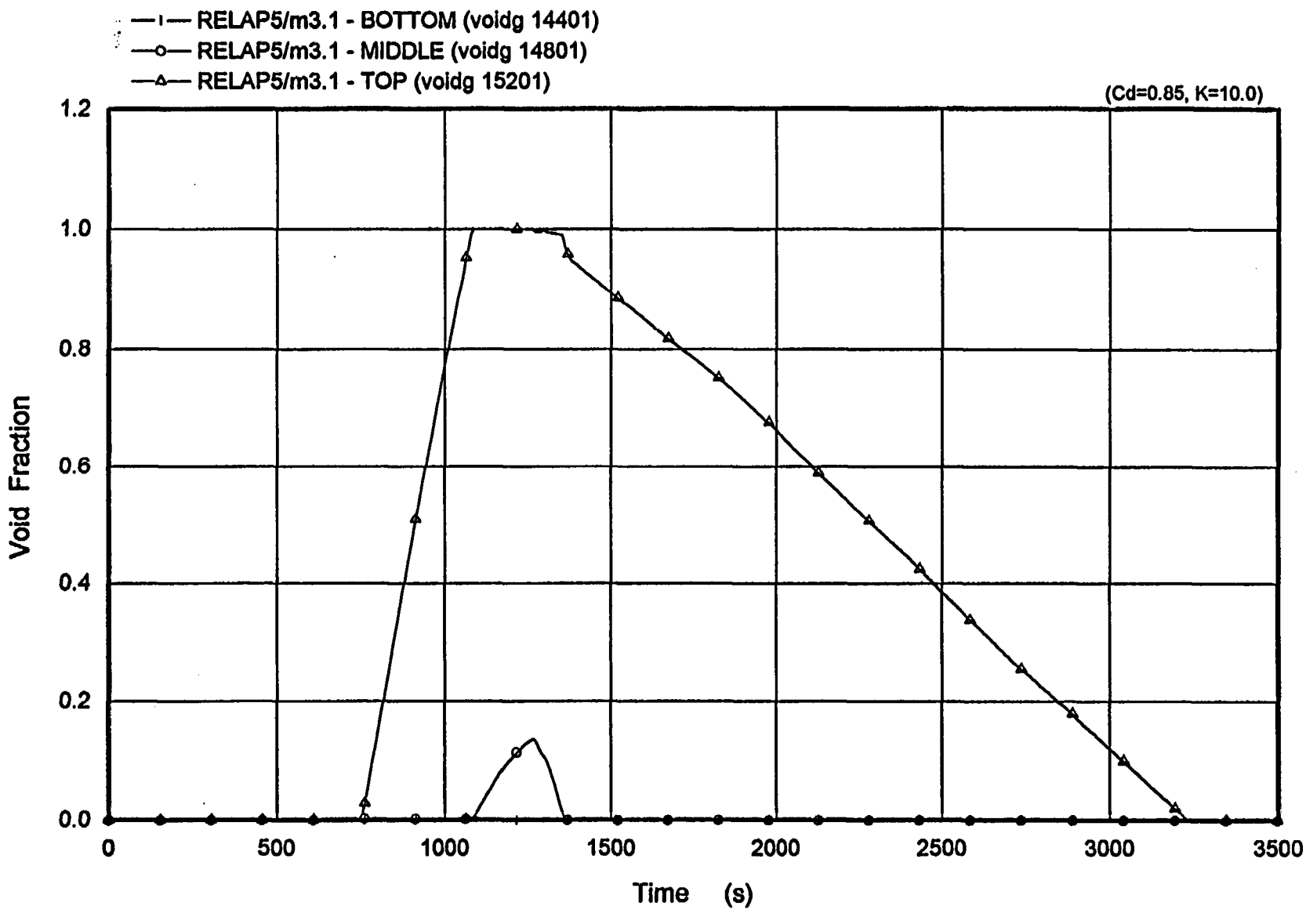

Figure 5.4 Vessel Upperhead Void Fraction

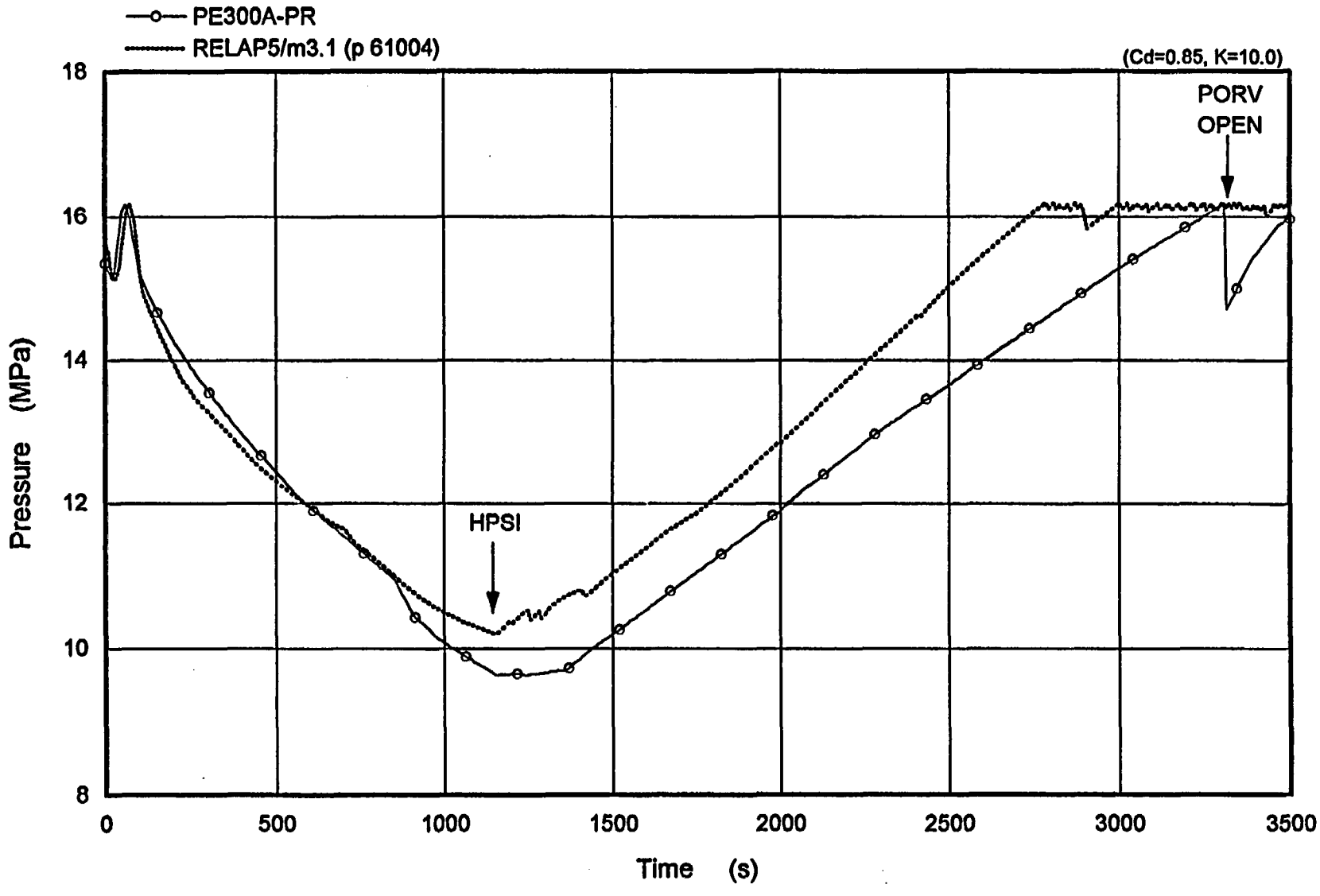

Figure 5.5 Pressurizer Pressure

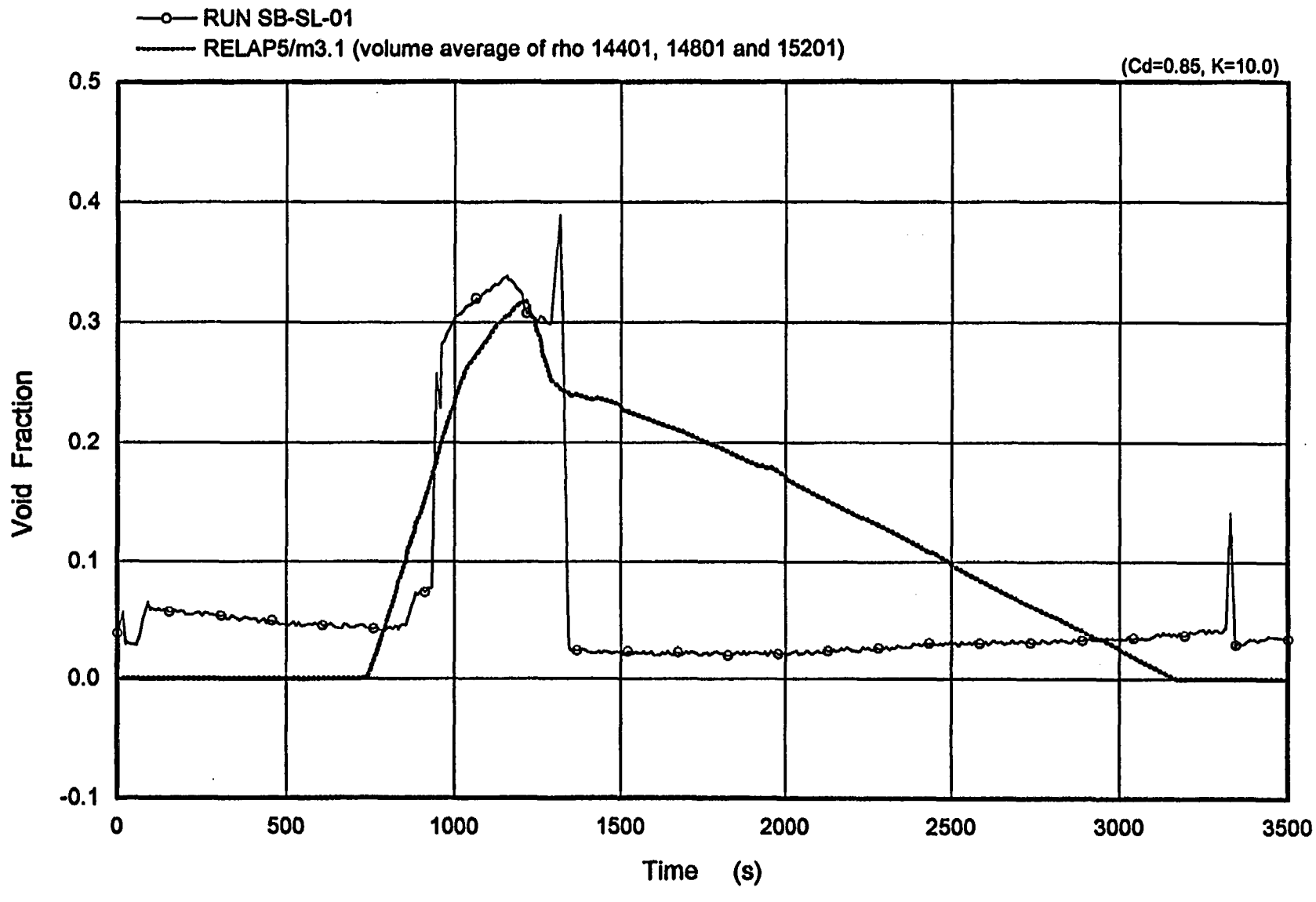

Figure 5.6 Volume Averaged Void Fraction of Three Upperhead Nodes

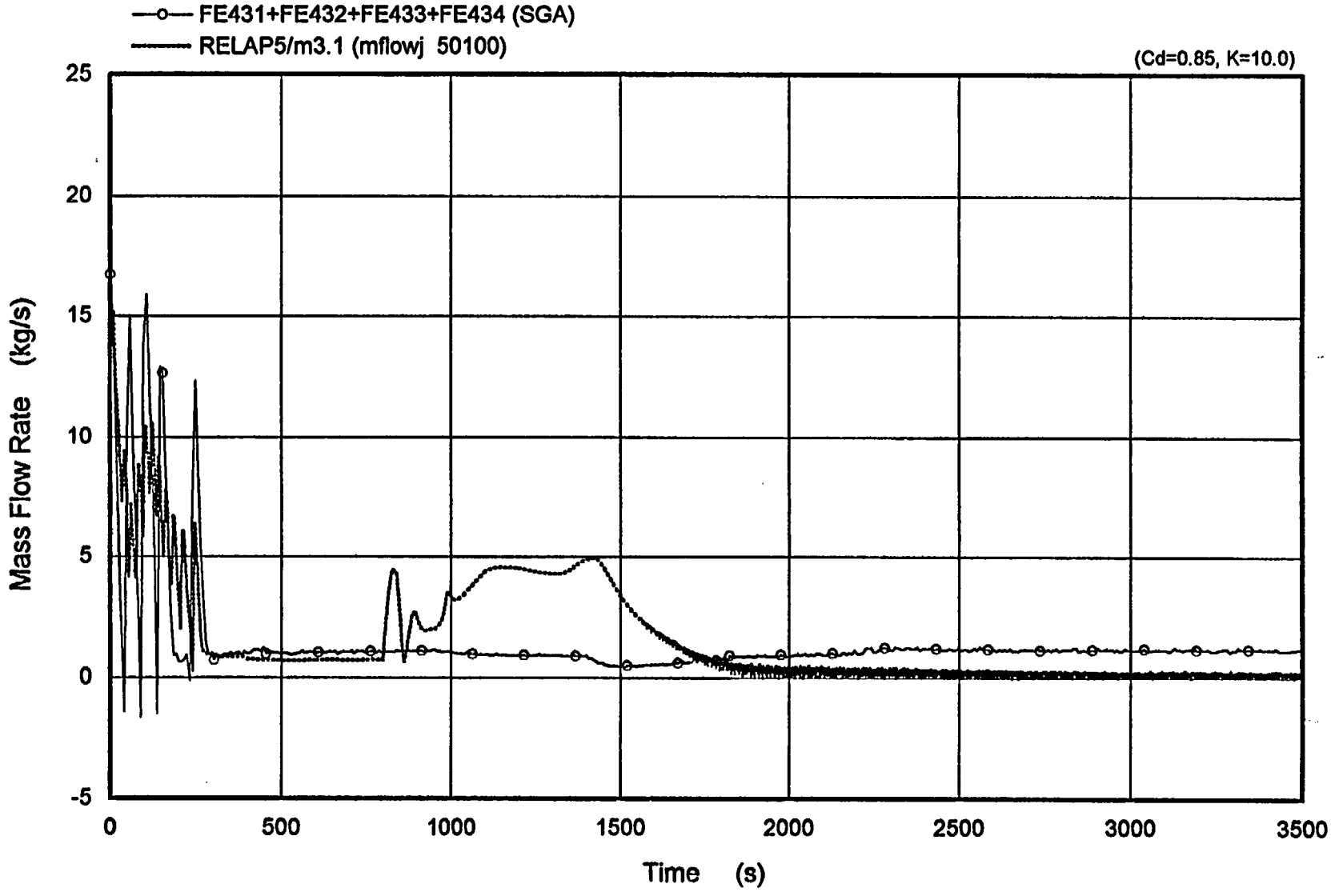

Figure 5.7 Downcomer Flow Rate of Intact Loop

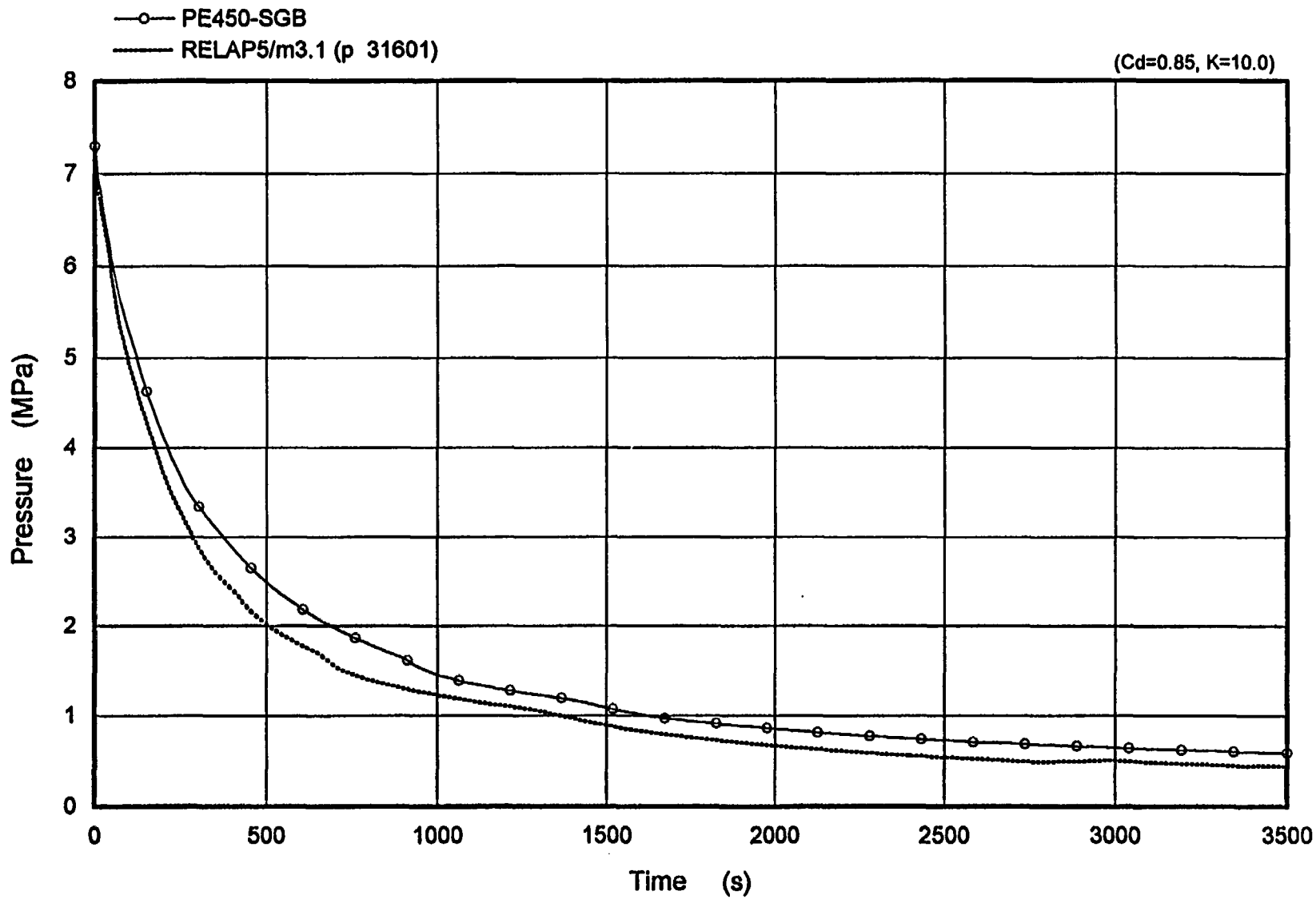

Figure 5.8 Secondary Pressure of Broken Loop

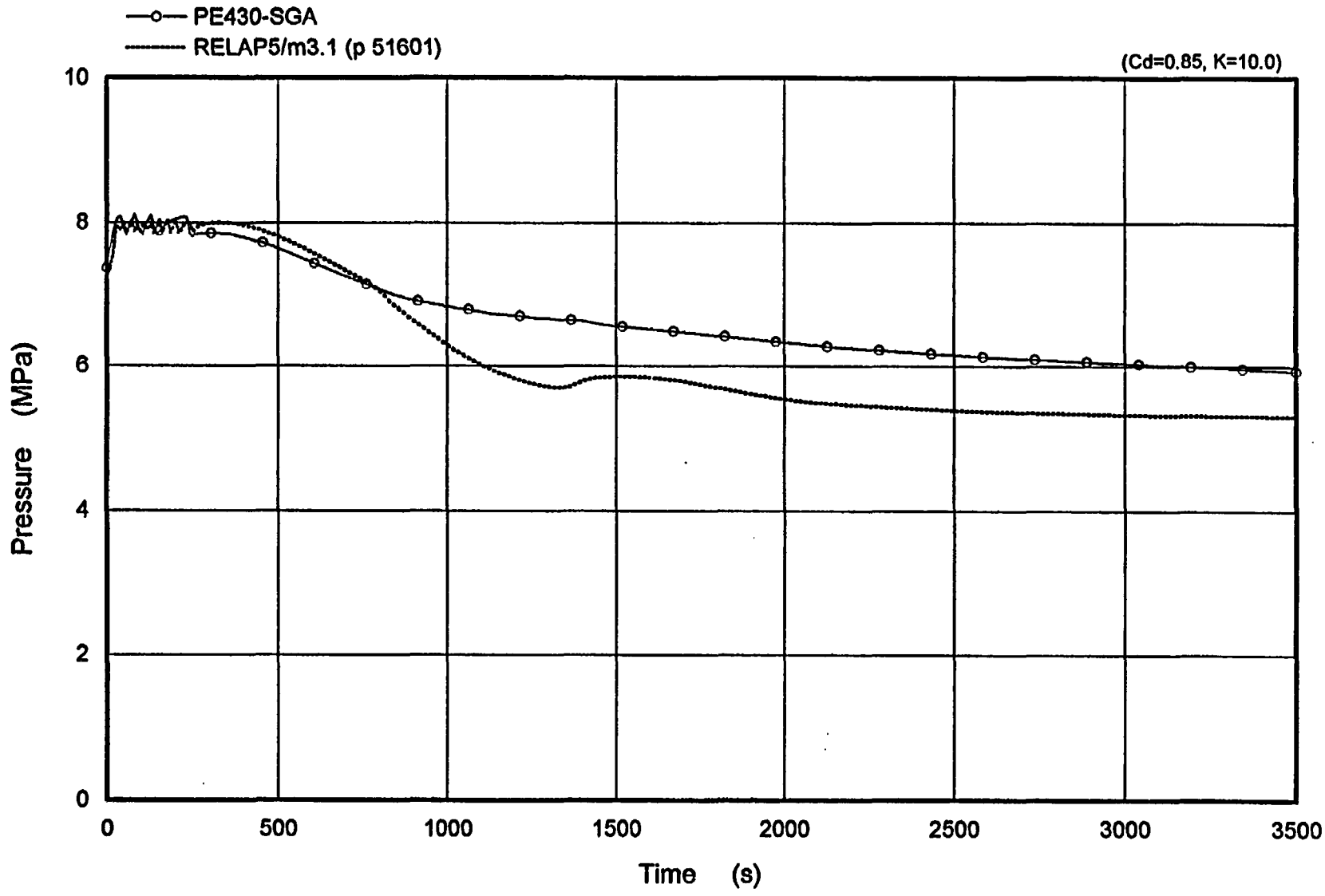

Figure 5.9 Secondary Pressure of Intact Loop

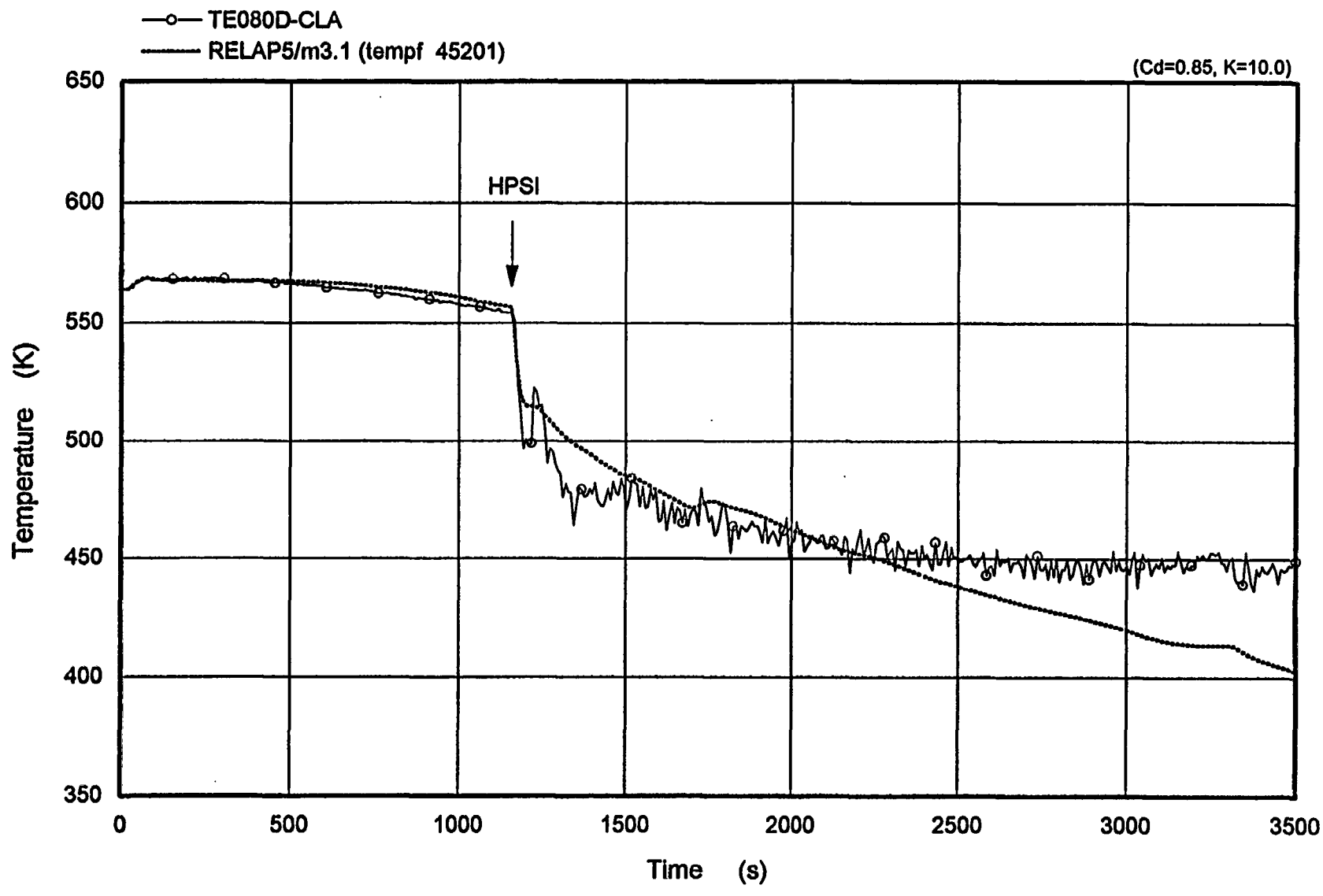

Figure 5.10 Coldleg Temperature of Intact Loop

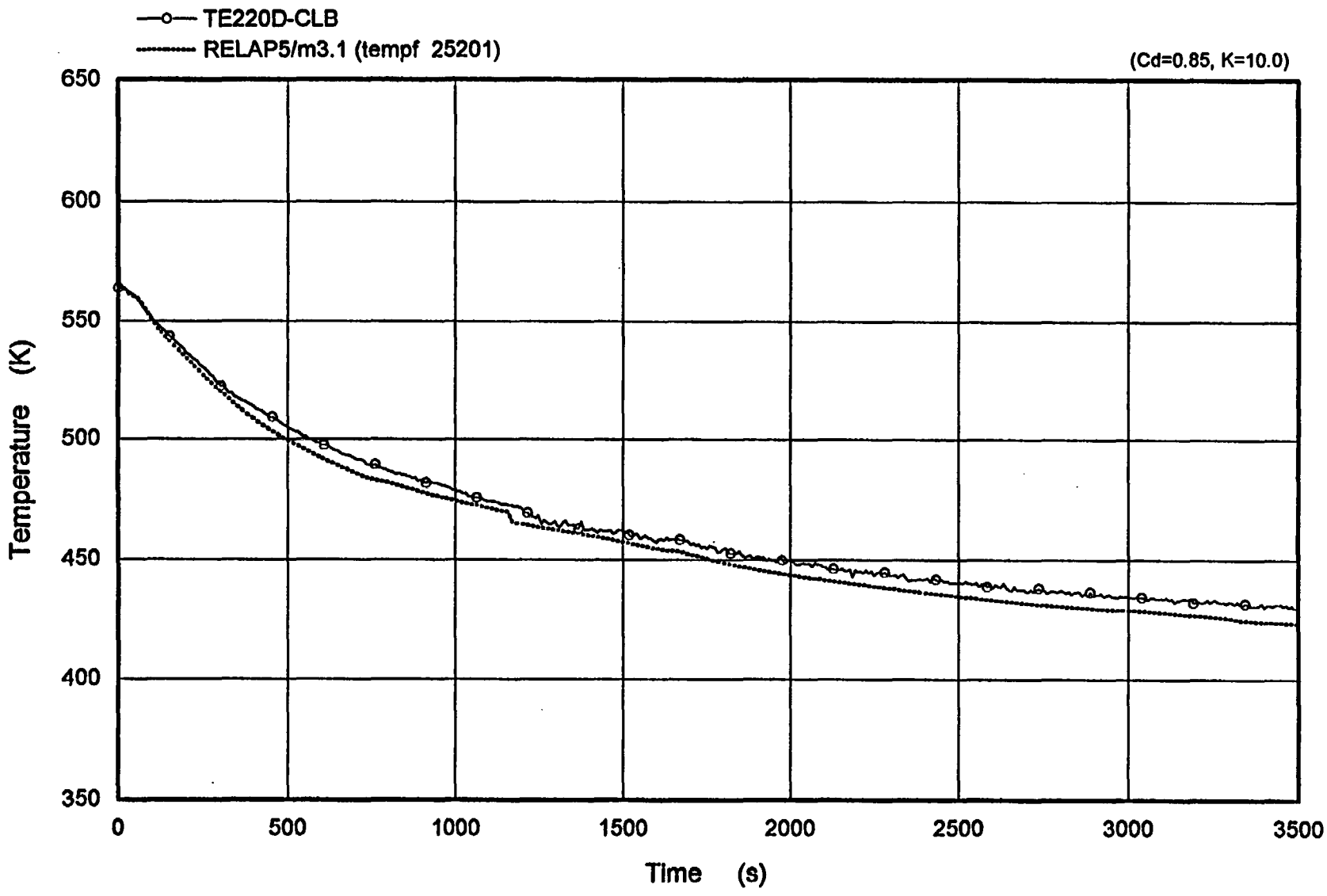

Figure 5.11 Coldleg Temperature of Broken Loop

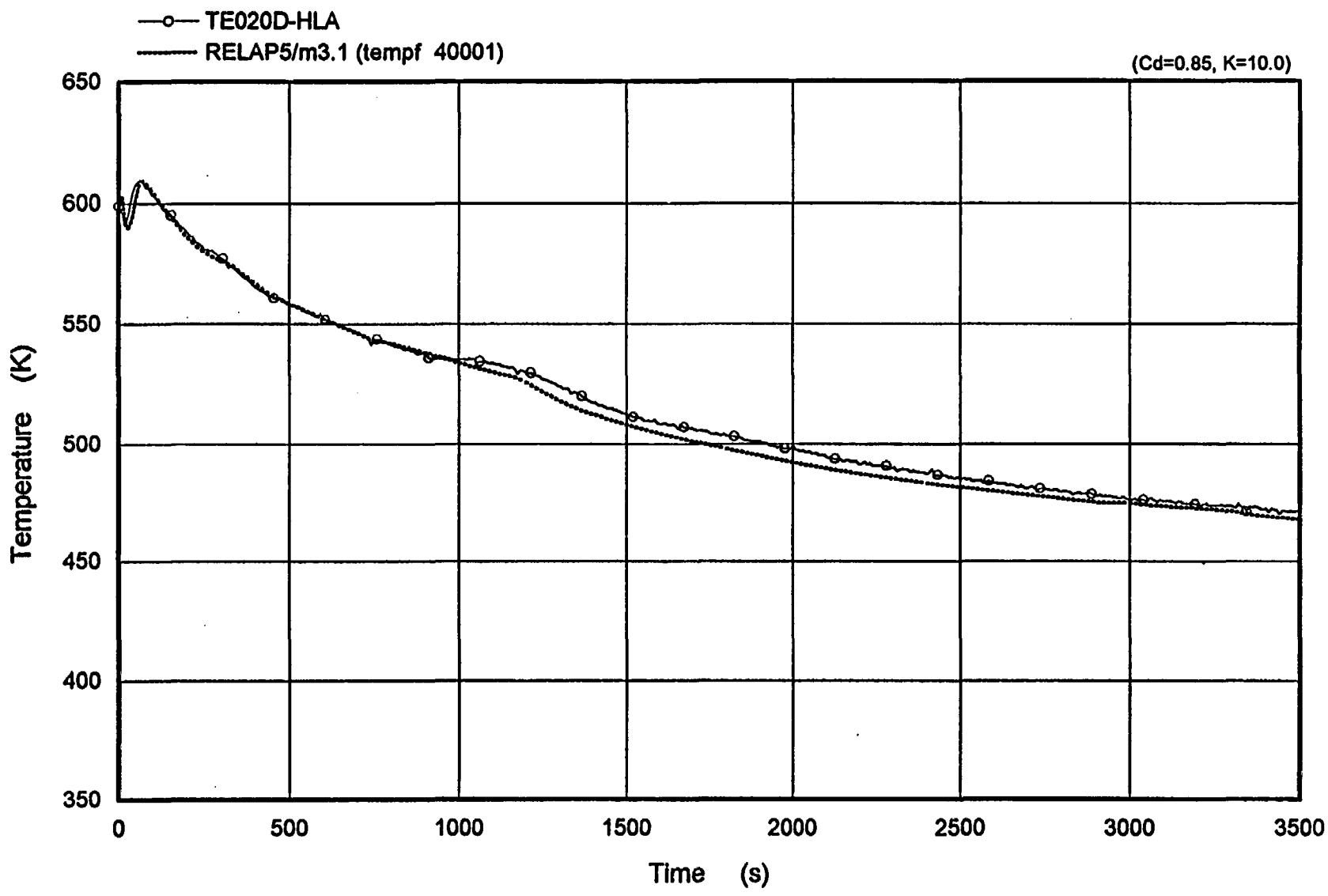

Figure 5.12 Hotleg Temperature of Intact Loop

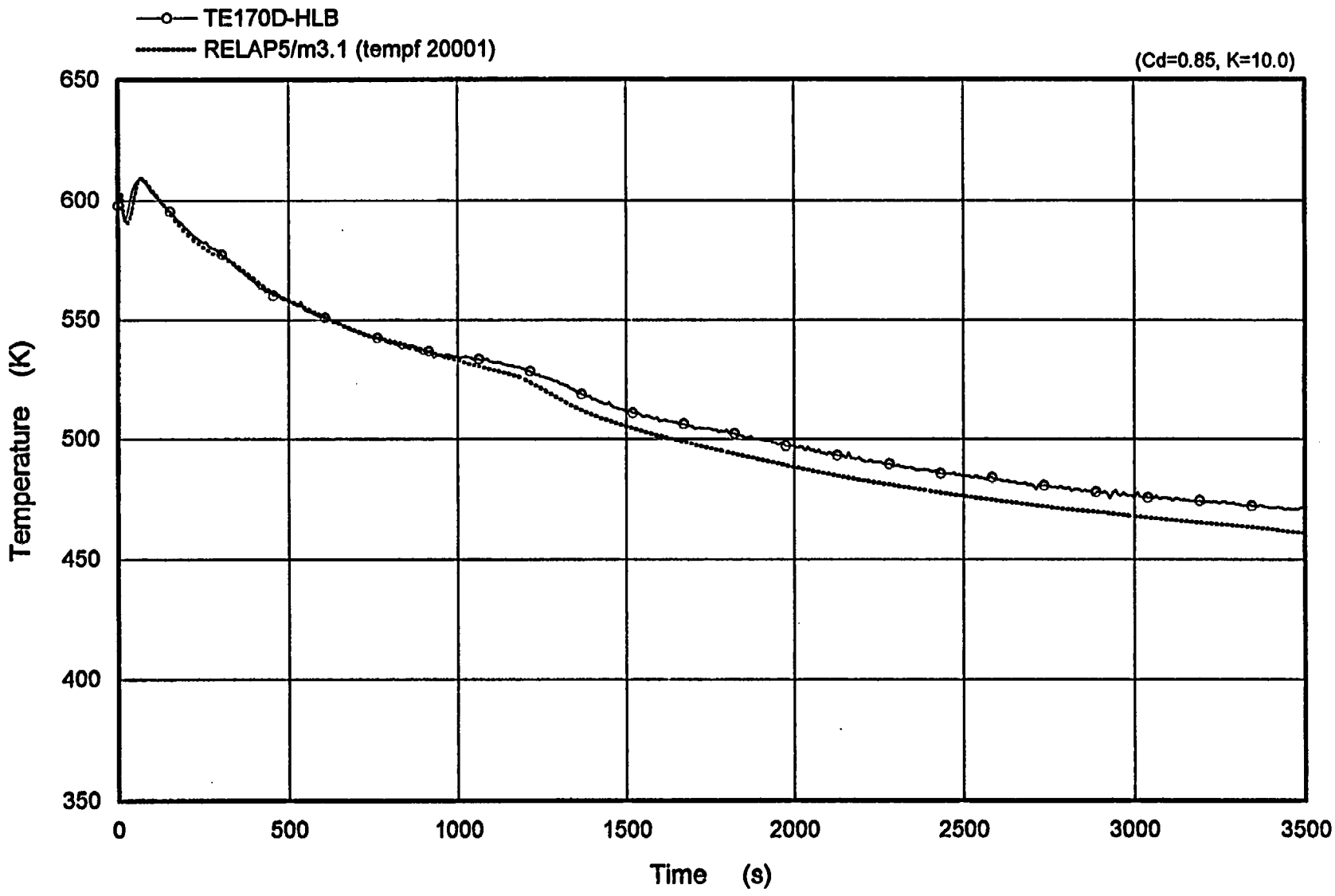

Figure 5.13 Hotleg Temperature of Broken Loop

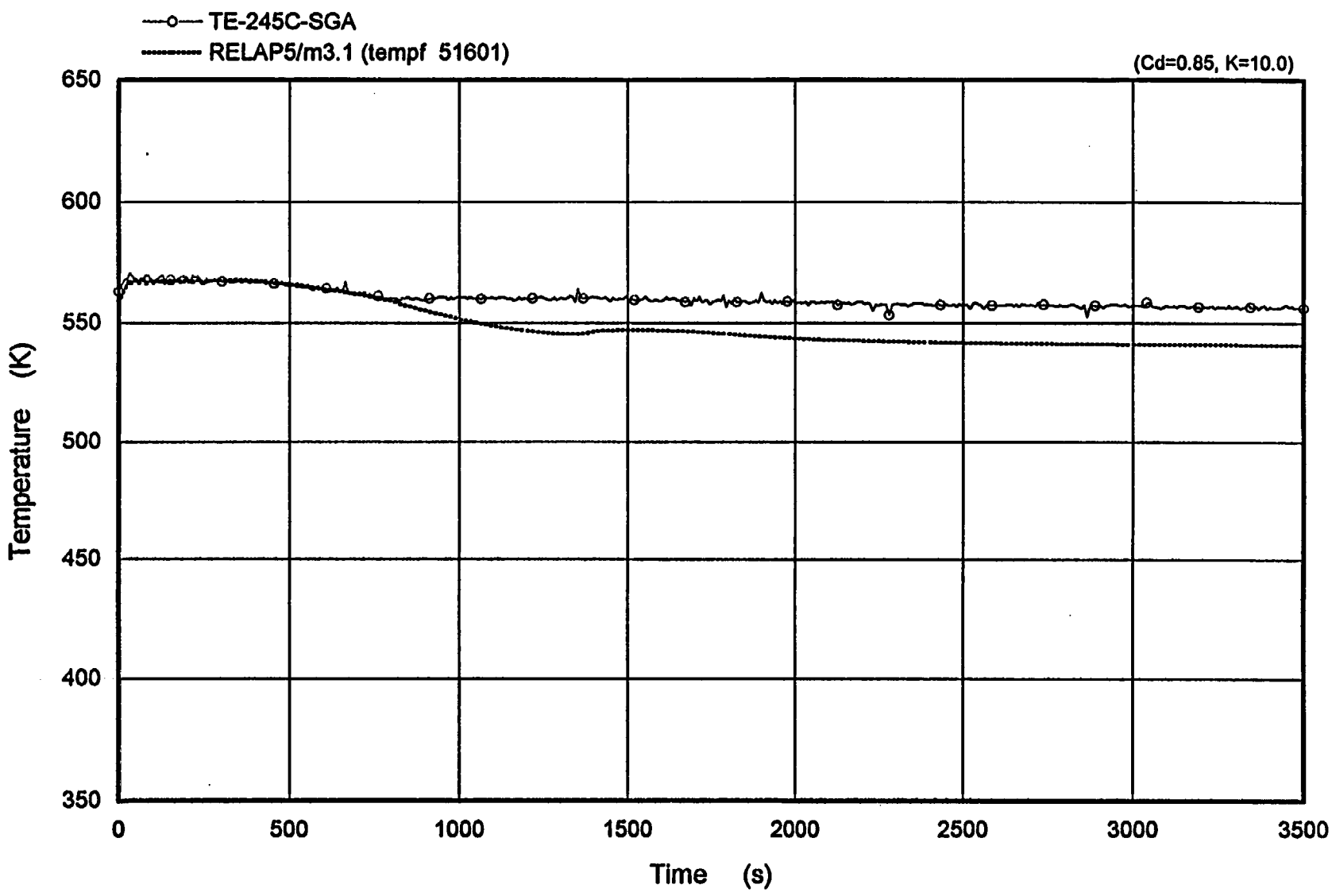

Figure 5.14 SG Steam Dome Temperature of Intact Loop

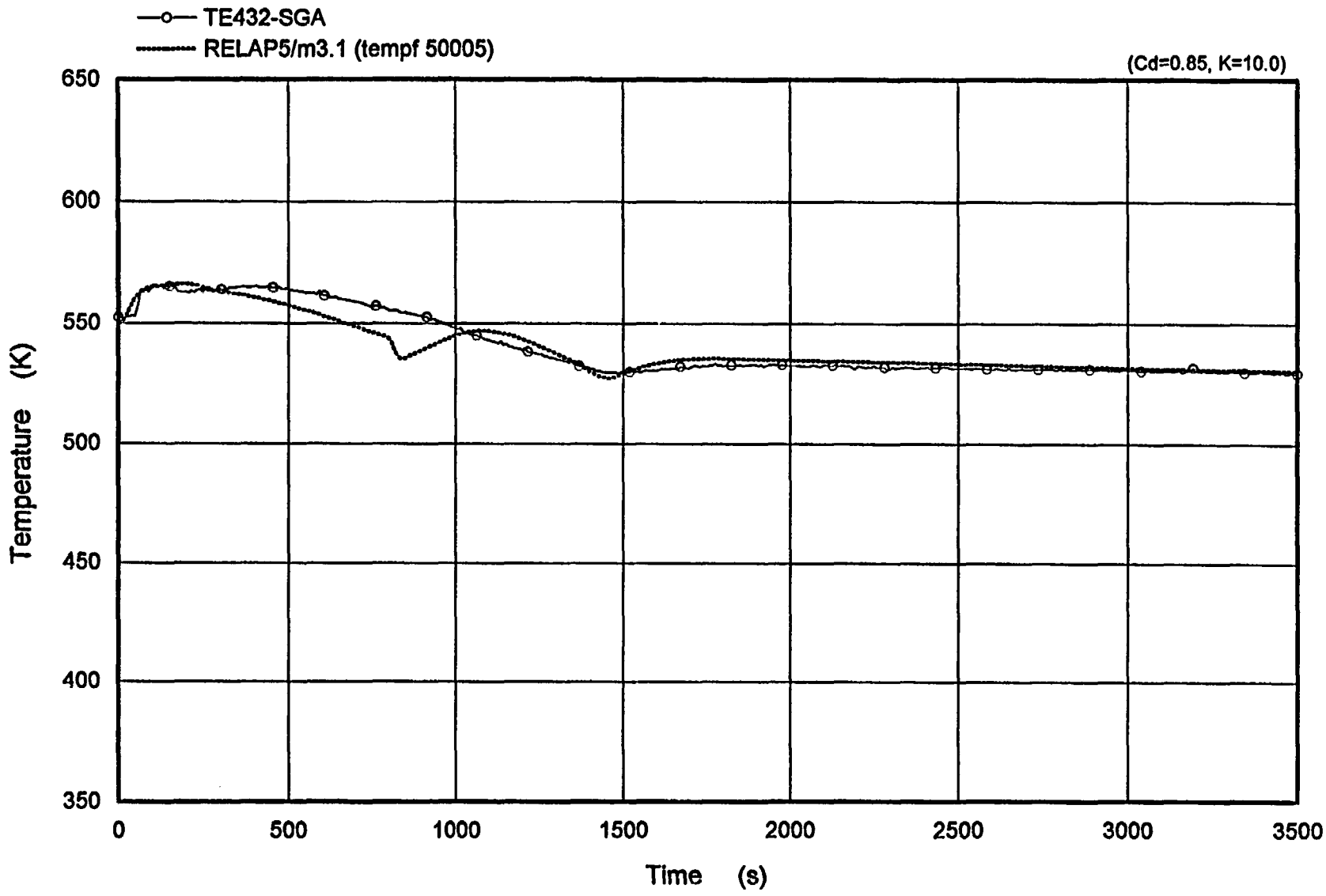

Figure 5.15 SG Downcomer Temperature of Intact Loop

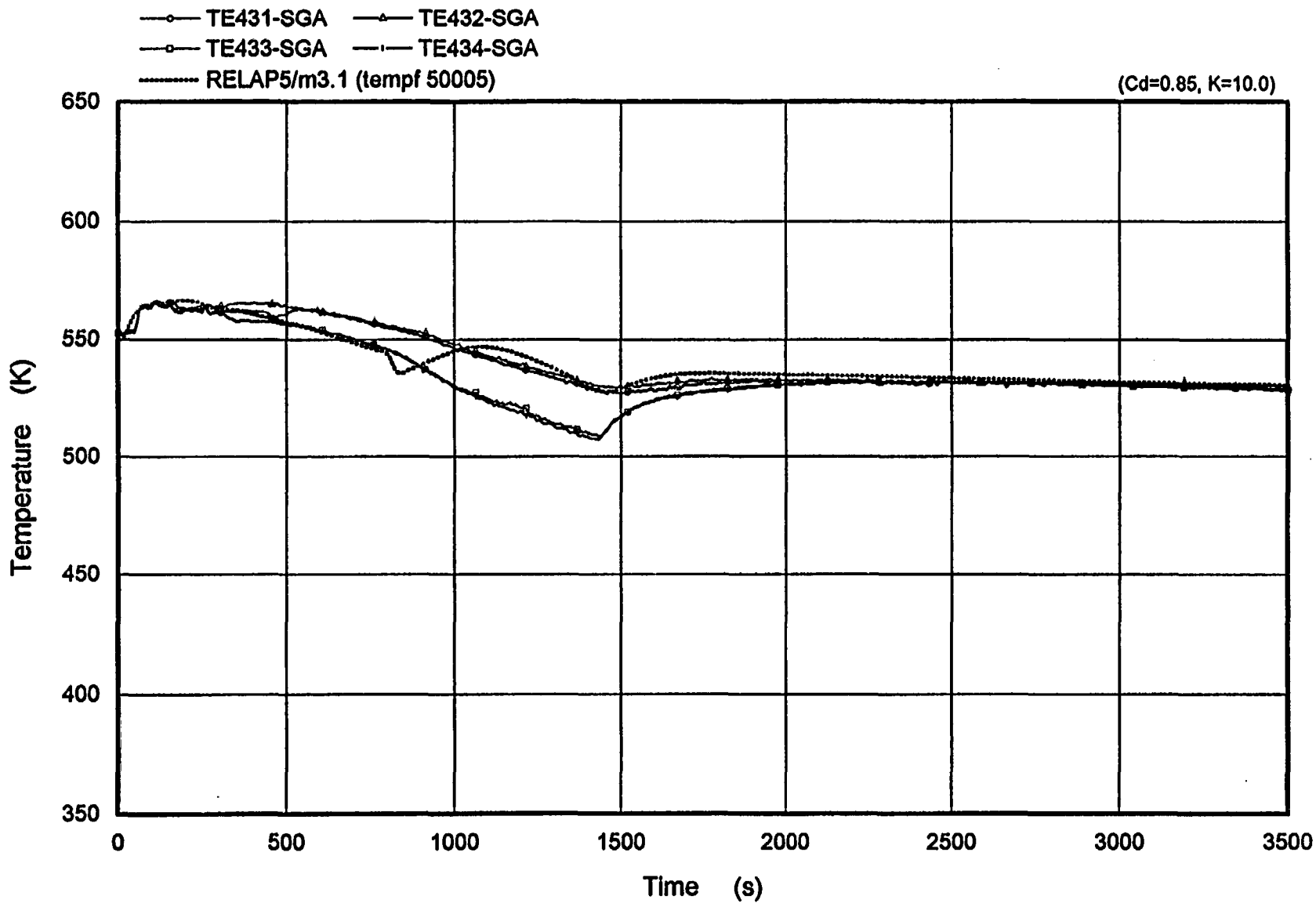

Figure 5.16 SG Downcomer Temperature of Intact Loop
(Downcomer is comprised of four loops)

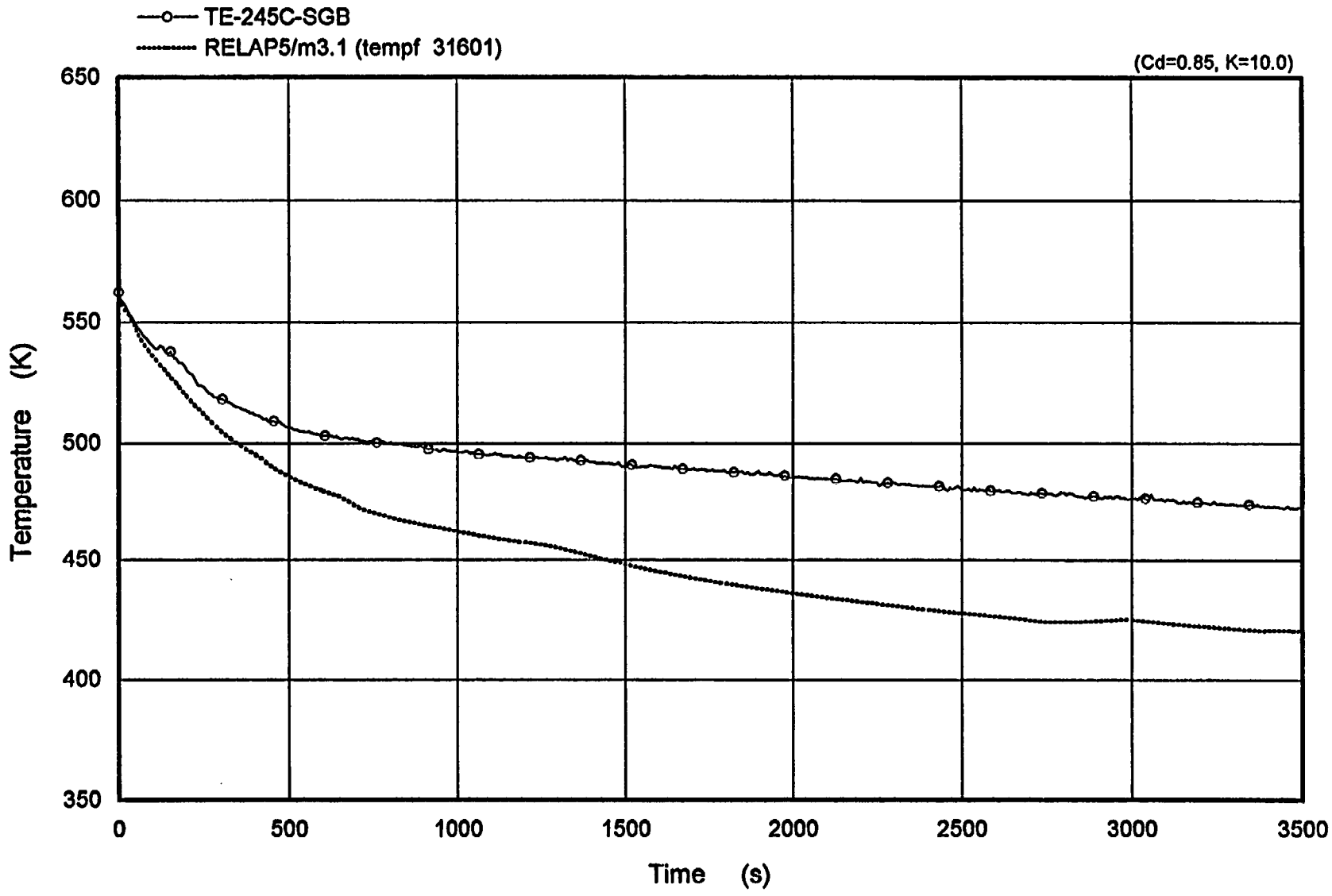

Figure 5.17 SG Dome Temperature of Broken Loop

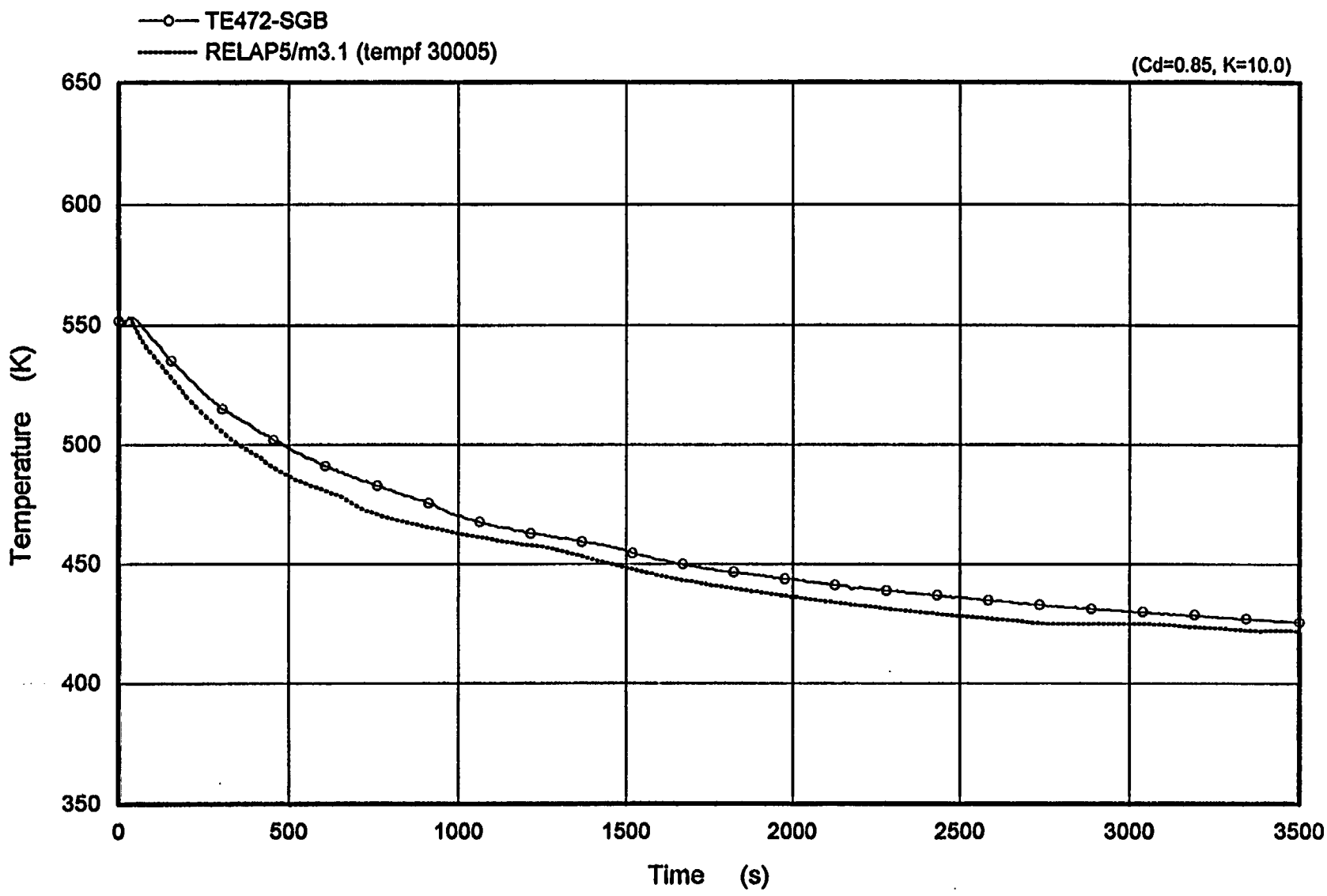

Figure 5.18 SG Downcomer Temperature of Broken Loop

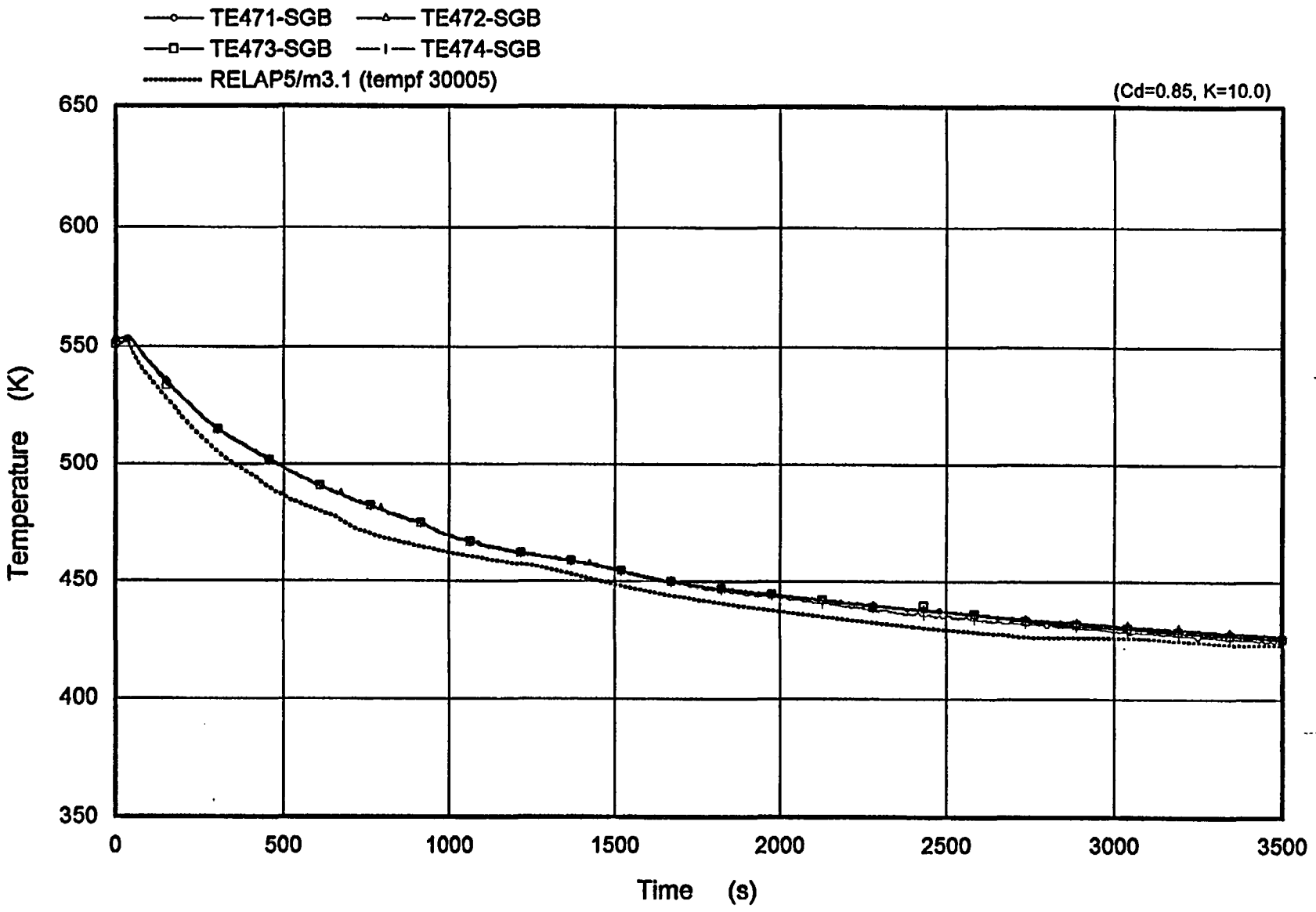

Figure 5.19 SG Downcomer Temperature of Broken Loop
(Downcomer is comprised of four loops)

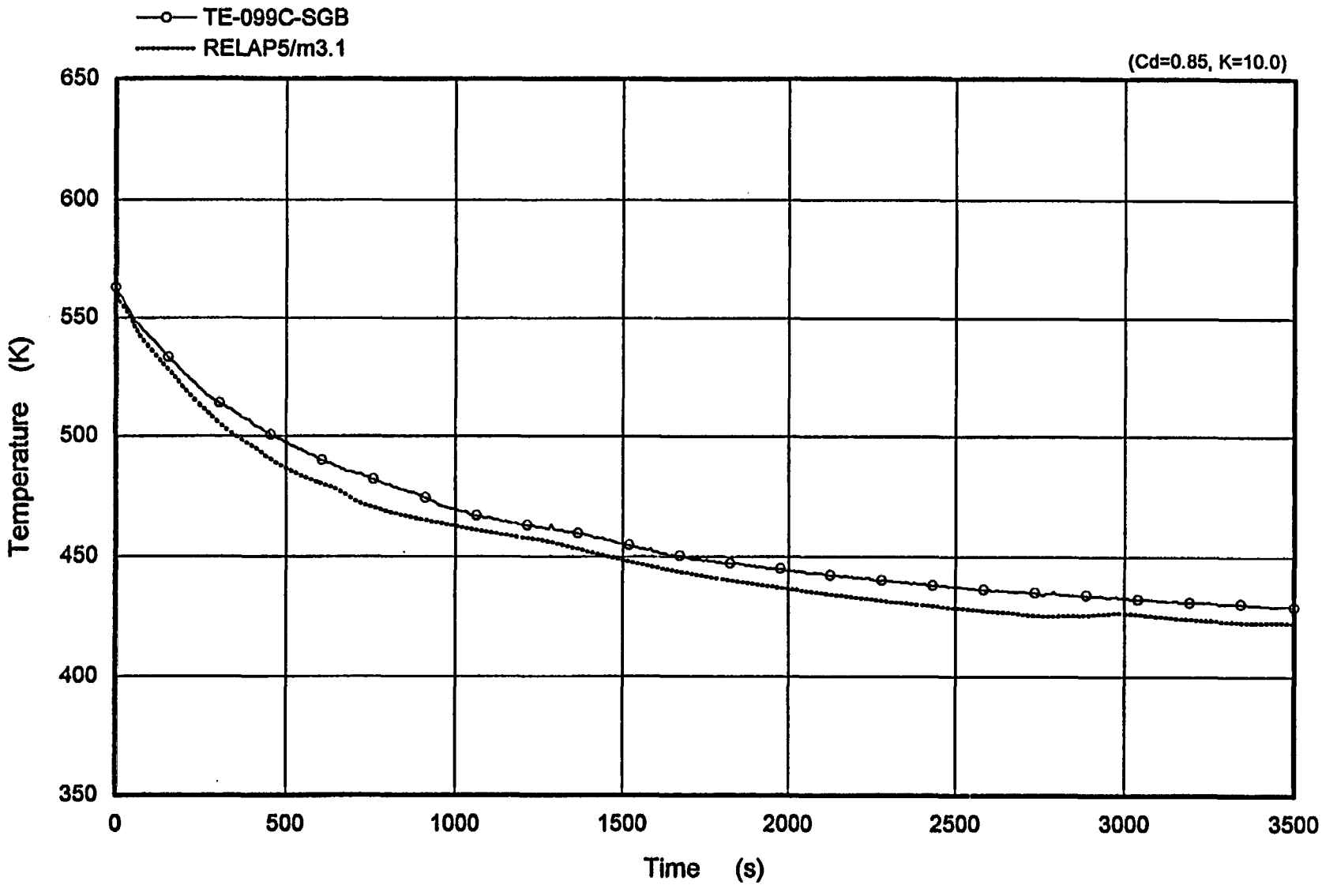

Figure 5.20 SG Boiler Bottom Temperature of Broken Loop

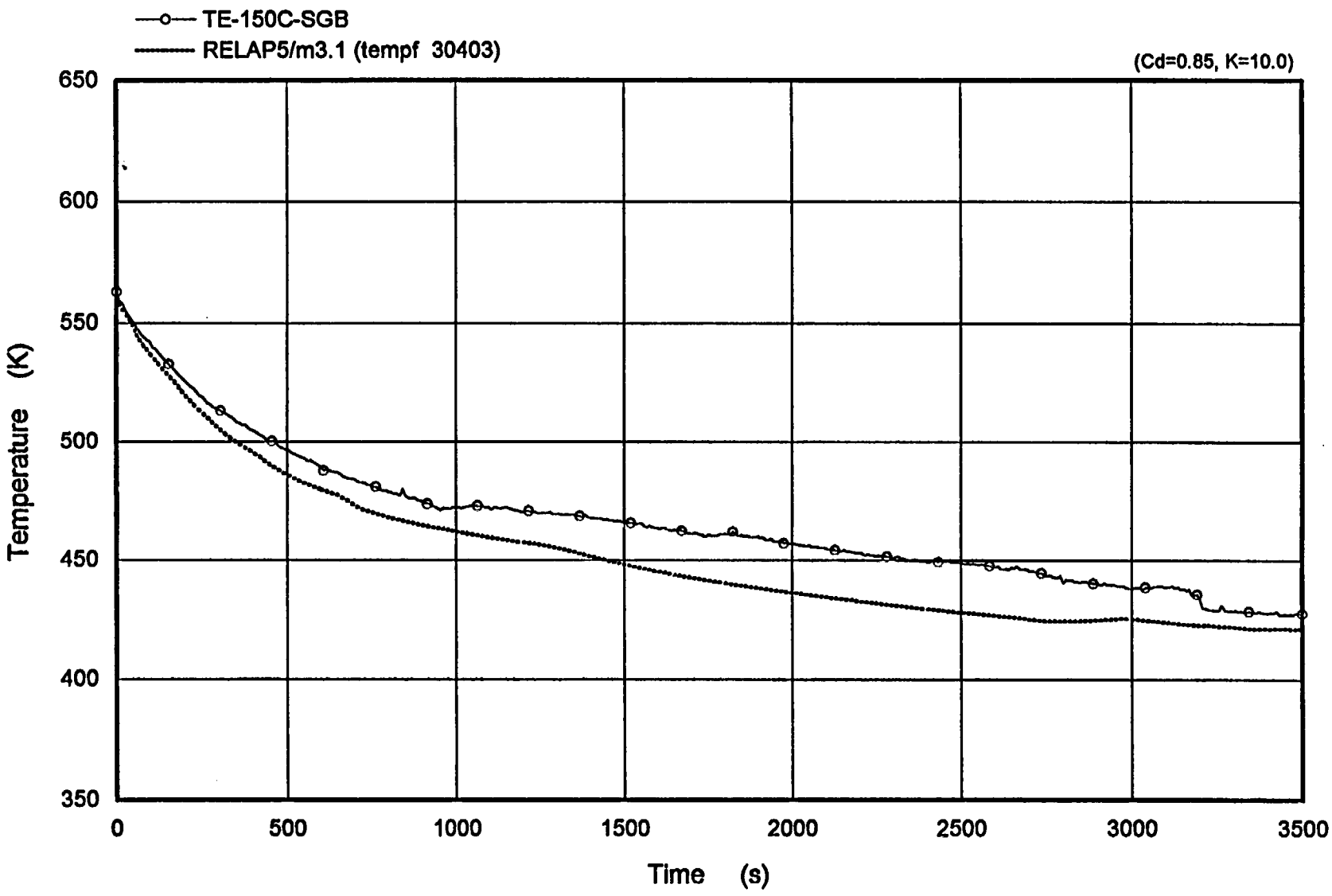

Figure 5.21 SG Boiler Middle Temperature of Broken Loop

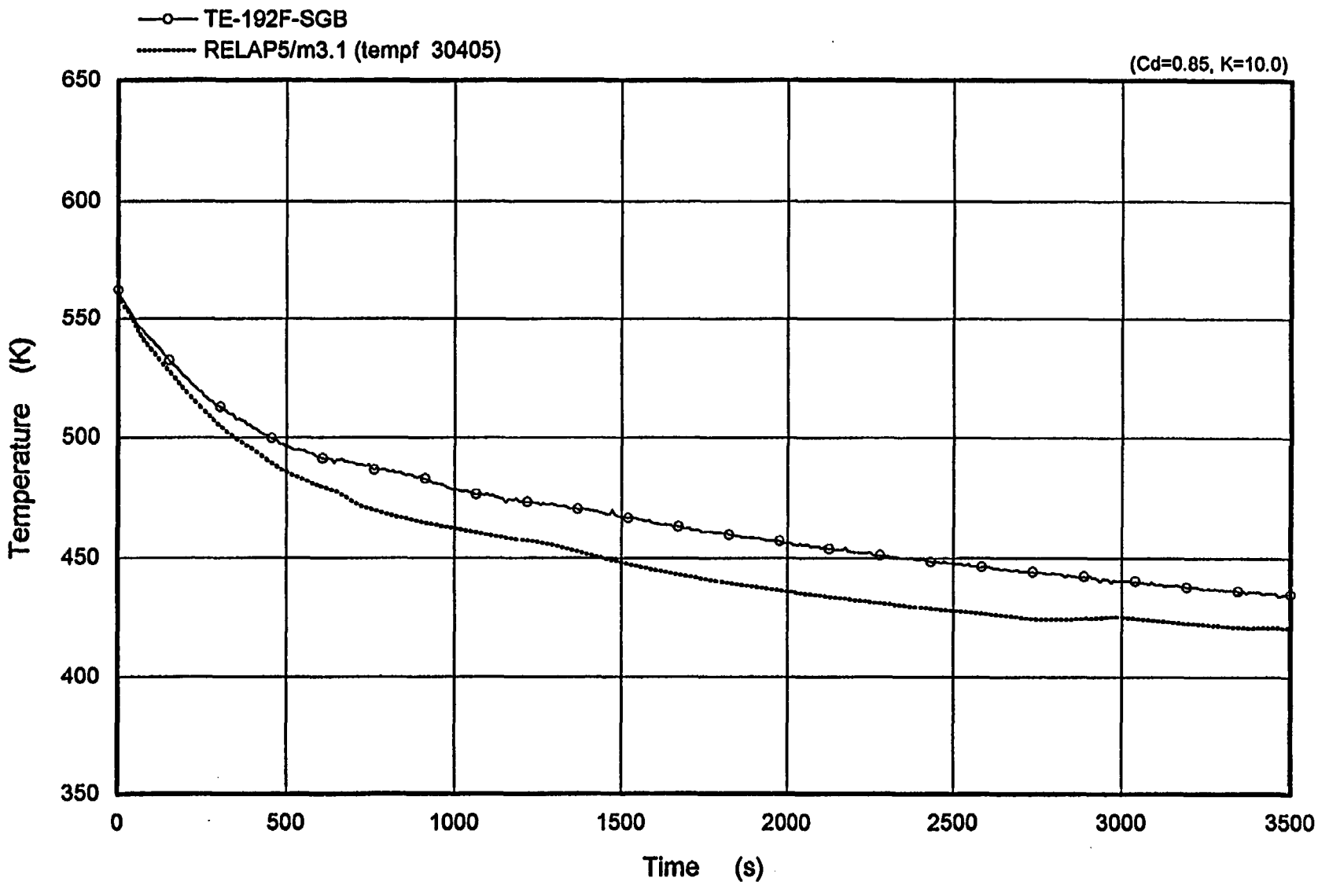

Figure 5.22 SG Boiler Top Temperature of Broken Loop

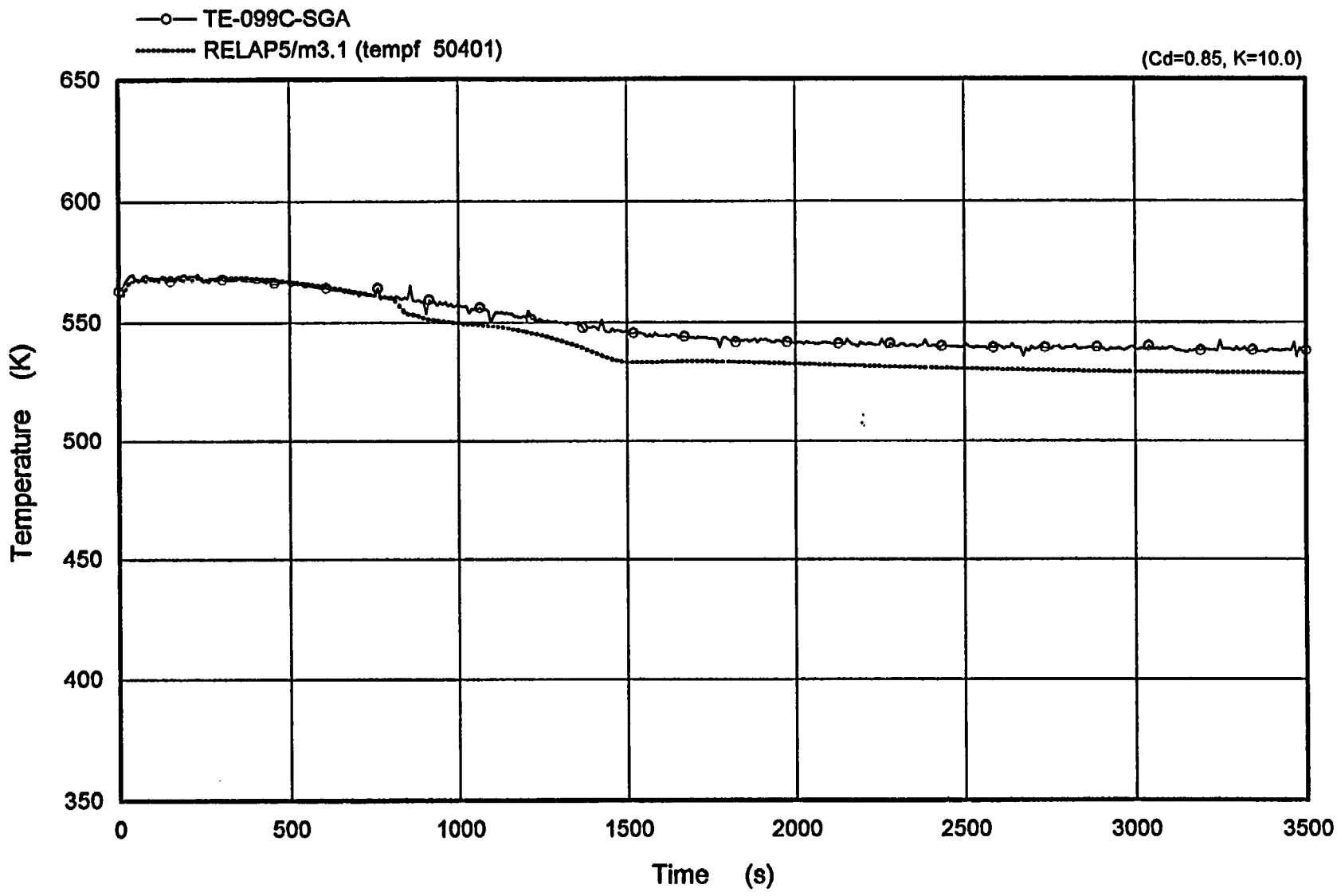

Figure 5.23 SG Boiler Bottom Temperature of Intact Loop

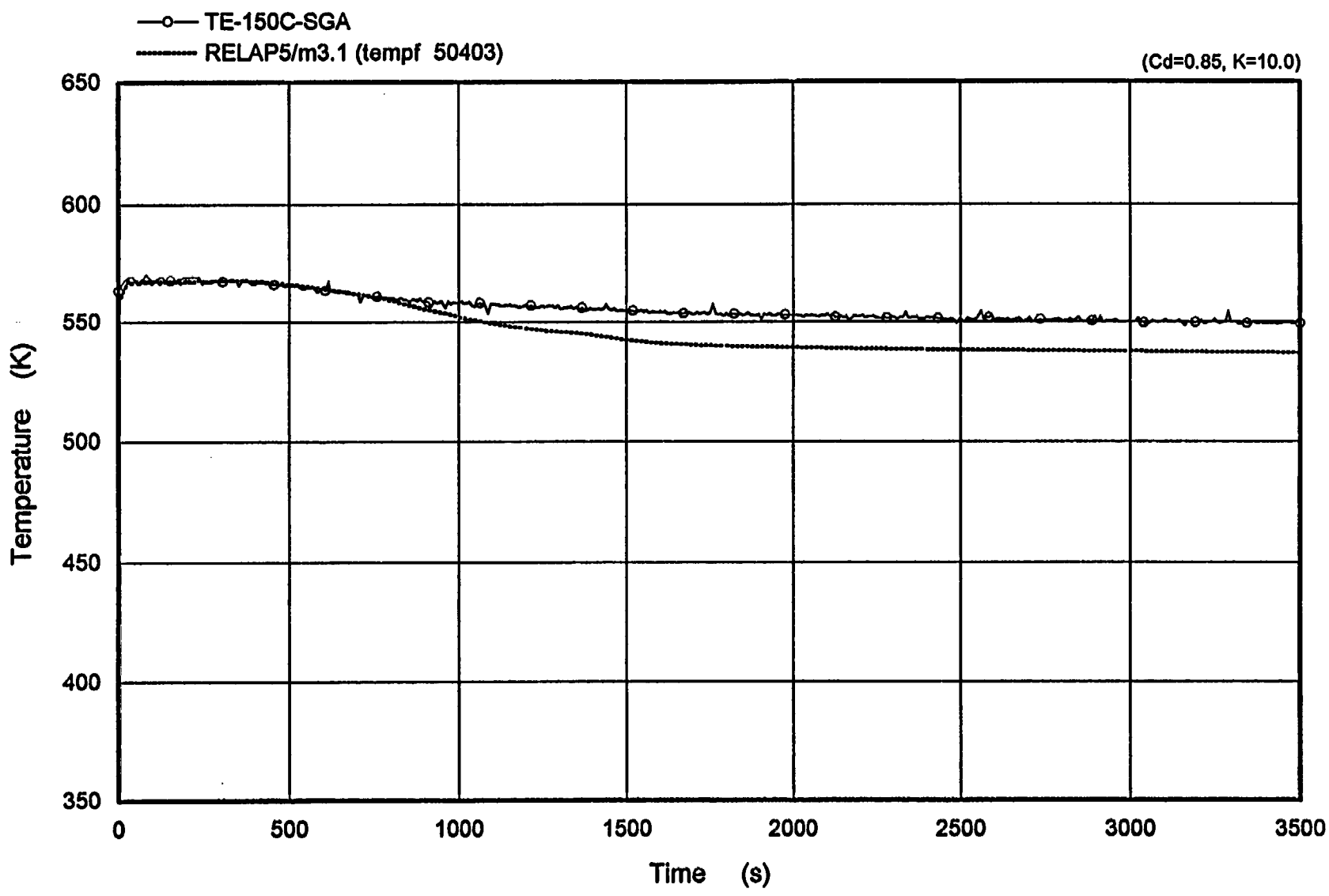

Figure 5.24 SG Boiler Middle Temperature of Intact Loop

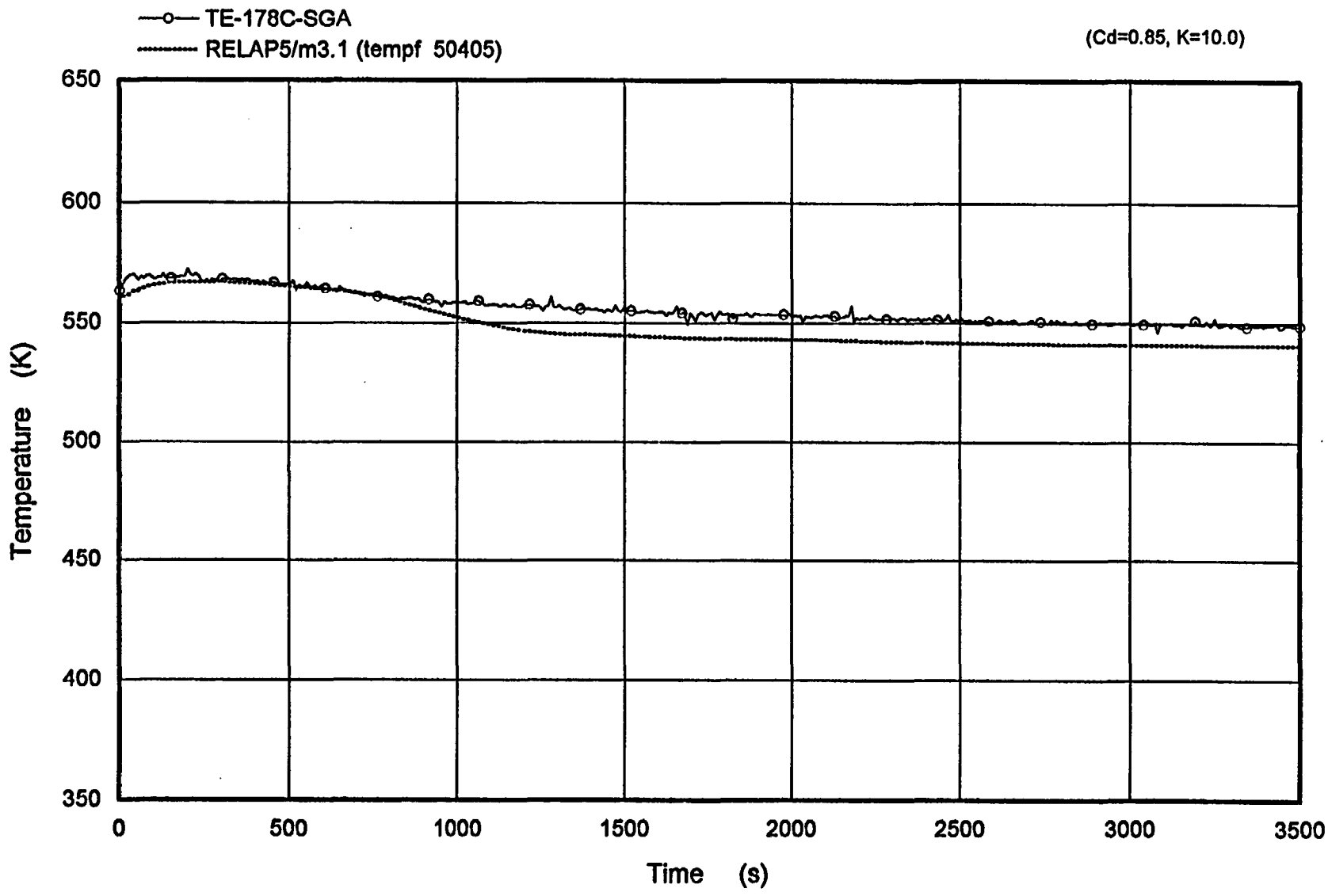

Figure 5.25 SG Boiler Top Temperature of Intact Loop

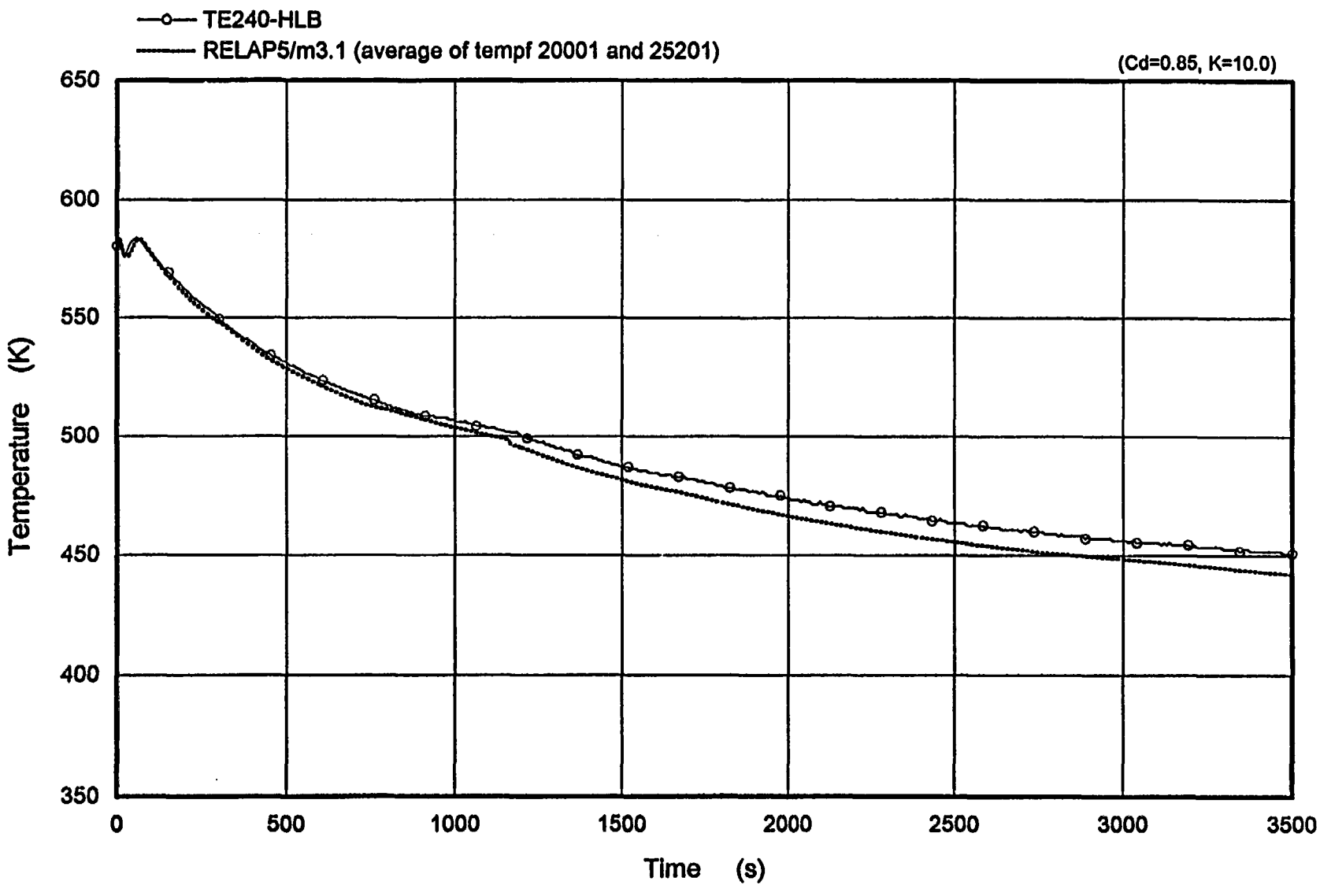

Figure 5.26 Average Temperature of RCS Broken Loop

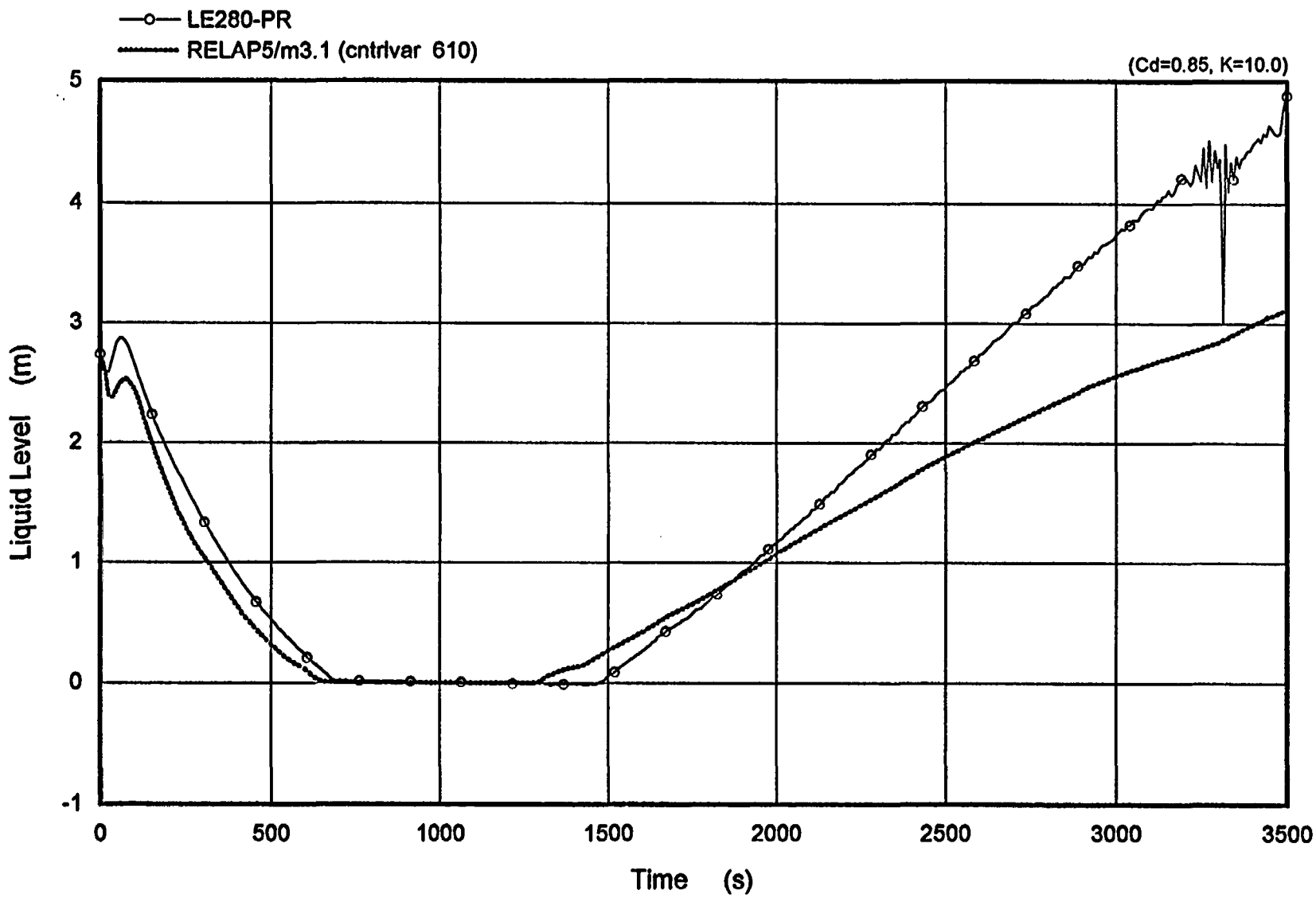

Figure 5.27 Collapsed Liquid Level of Pressurizer

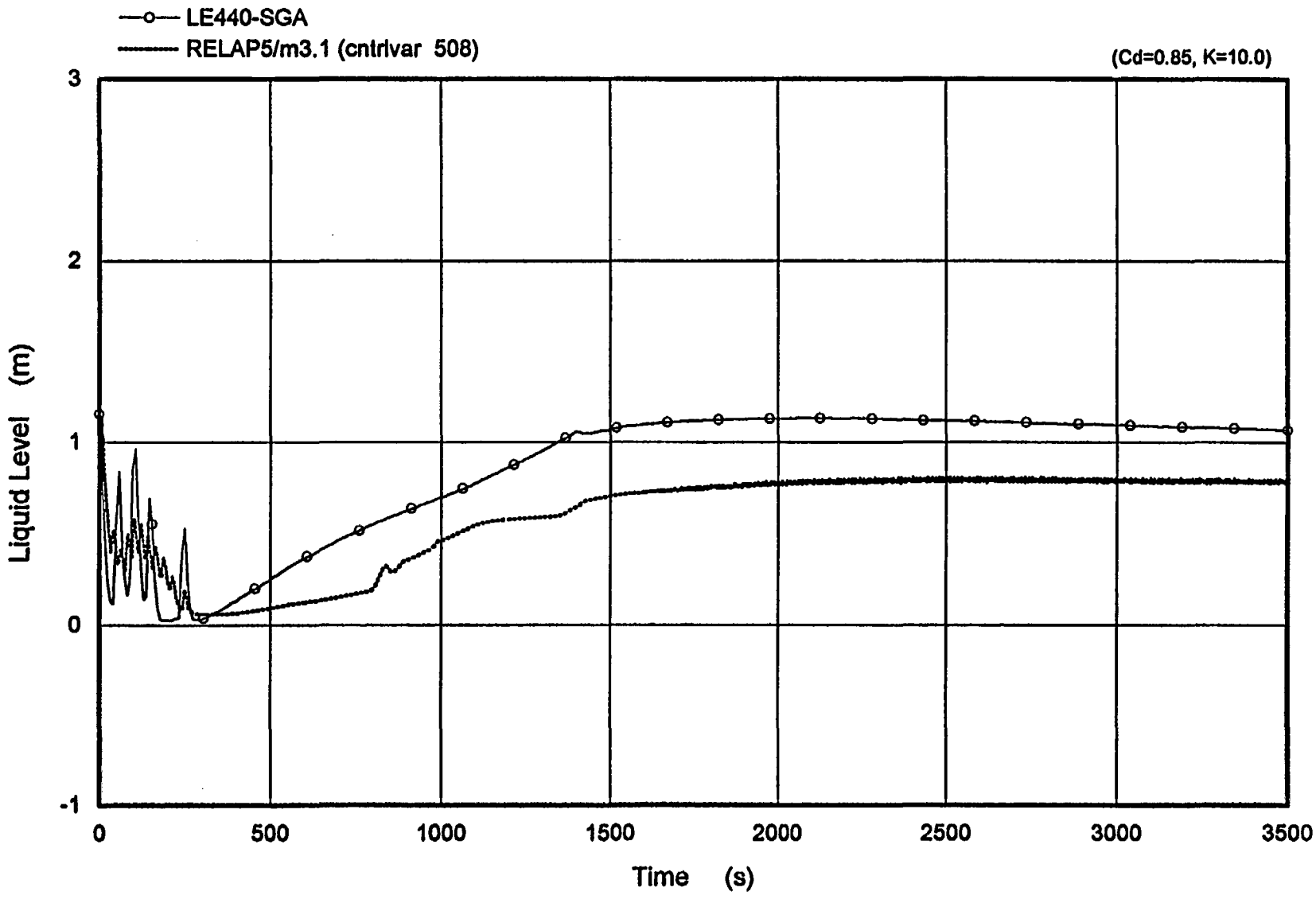

Figure 5.28 Narrow Range of SG Level of Intact Loop

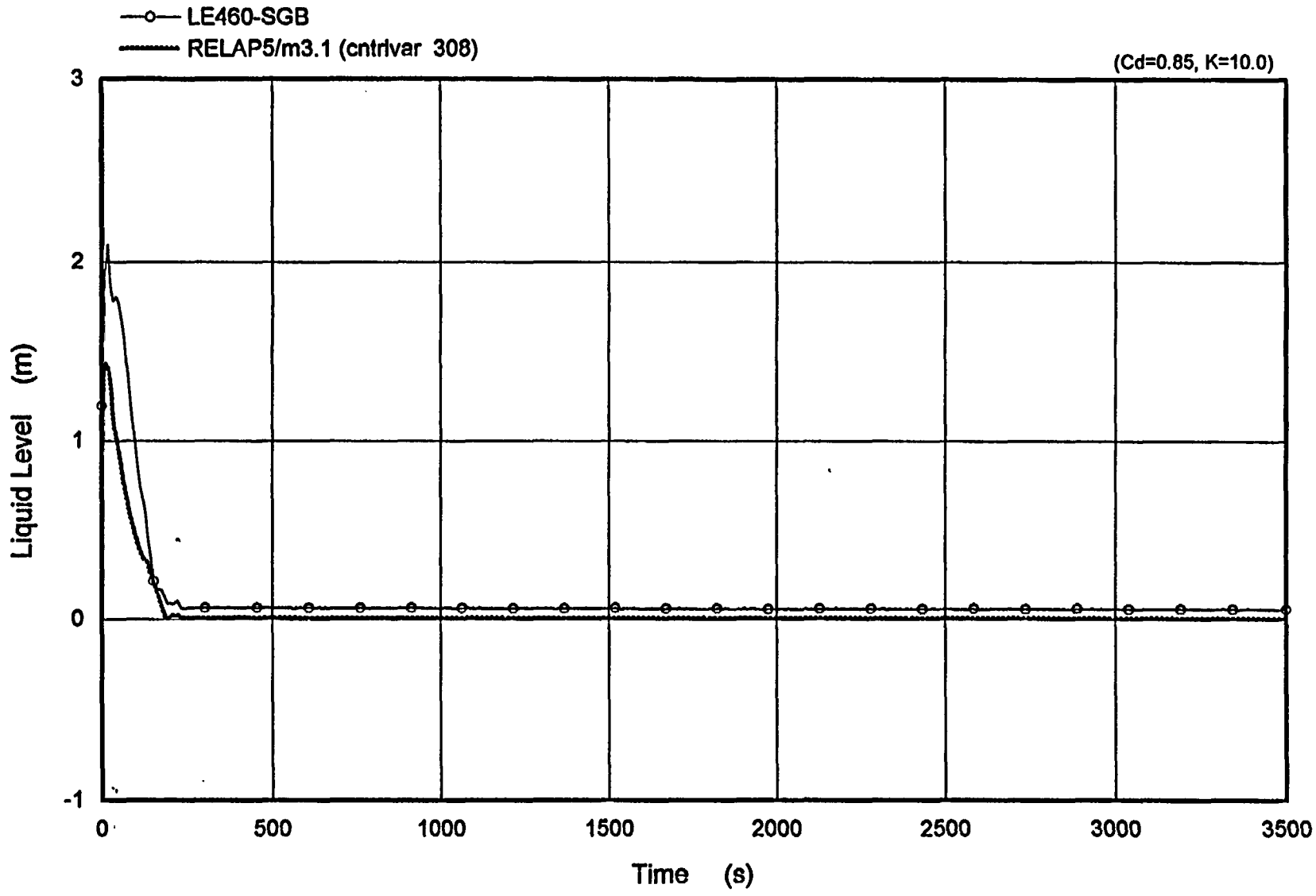

Figure 5.29 Narrow Range of SG Level of Broken Loop

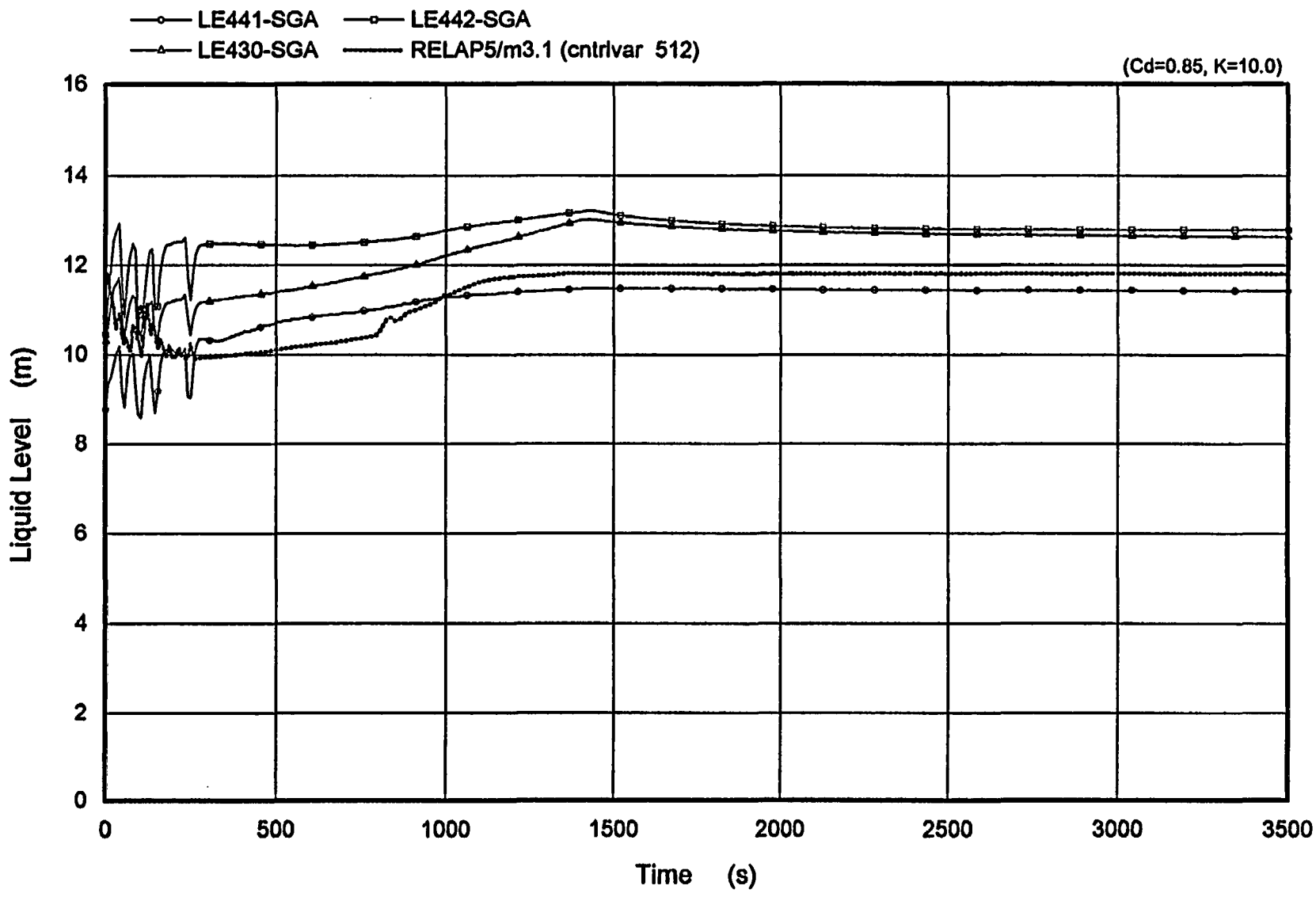

Figure 5.30 Liquid Level of SG Intact Loop

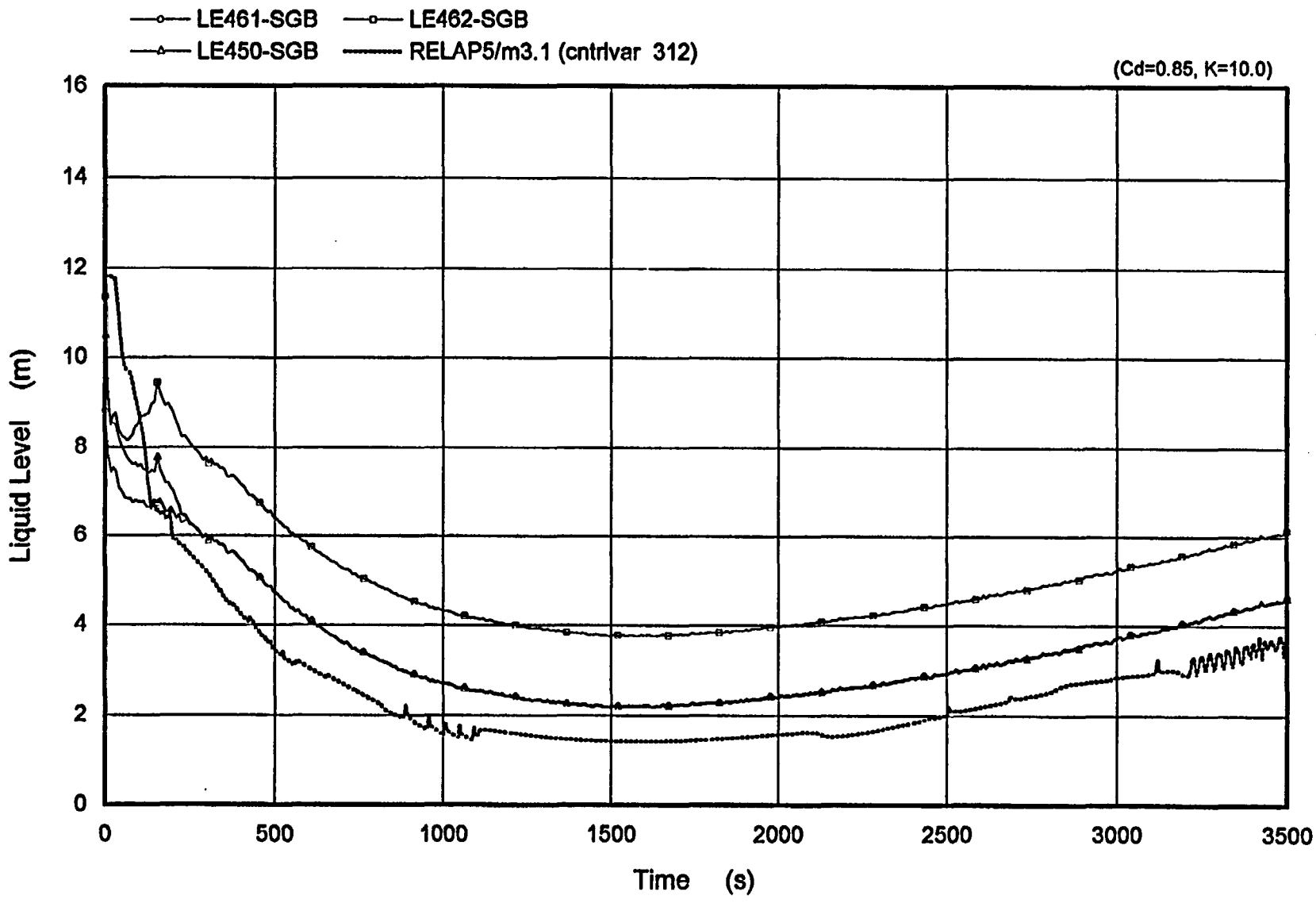

Figure 5.31 Liquid Level of SG Broken Loop

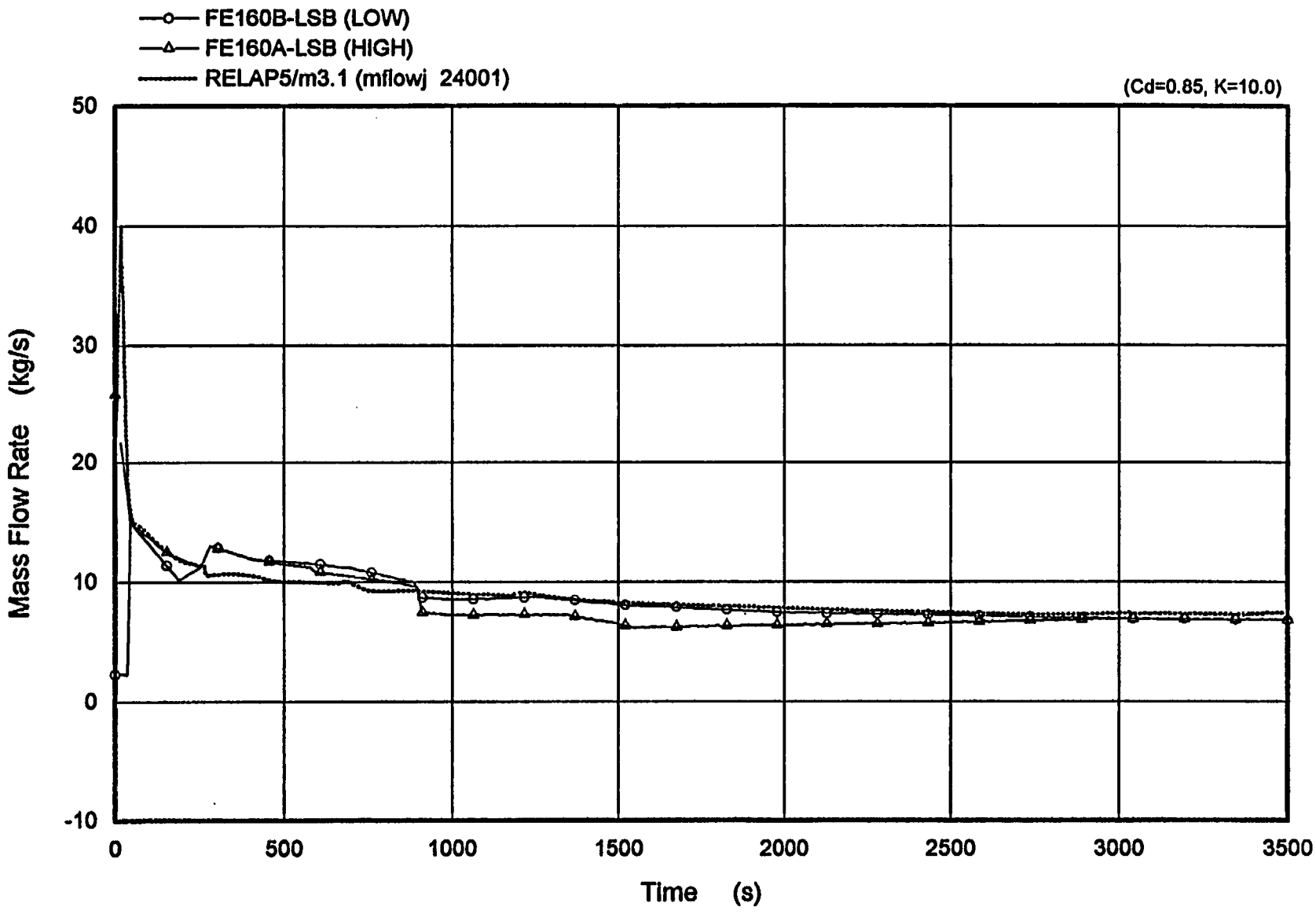

Figure 5.32 Pump Suction Flow Rate of Broken Loop

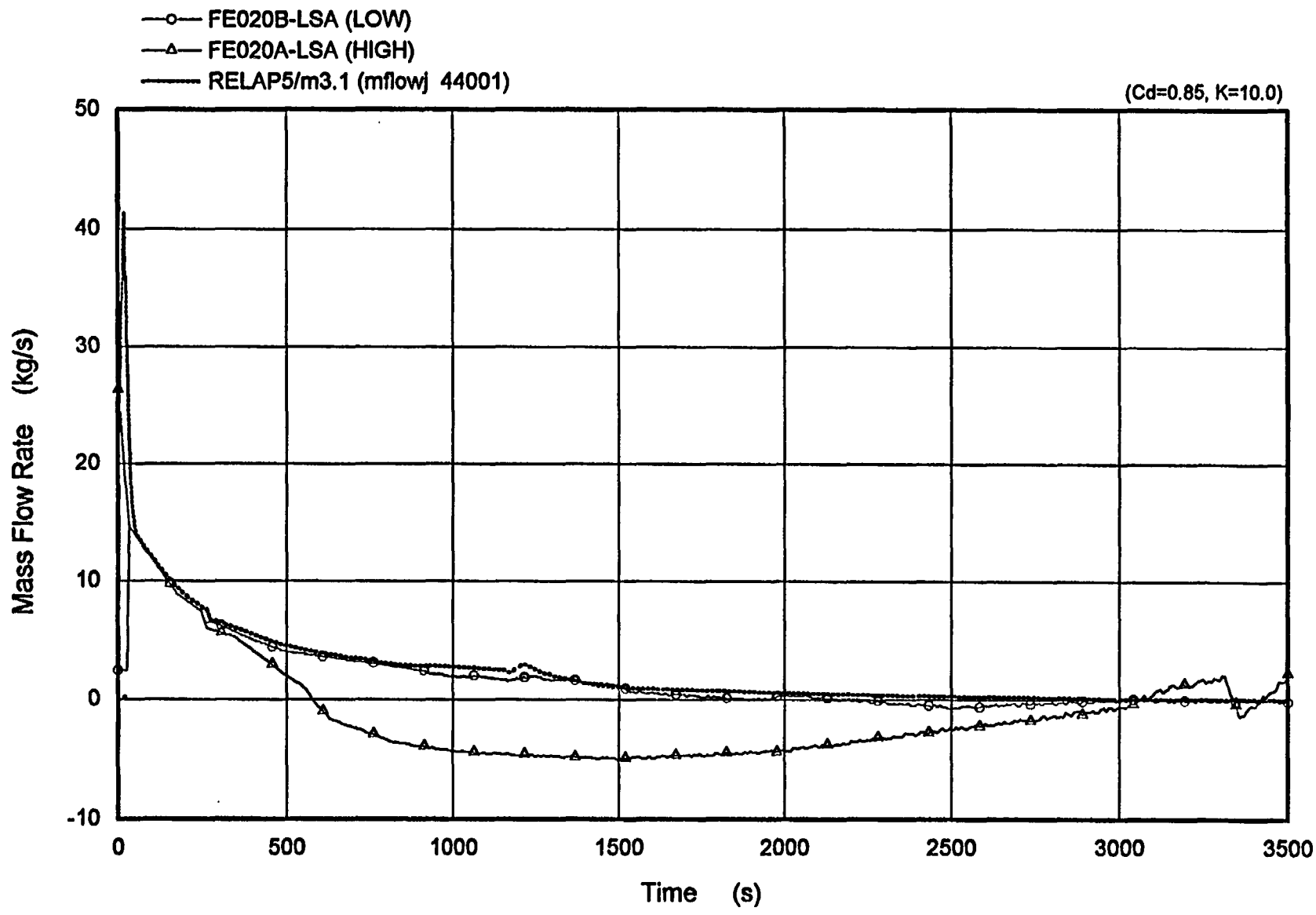

Figure 5.33 Pump Suction Flow Rate of Intact Loop

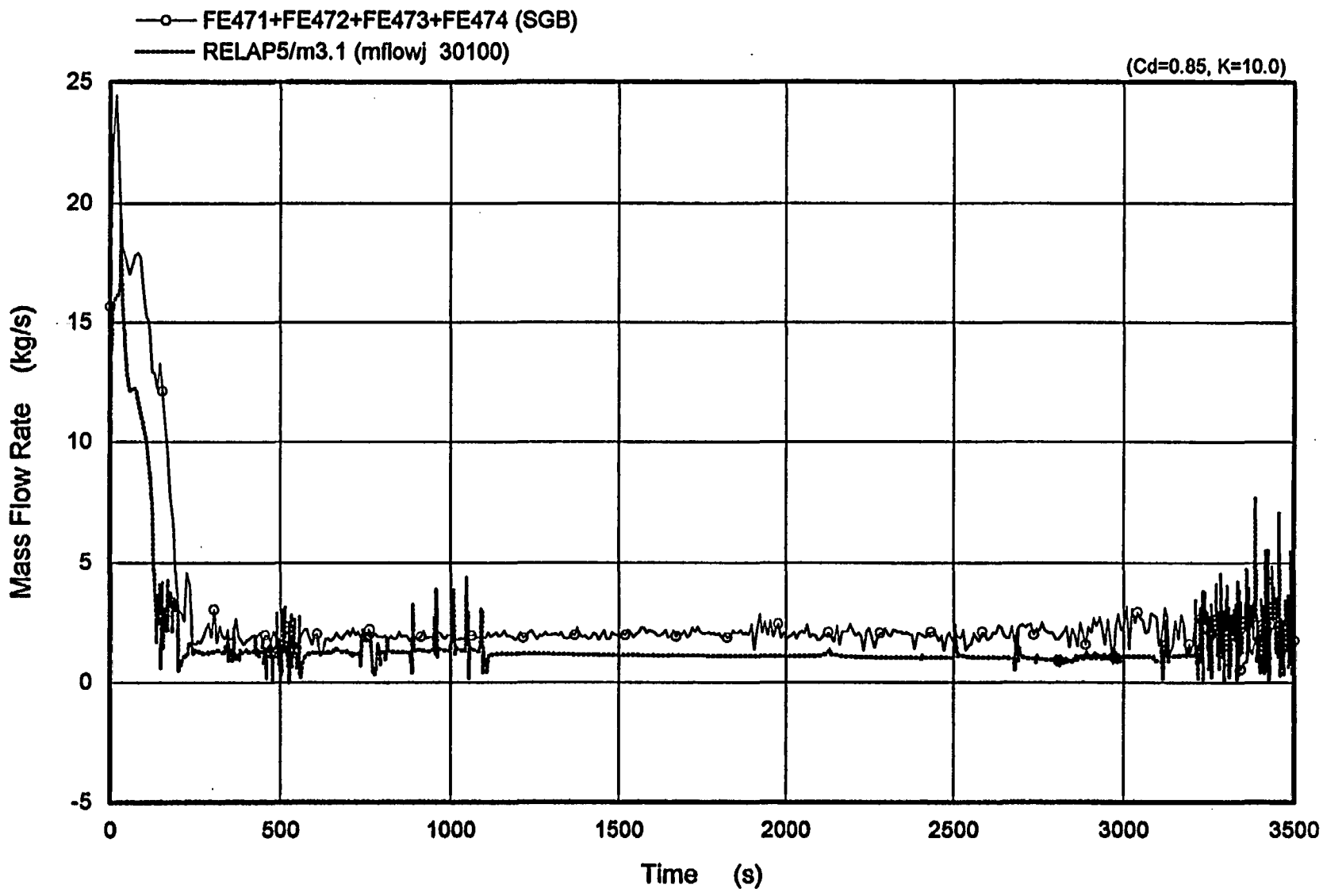

Figure 5.34 Downcomer Flow Rate of Broken Loop

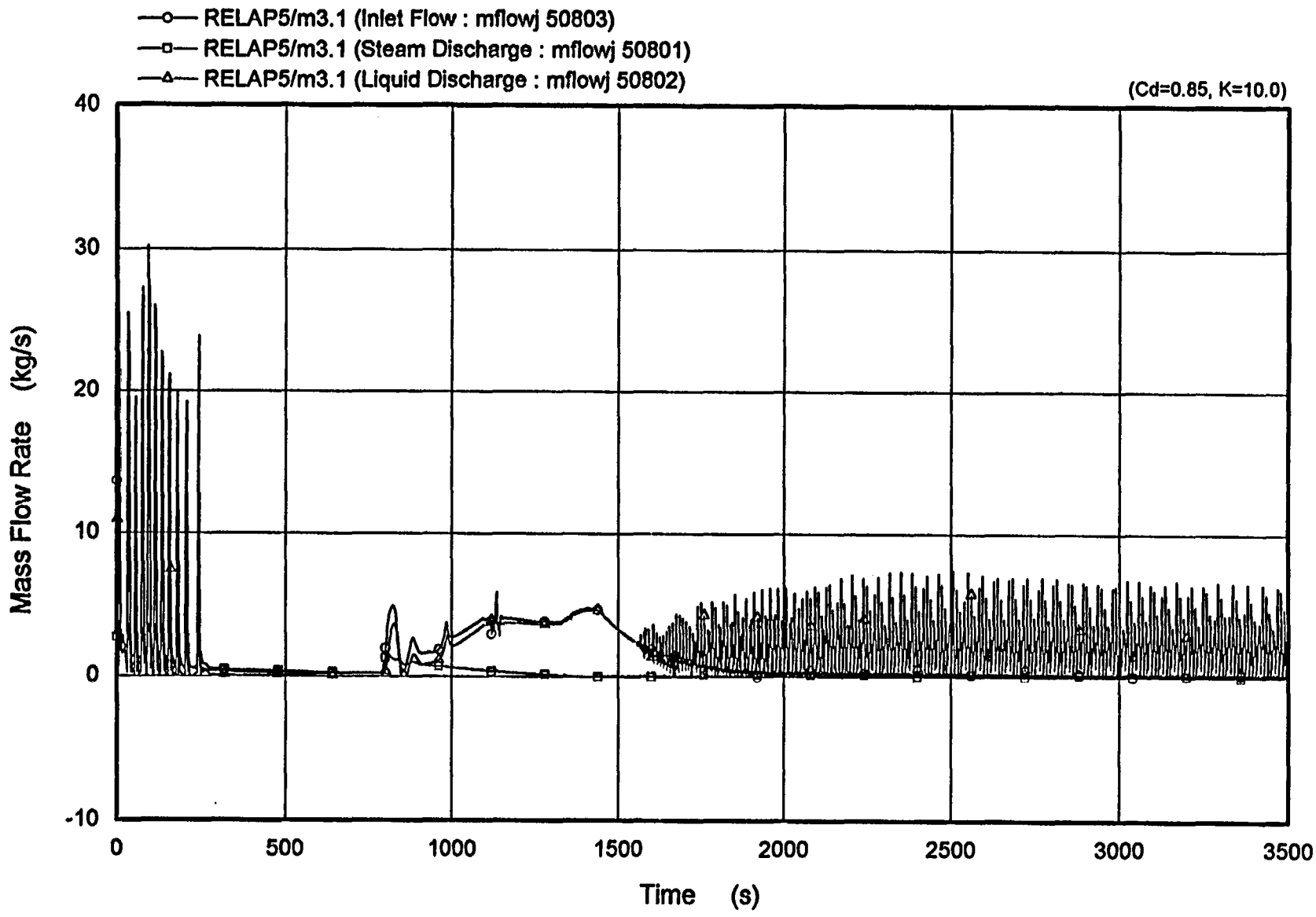

Figure 5.35 Separator Flow Rate of Intact Loop

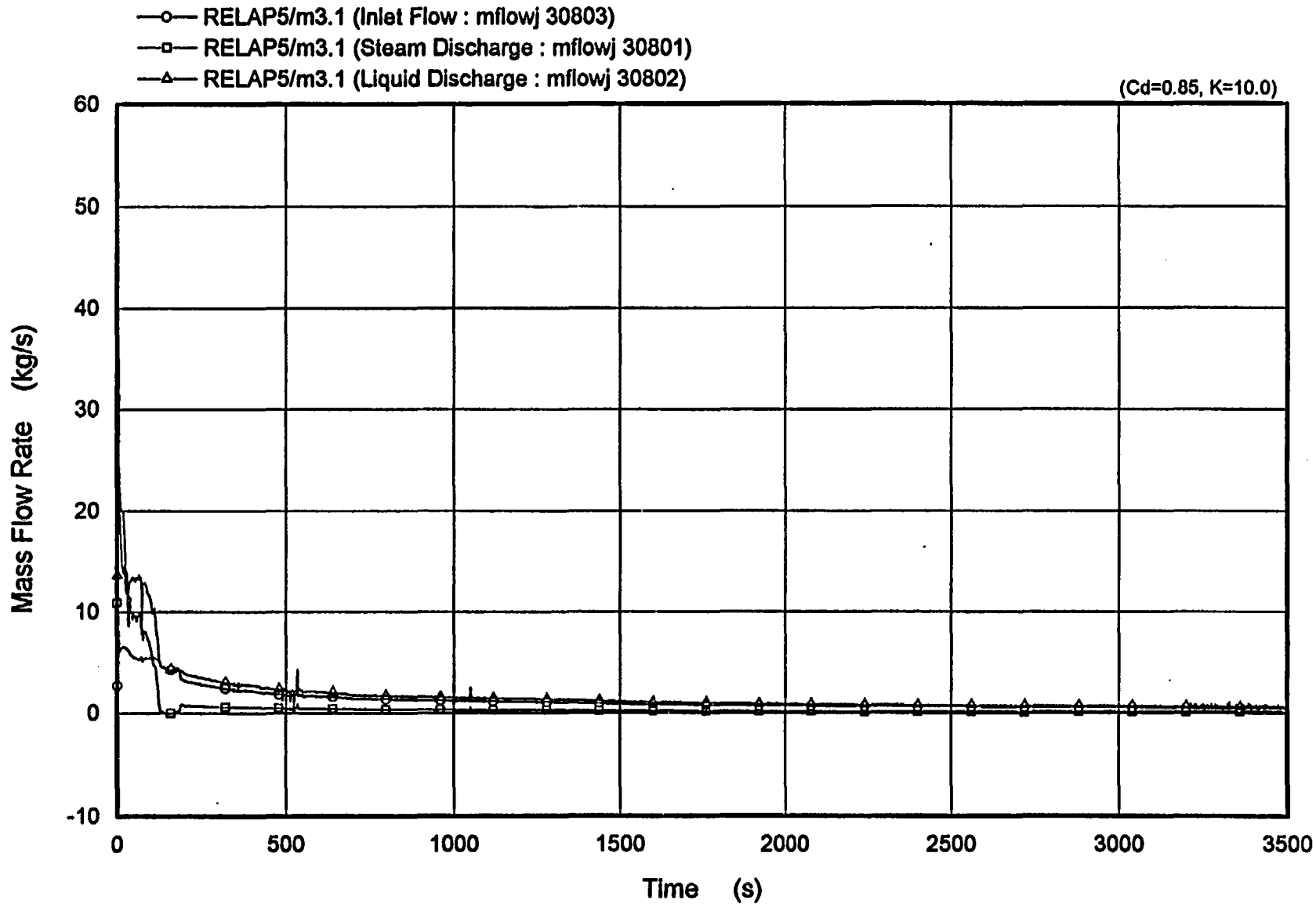

Figure 5.36 Separator Flow Rate of Broken Loop

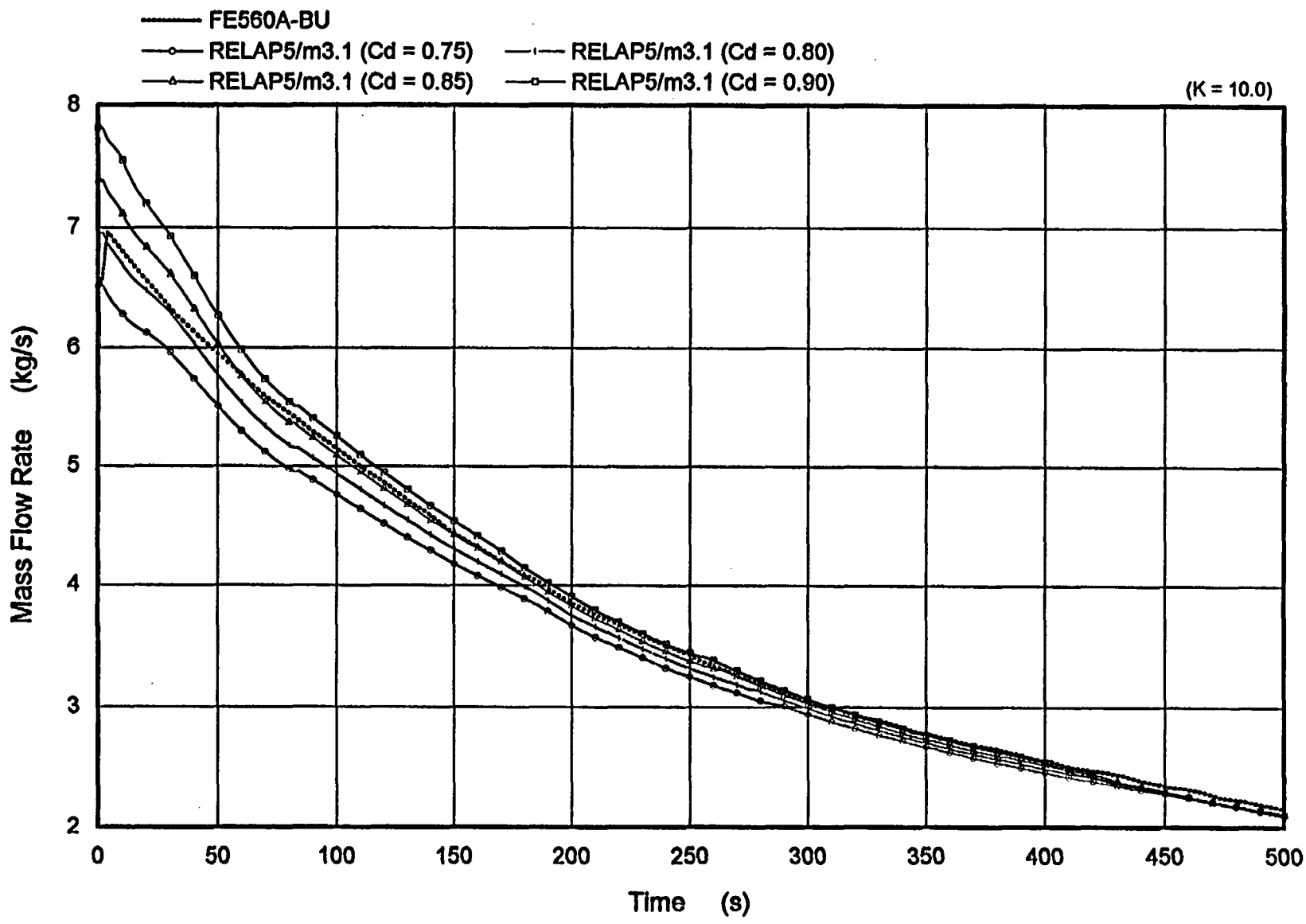

Figure 7.1 Comparison of Break Flow Rate (Cd Value Sensitivity)

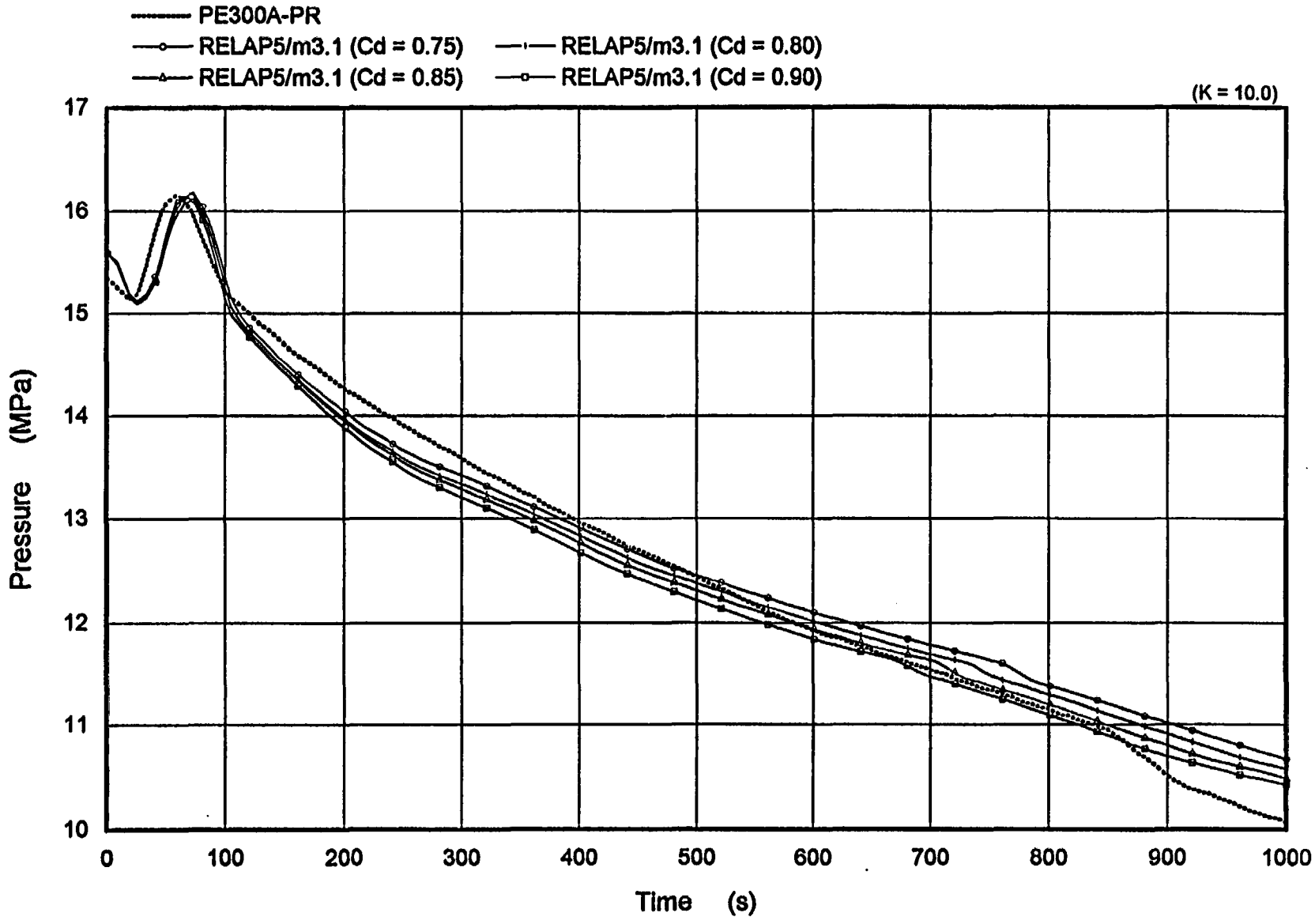

Figure 7.2 Comparison of Pressurizer Pressure (Cd Value Sensitivity)

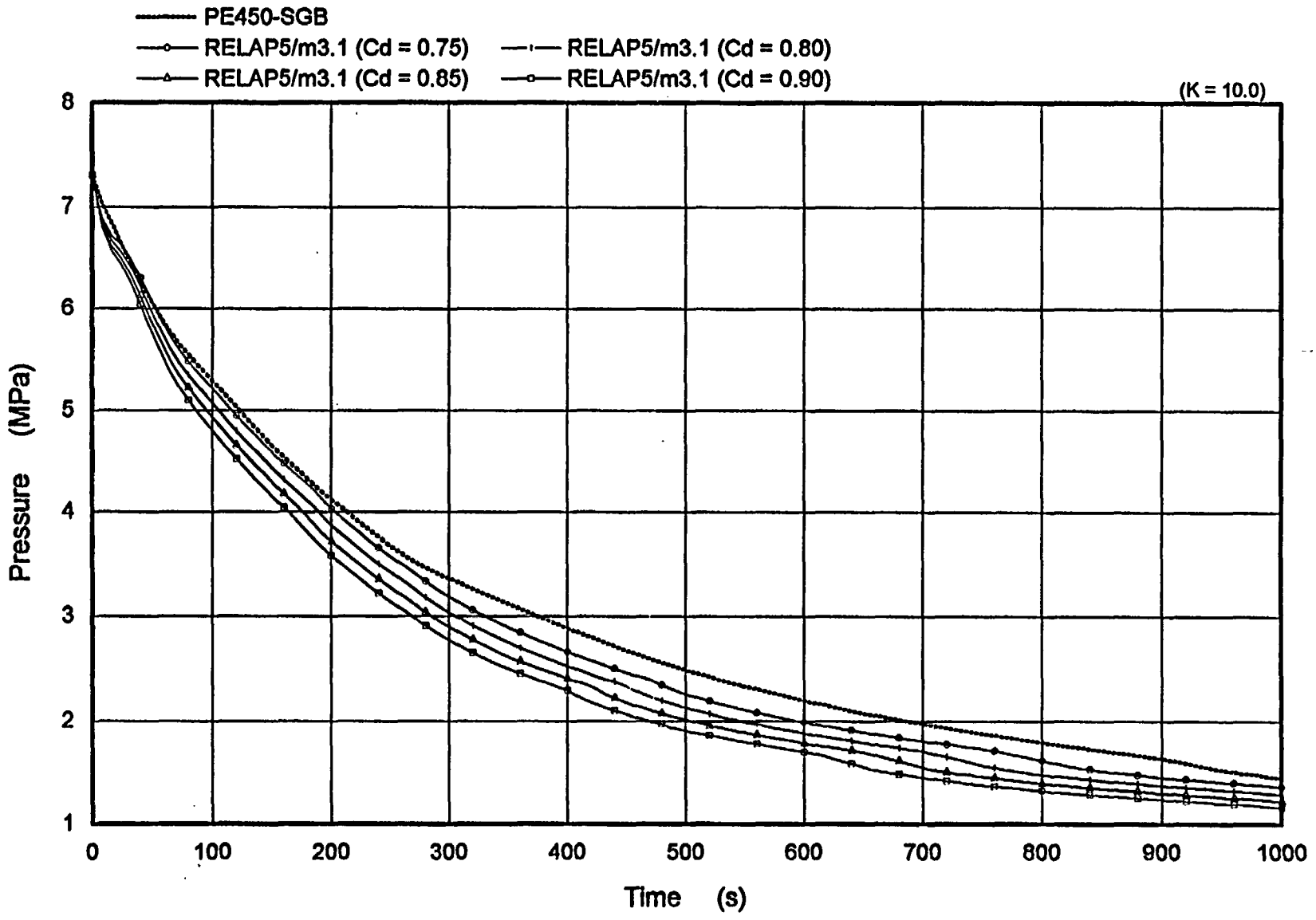

Figure 7.3 Comparison of Secondary Pressure of Broken Loop (Cd Value Sensitivity)

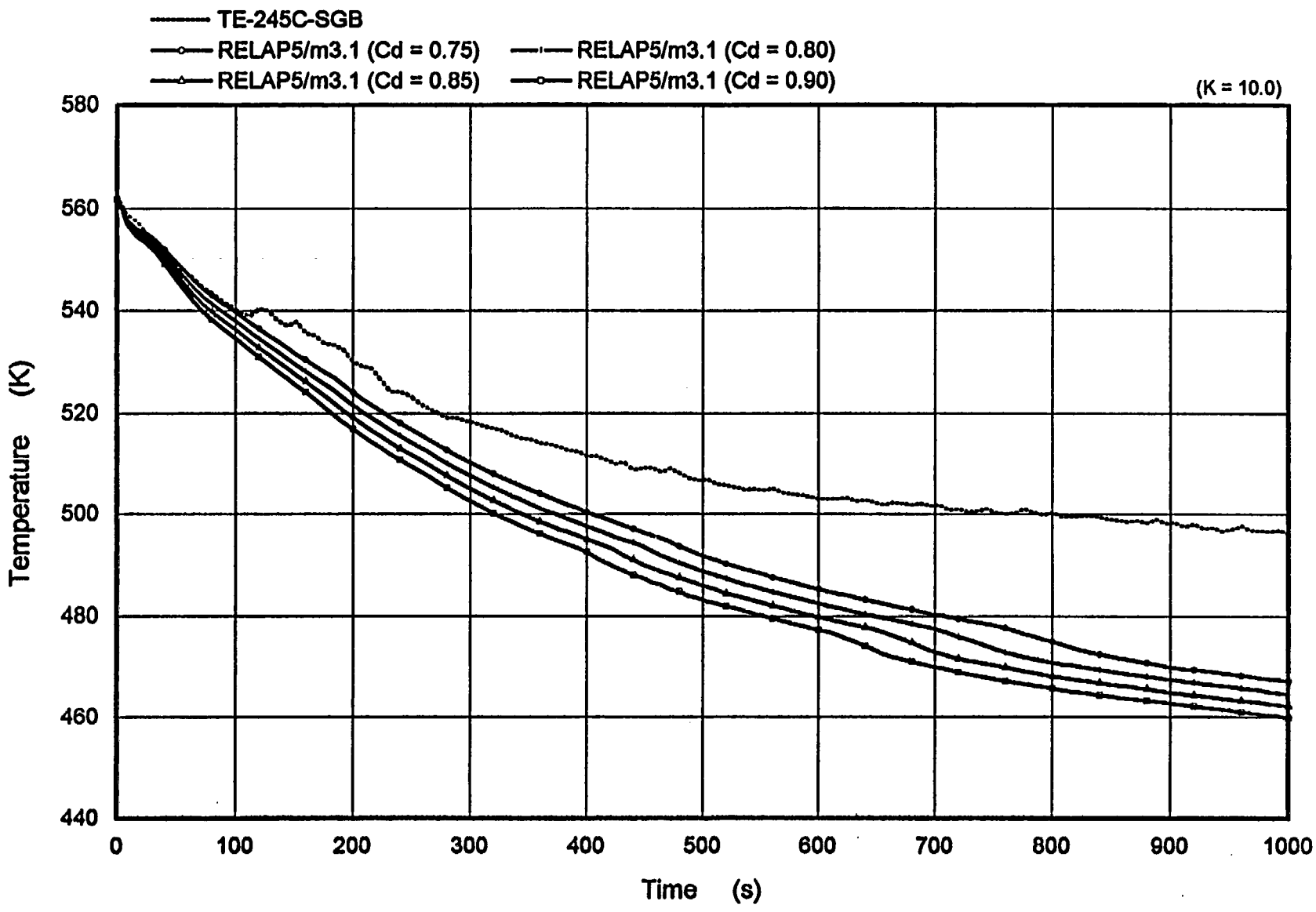

Figure 7.4 Comparison of Secondary Temperature of Broken Loop (Cd Value Sensitivity)

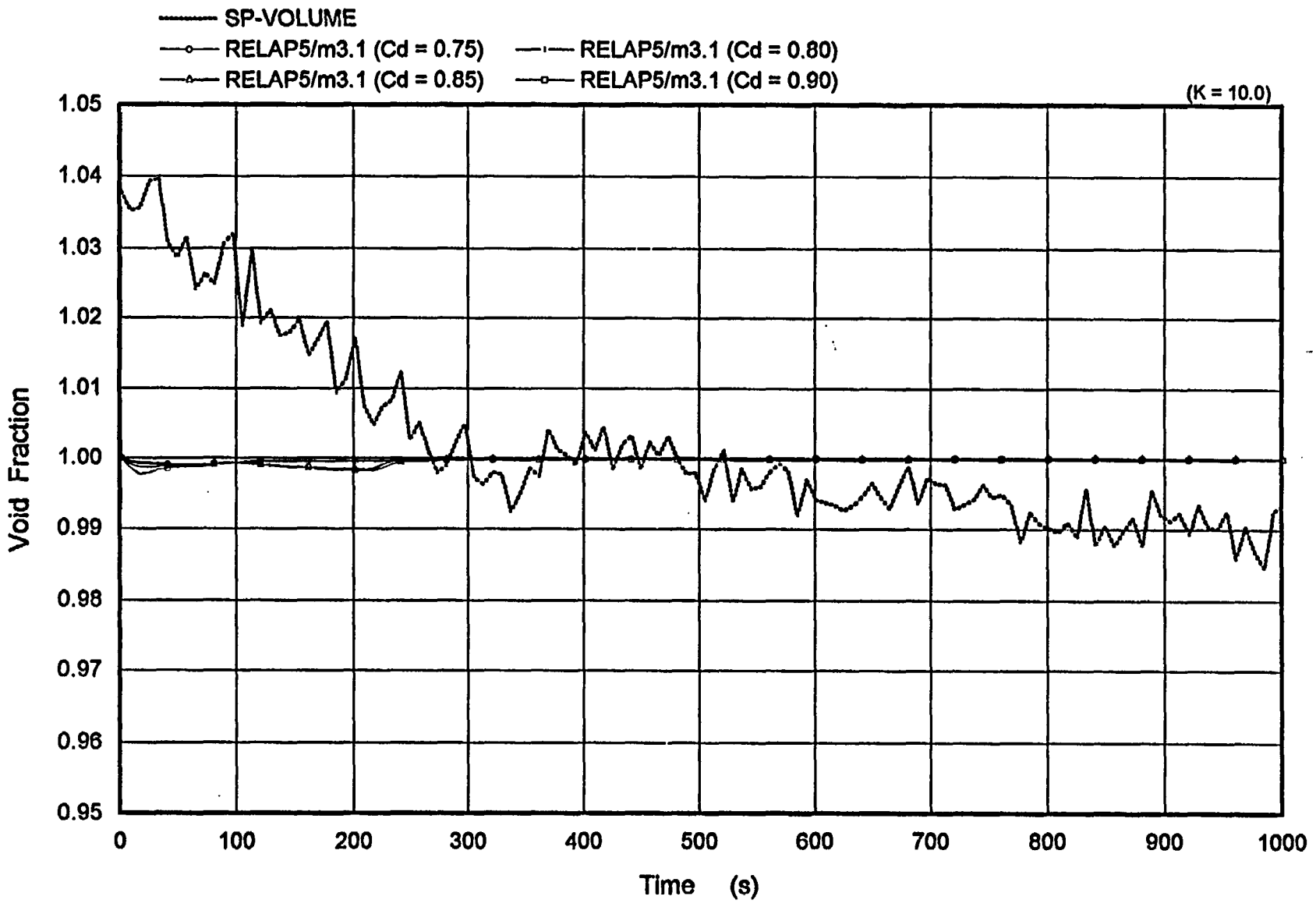

Figure 7.5 Comparison of Break Void Fraction (Cd Value Sensitivity)

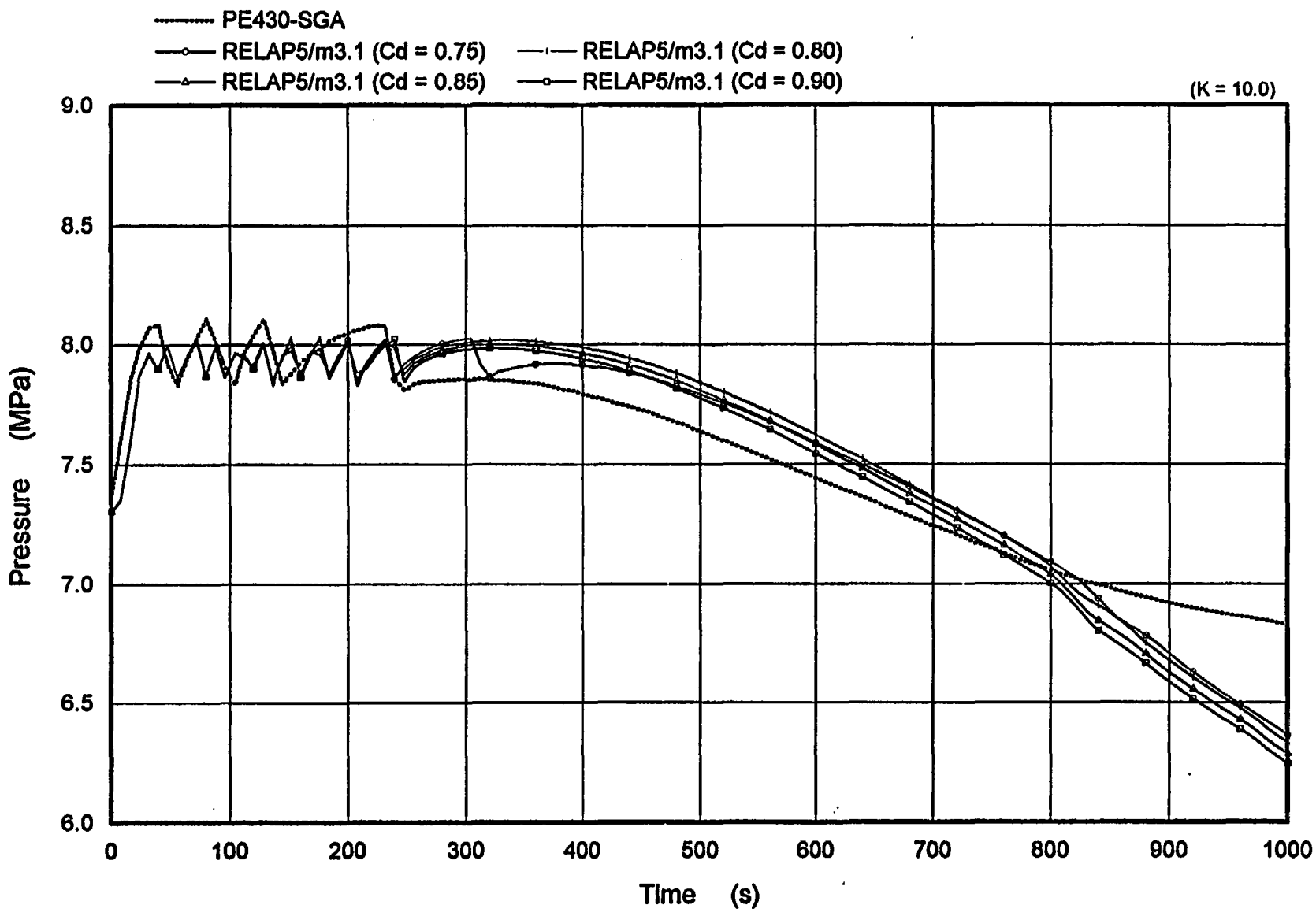

Figure 7.6 Comparison of Secondary Pressure of Intact Loop (Cd Value Sensitivity)

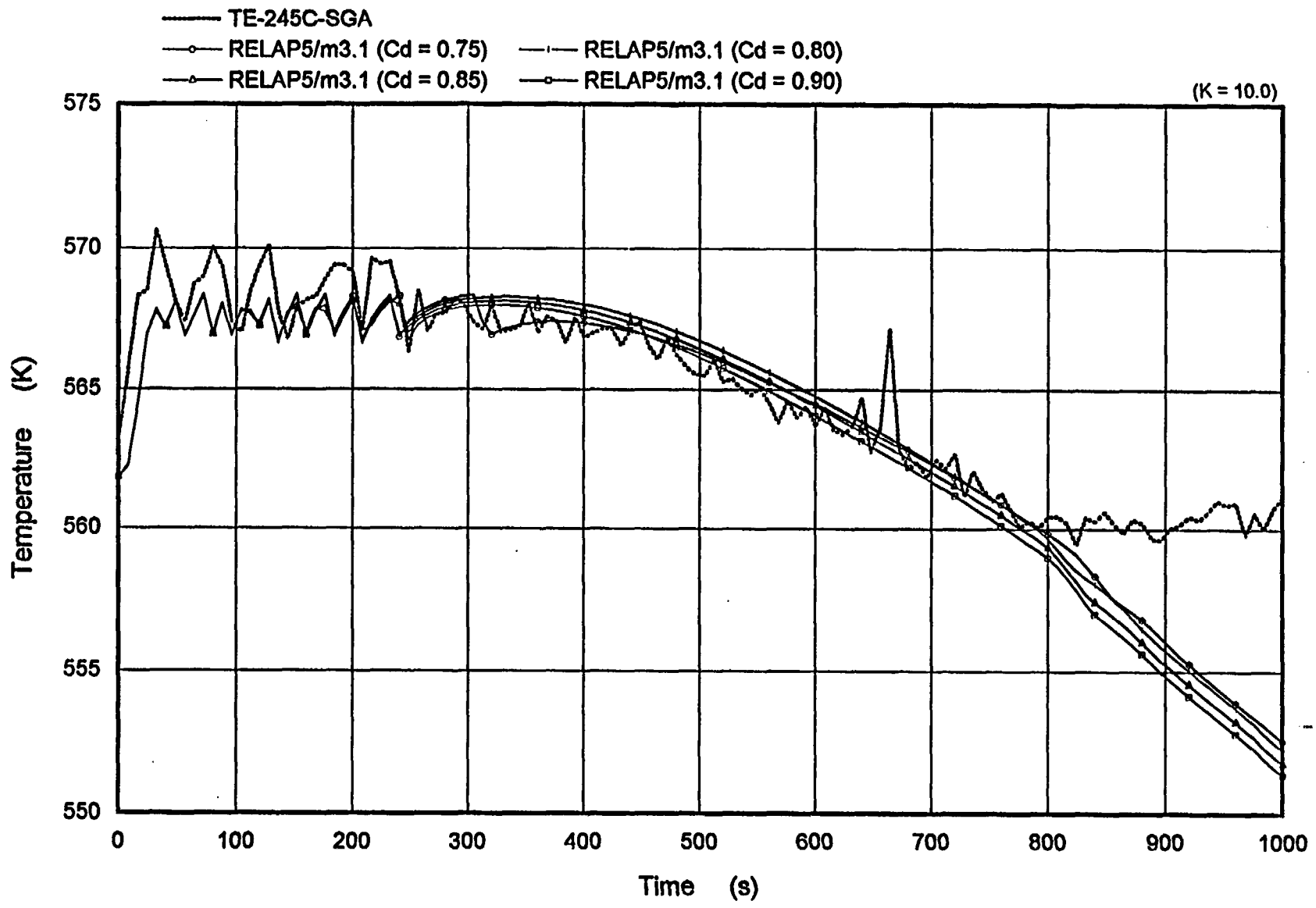

Figure 7.7 Comparison of Secondary Temperature of Intact Loop (Cd Value Sensitivity)

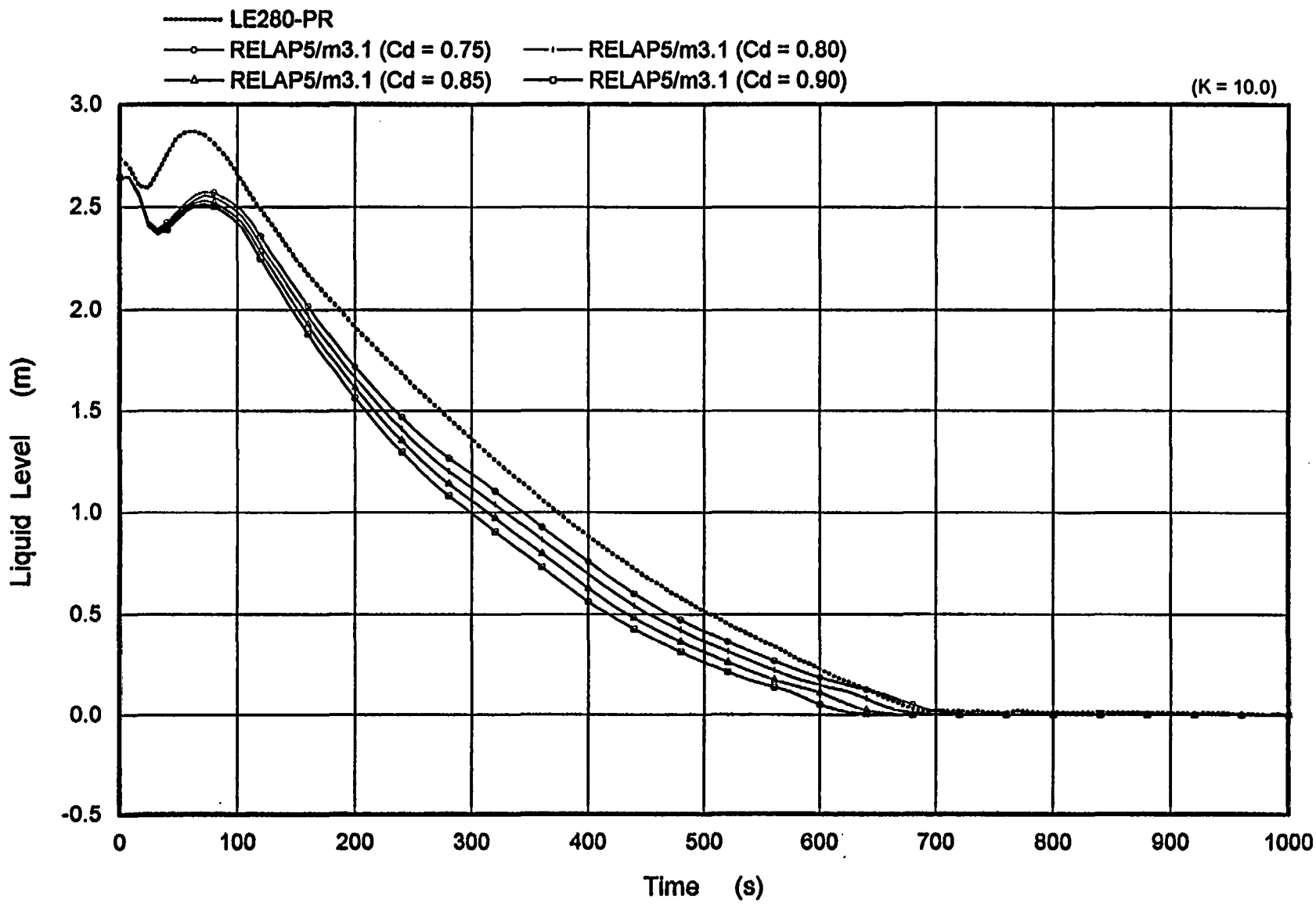

Figure 7.8 Collapsed Liquid Level of Pressurizer (Cd Value Sensitivity)

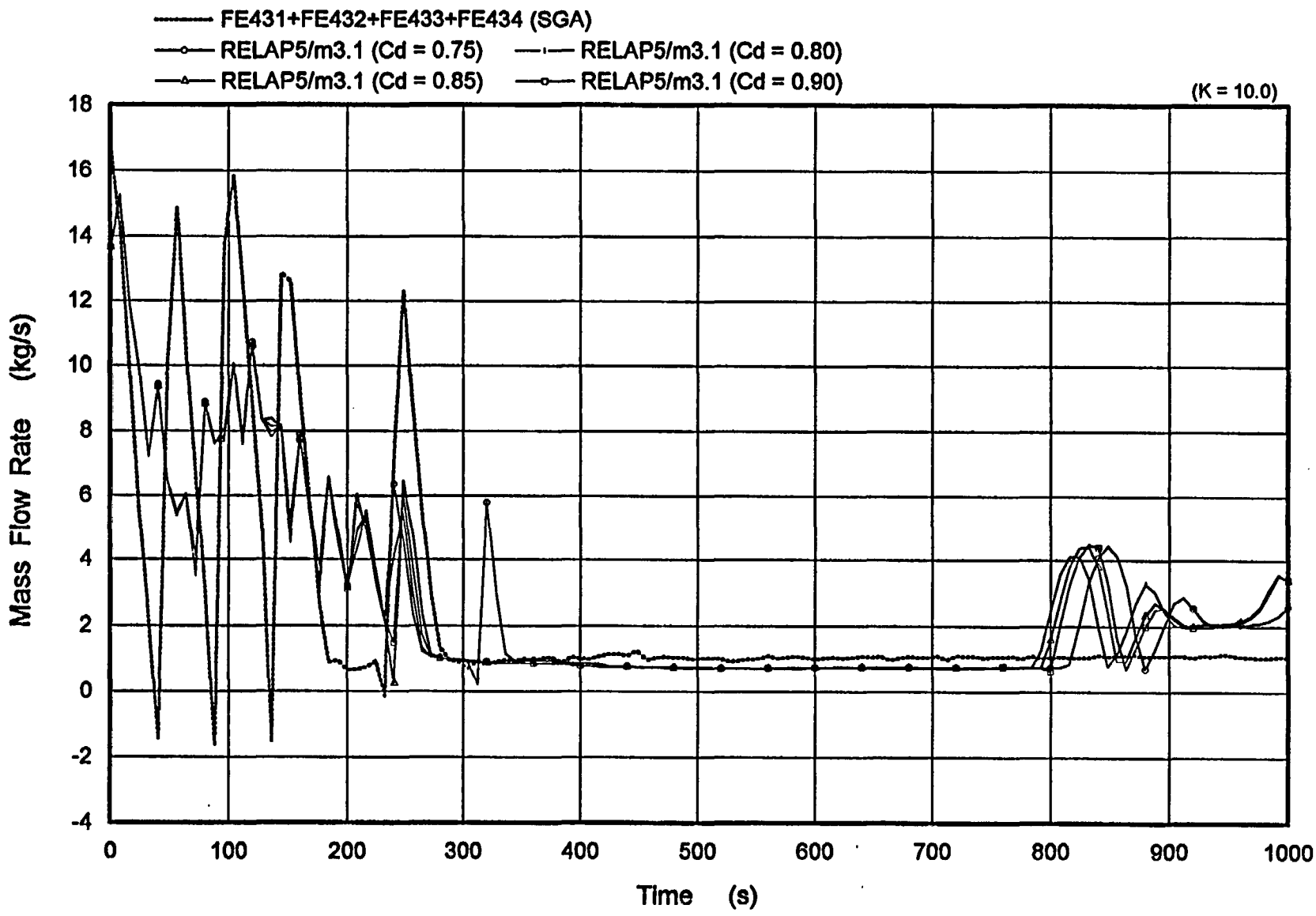

Figure 7.9 Downcomer Flow Rate of Intact Loop (Cd Value Sensitivity)

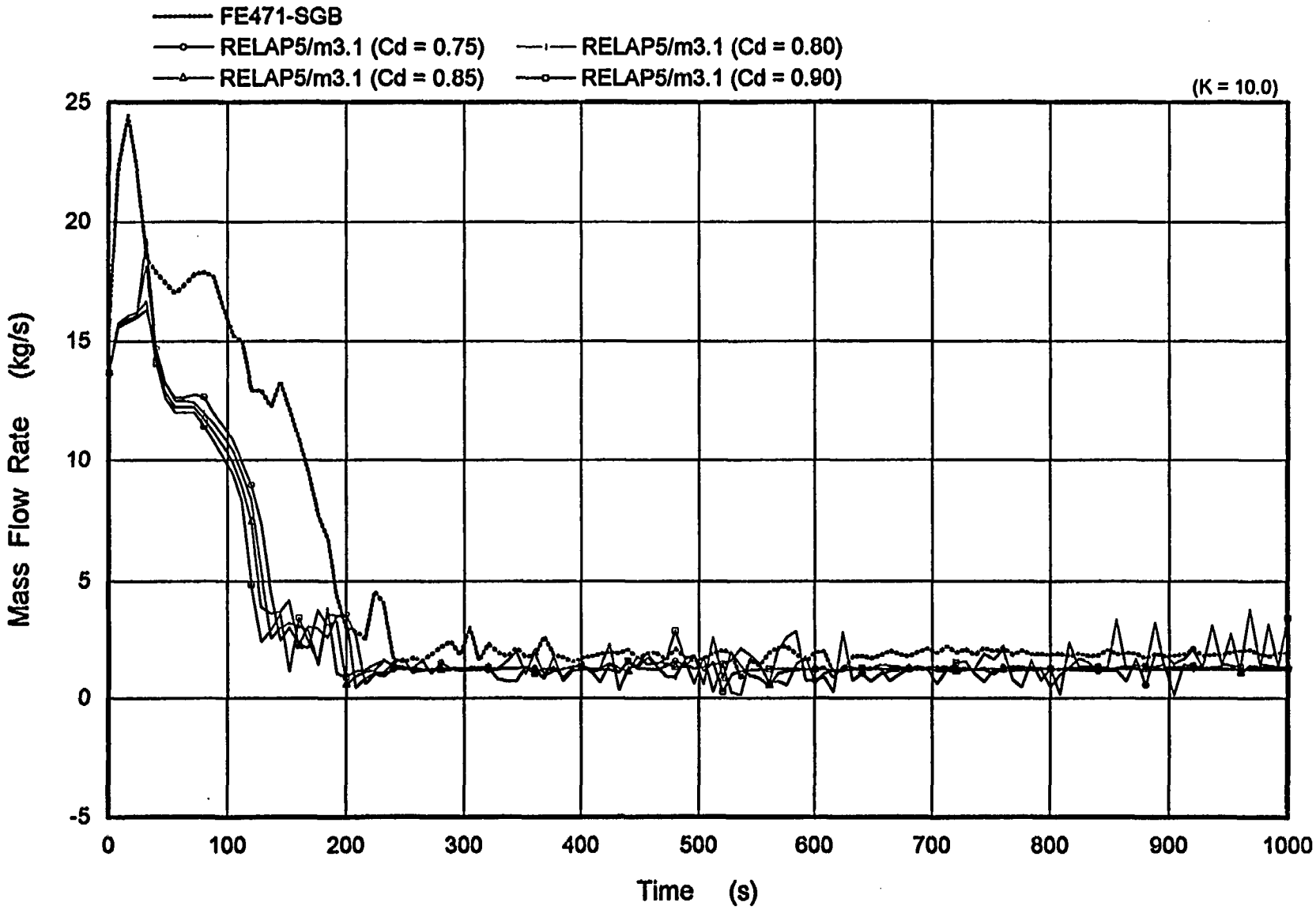

Figure 7.10 Downcomer Flow Rate of Broken Loop (Cd Value Sensitivity)

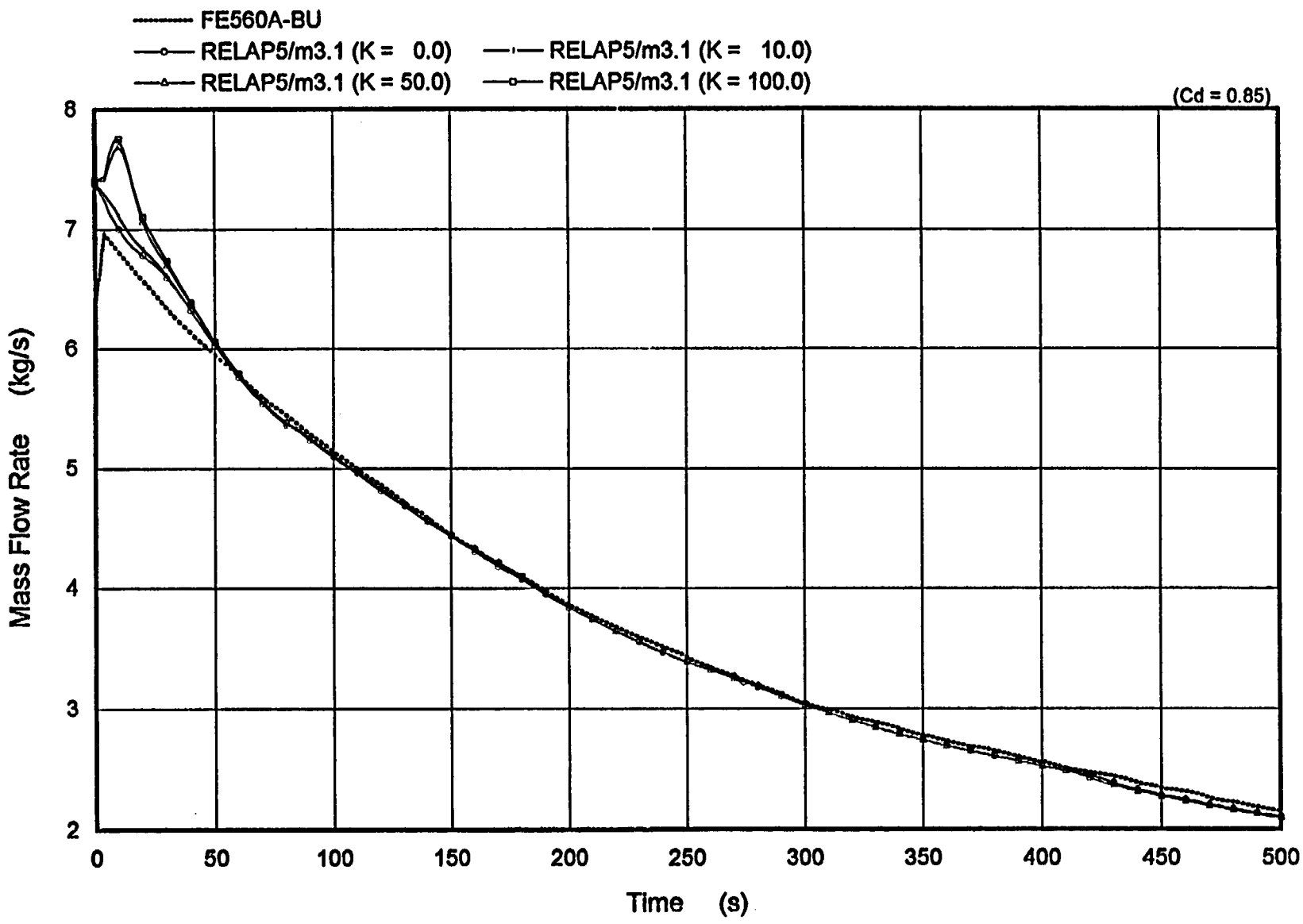

Figure 7.11 Comparison of Break Flow Rate (K Value Sensitivity)

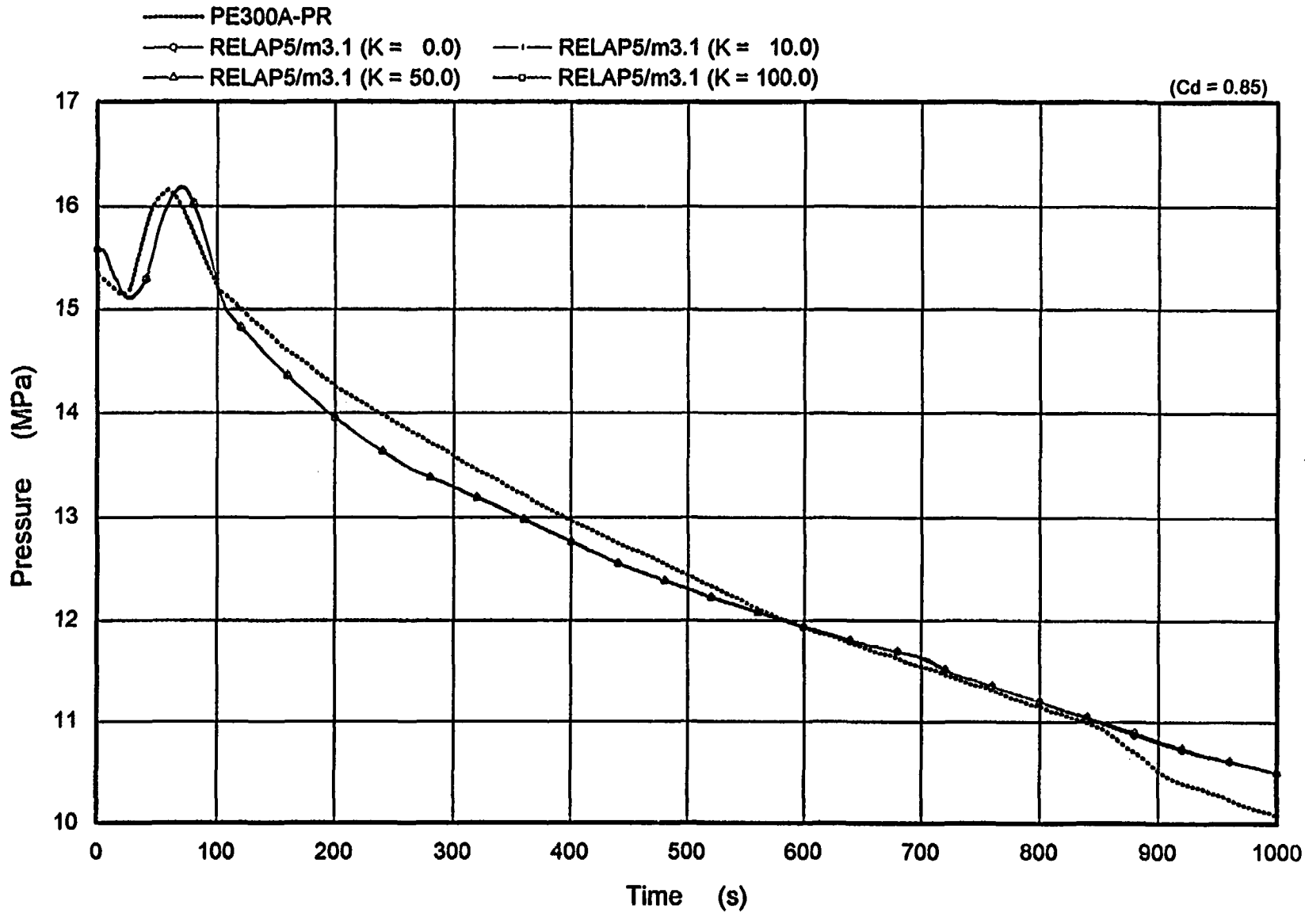

Figure 7.12 Comparison of Pressurizer Pressure (K Value Sensitivity)

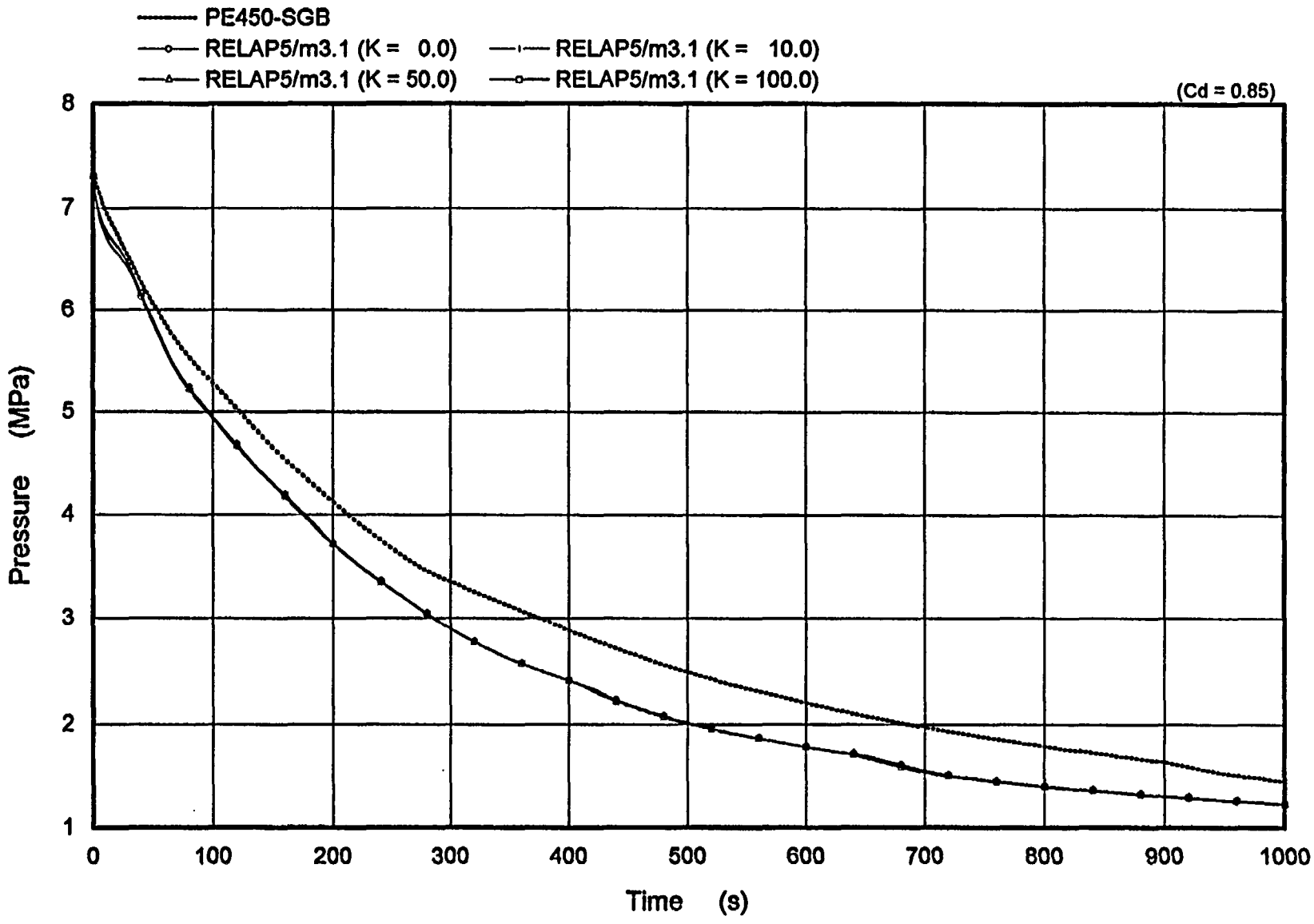

Figure 7.13 Comparison of Secondary Pressure of Broken Loop (K Value Sensitivity)

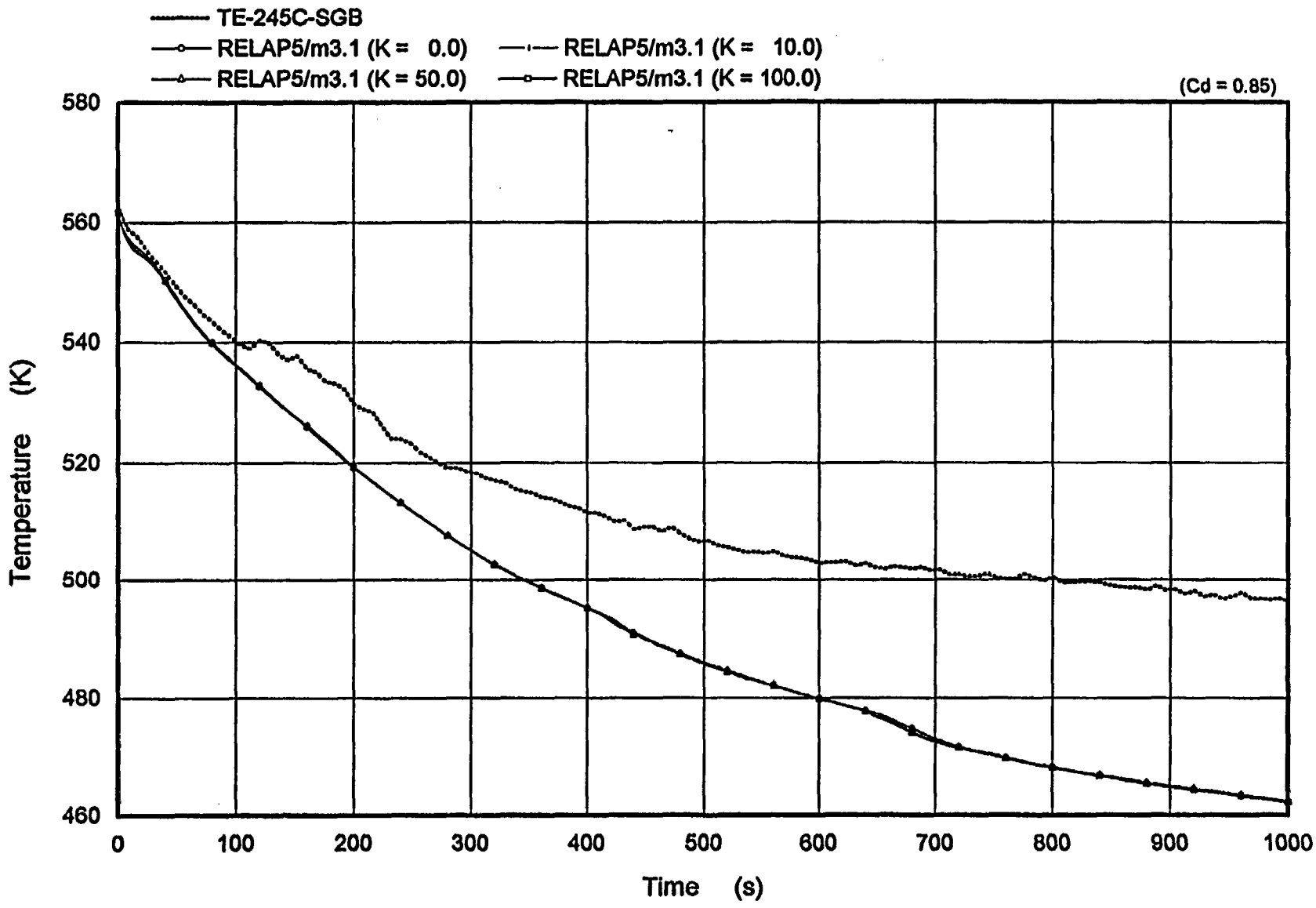

Figure 7.14 Comparison of Secondary Temperature of Broken Loop (K Value Sensitivity)

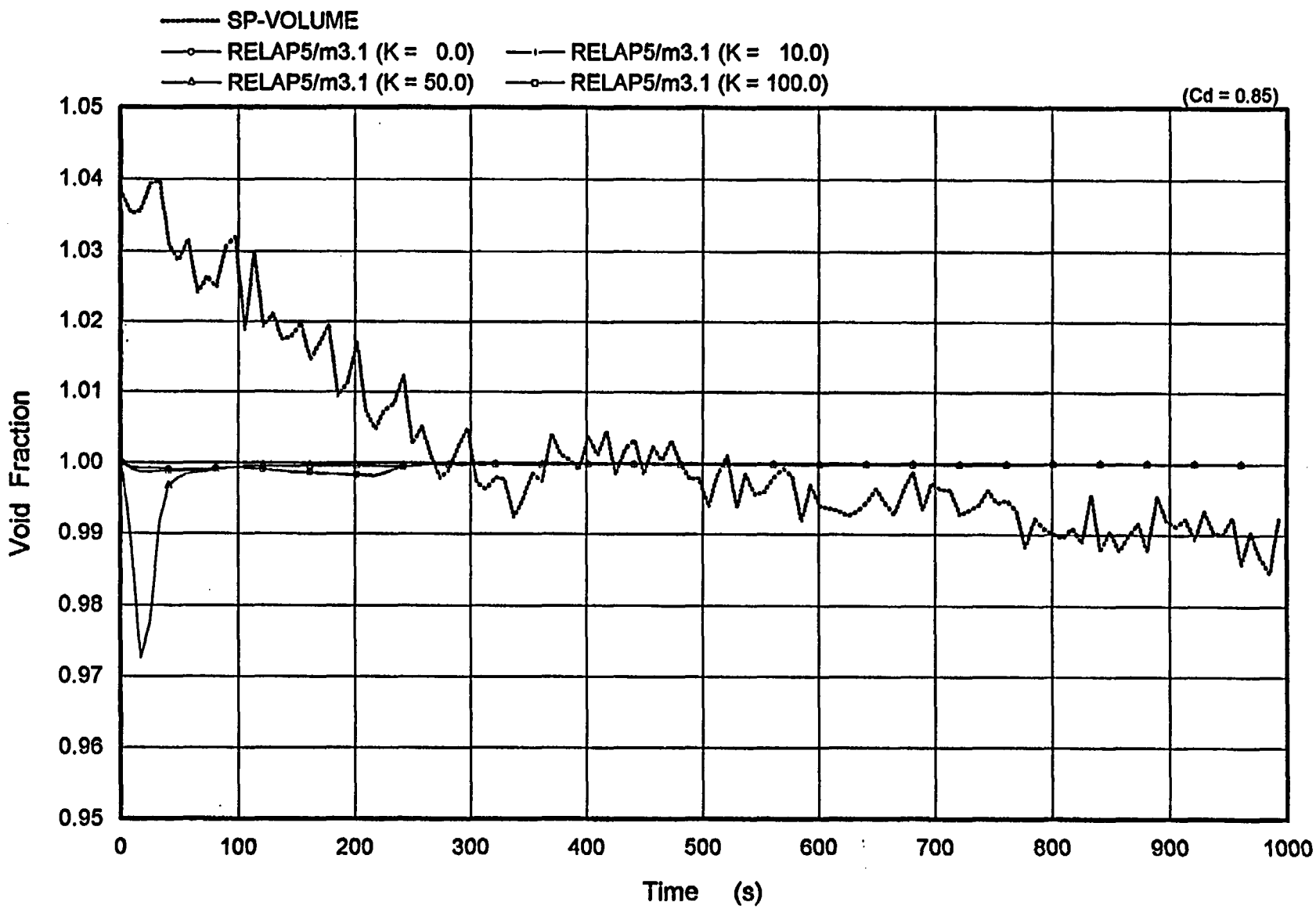

Figure 7.15 Comparison of Break Void Fraction (K Value Sensitivity)

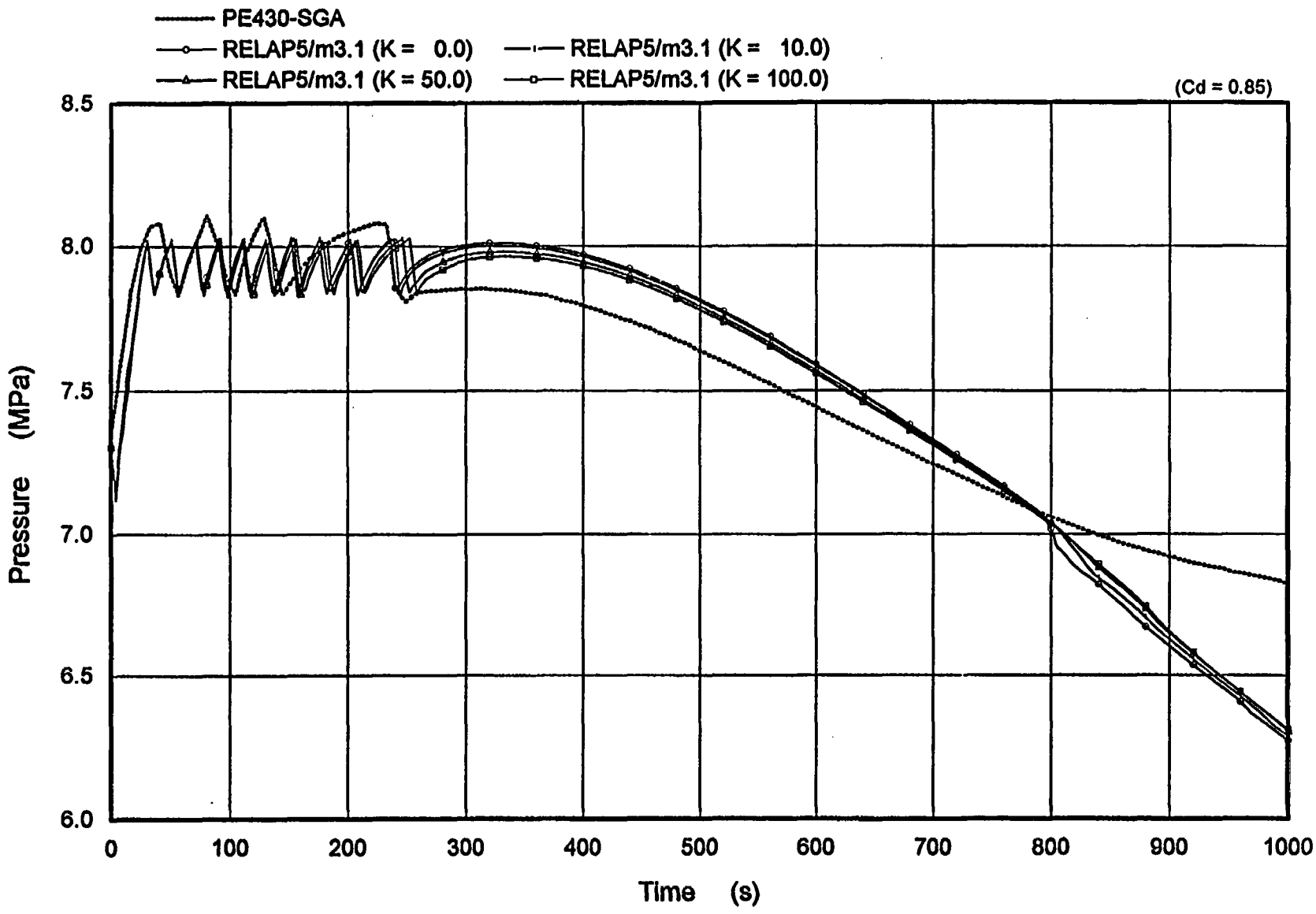

Figure 7.16 Comparison of Secondary Pressure of Intact Loop (K Value Sensitivity)

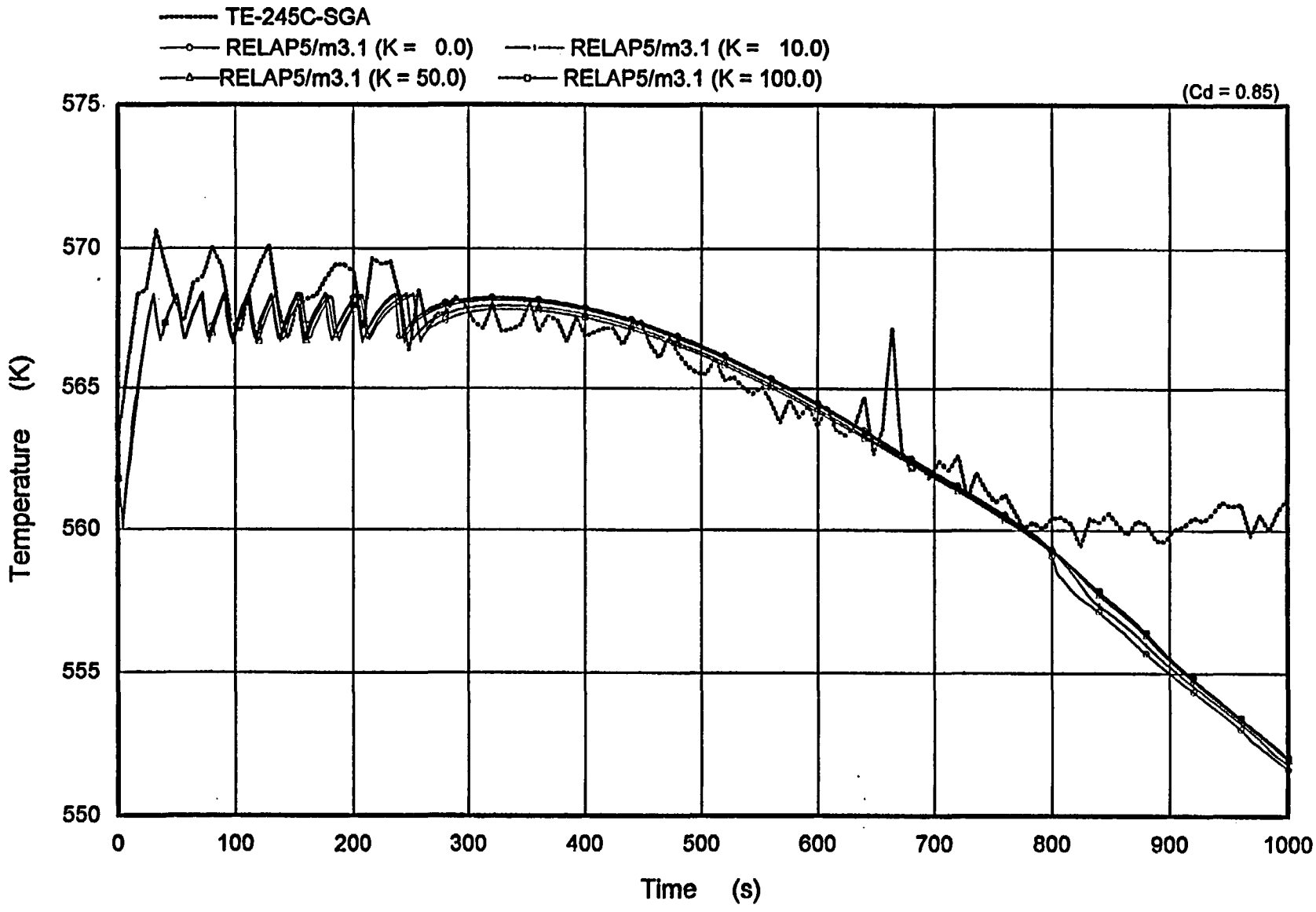

Figure 7.17 Comparison of Secondary Temperature of Intact Loop (K Value Sensitivity)

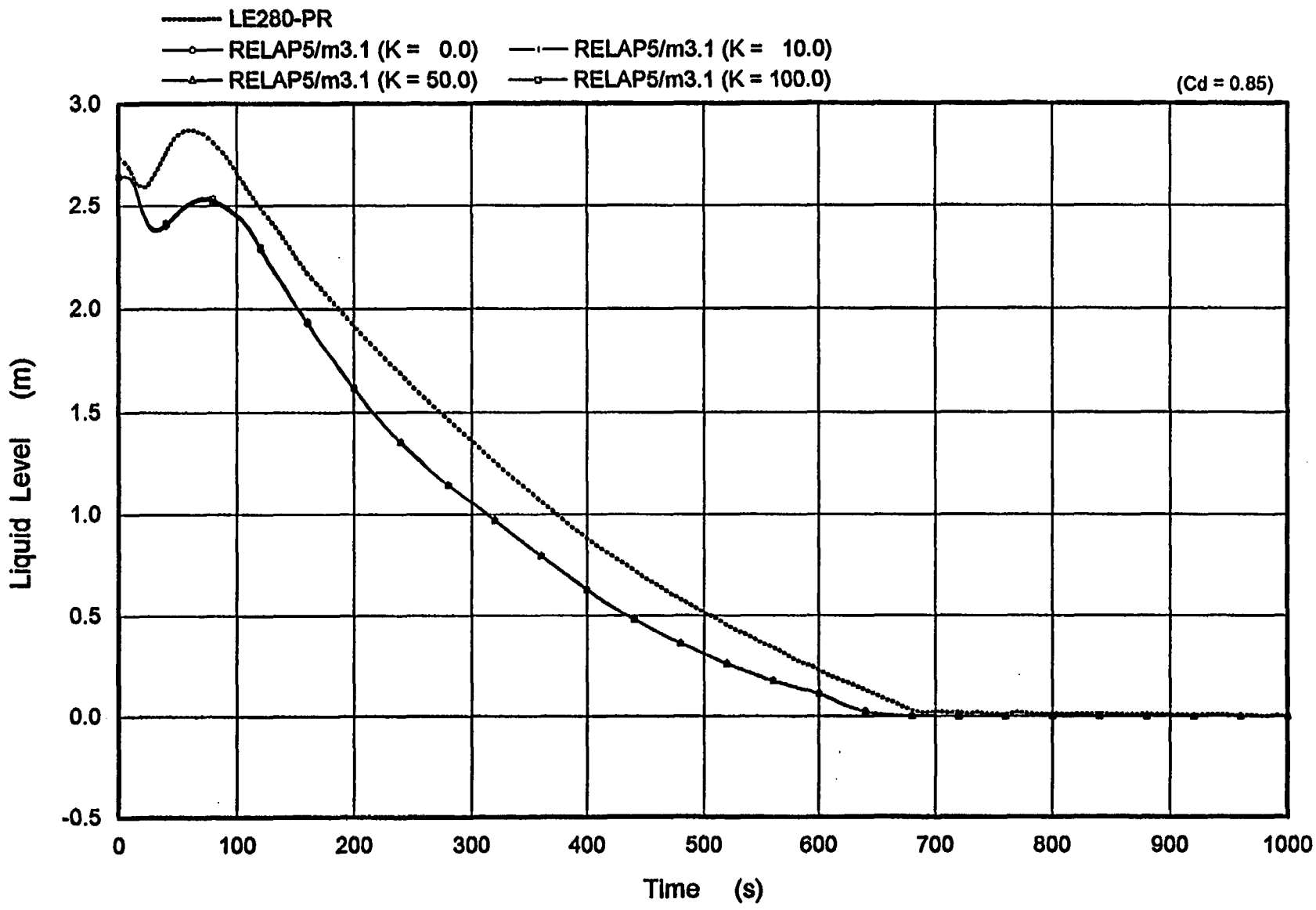

Figure 7.18 Collapsed Liquid Level of Pressurizer (K Value Sensitivity)

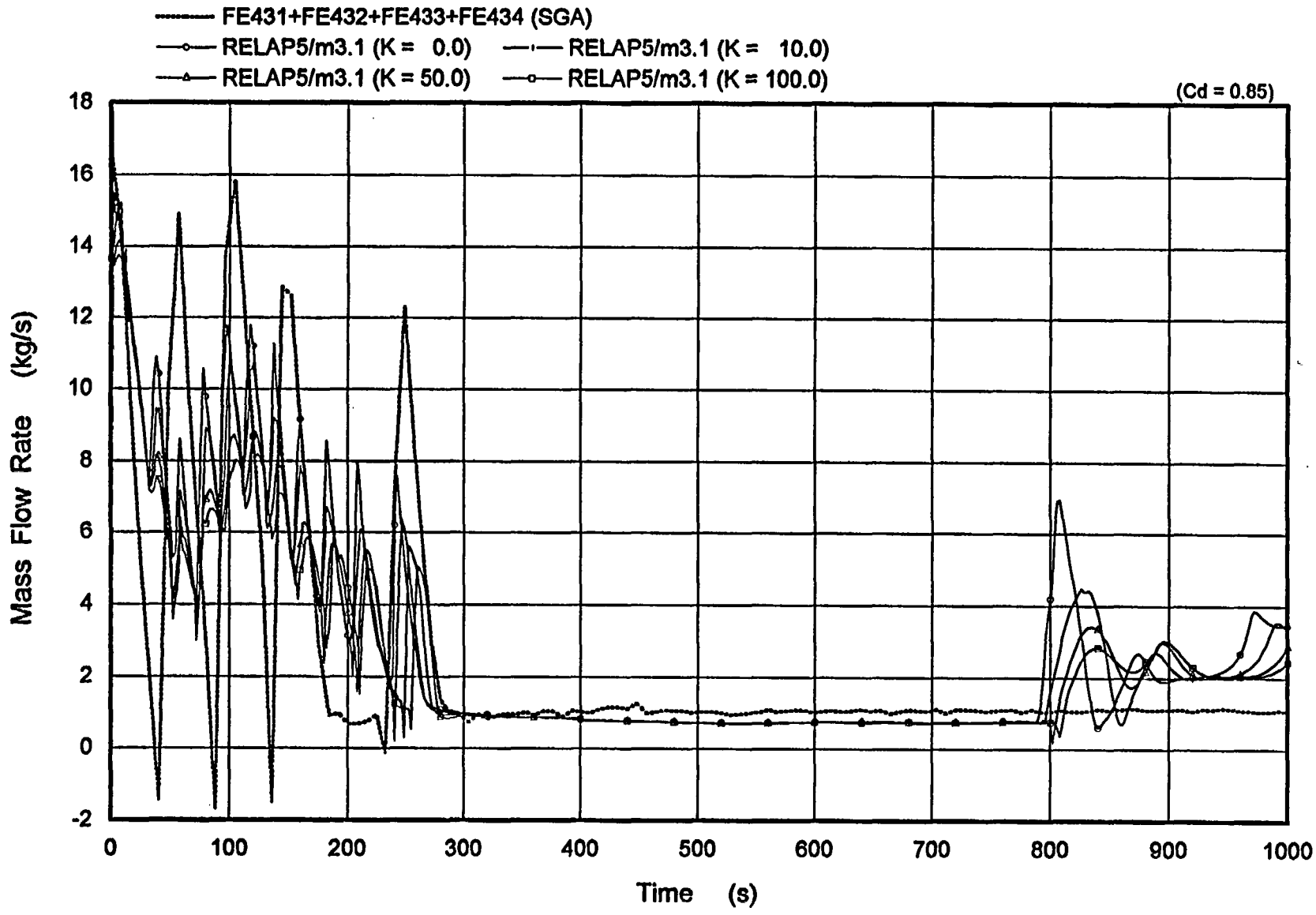

Figure 7.19 Downcomer Flow Rate of Intact Side (K Value Sensitivity)

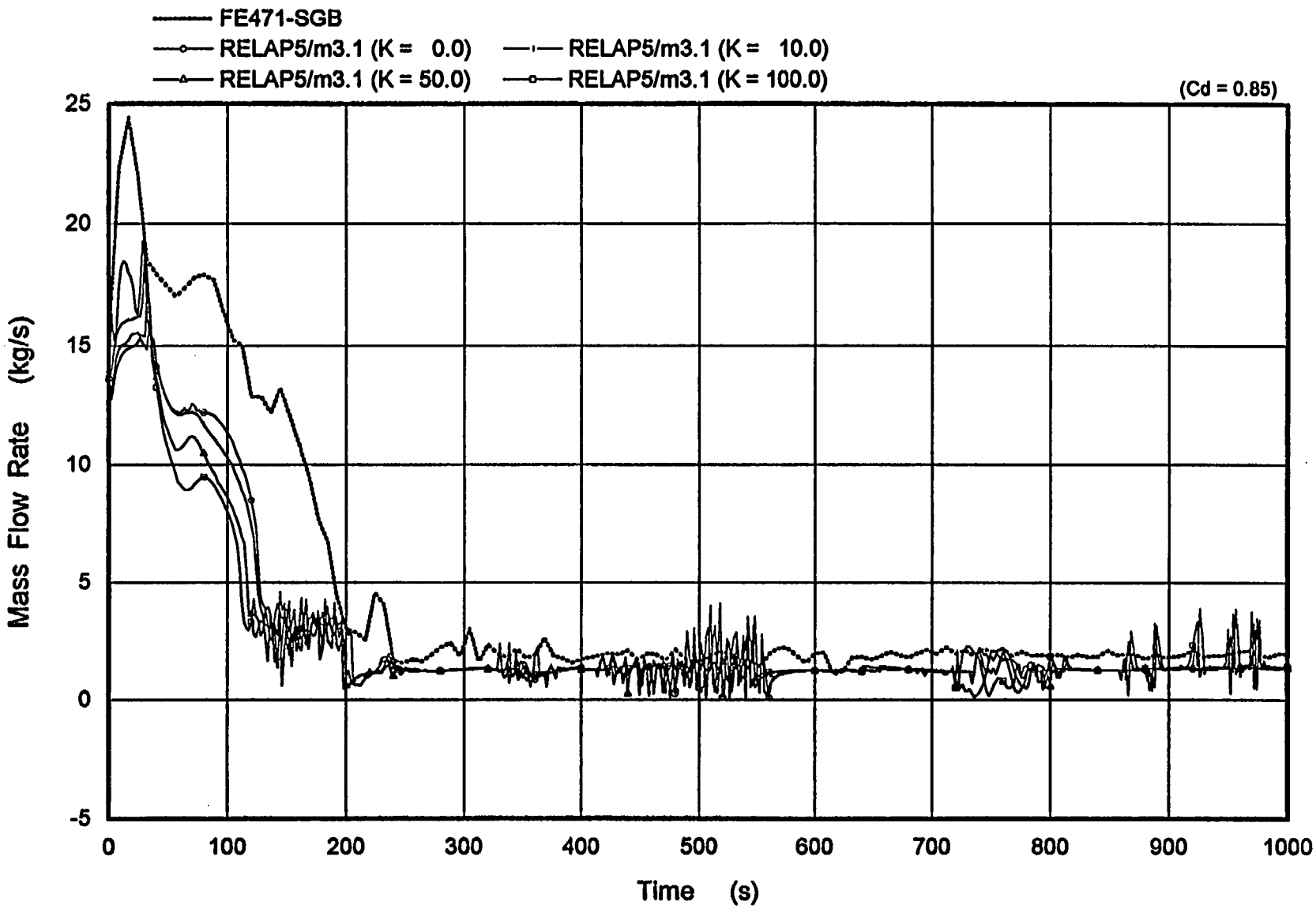

Figure 7.20 Downcomer Flow Rate of Broken Side (K Value Sensitivity)

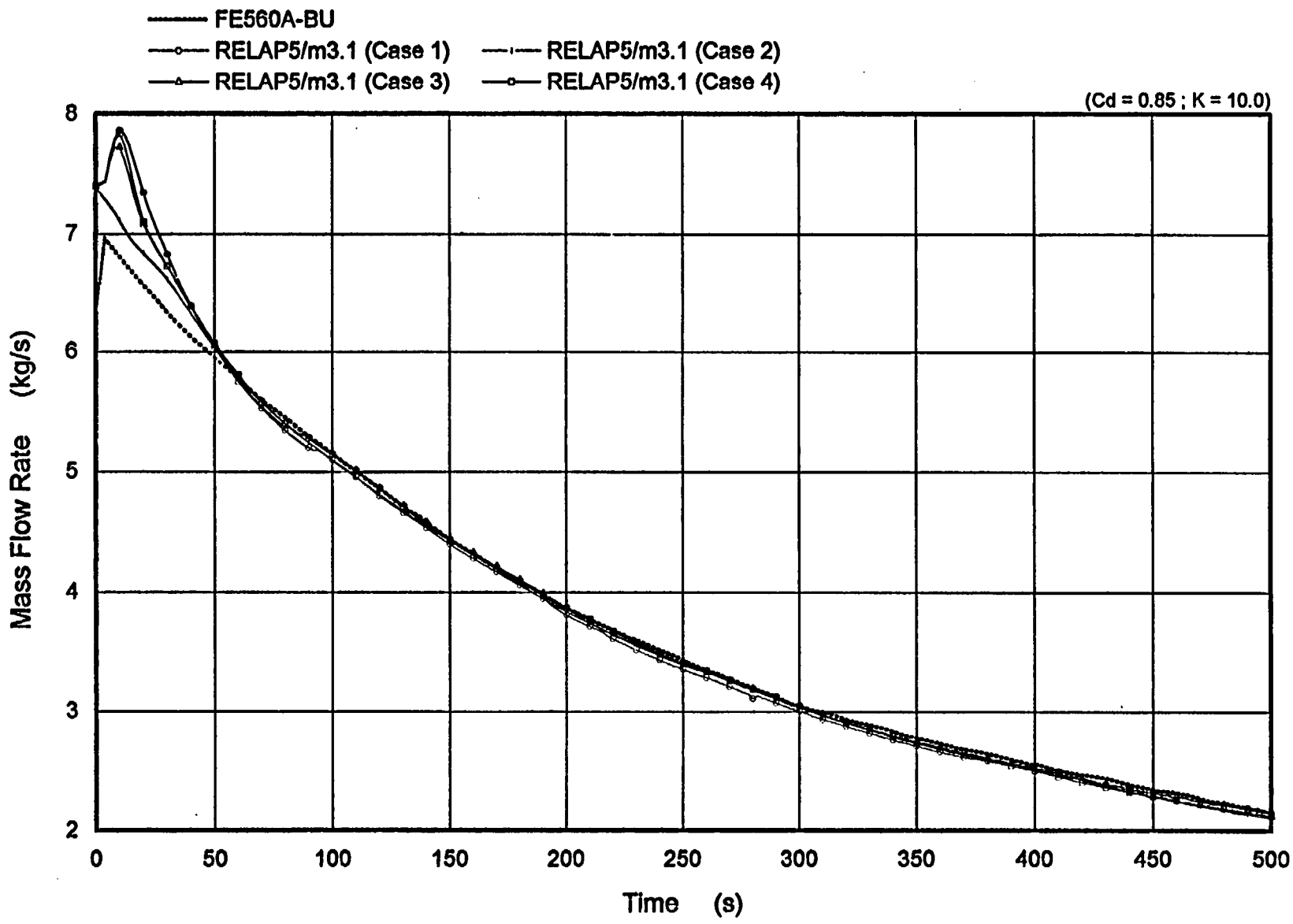

Figure 7.21 Comparison of Break Flow Rate (S/G Nodes Sensitivity)

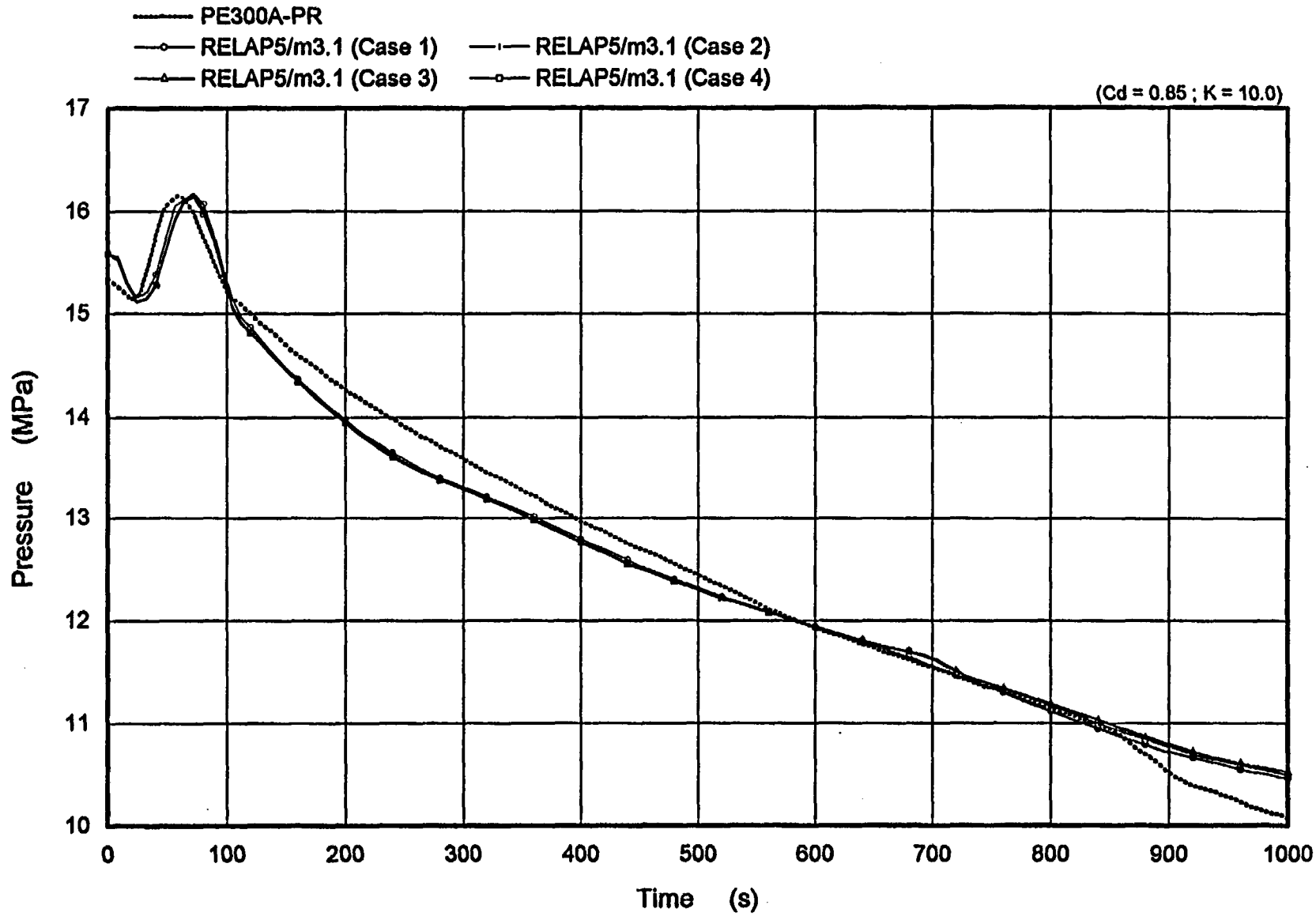

Figure 7.22 Comparison of Pressurizer Pressure (S/G Nodes Sensitivity)

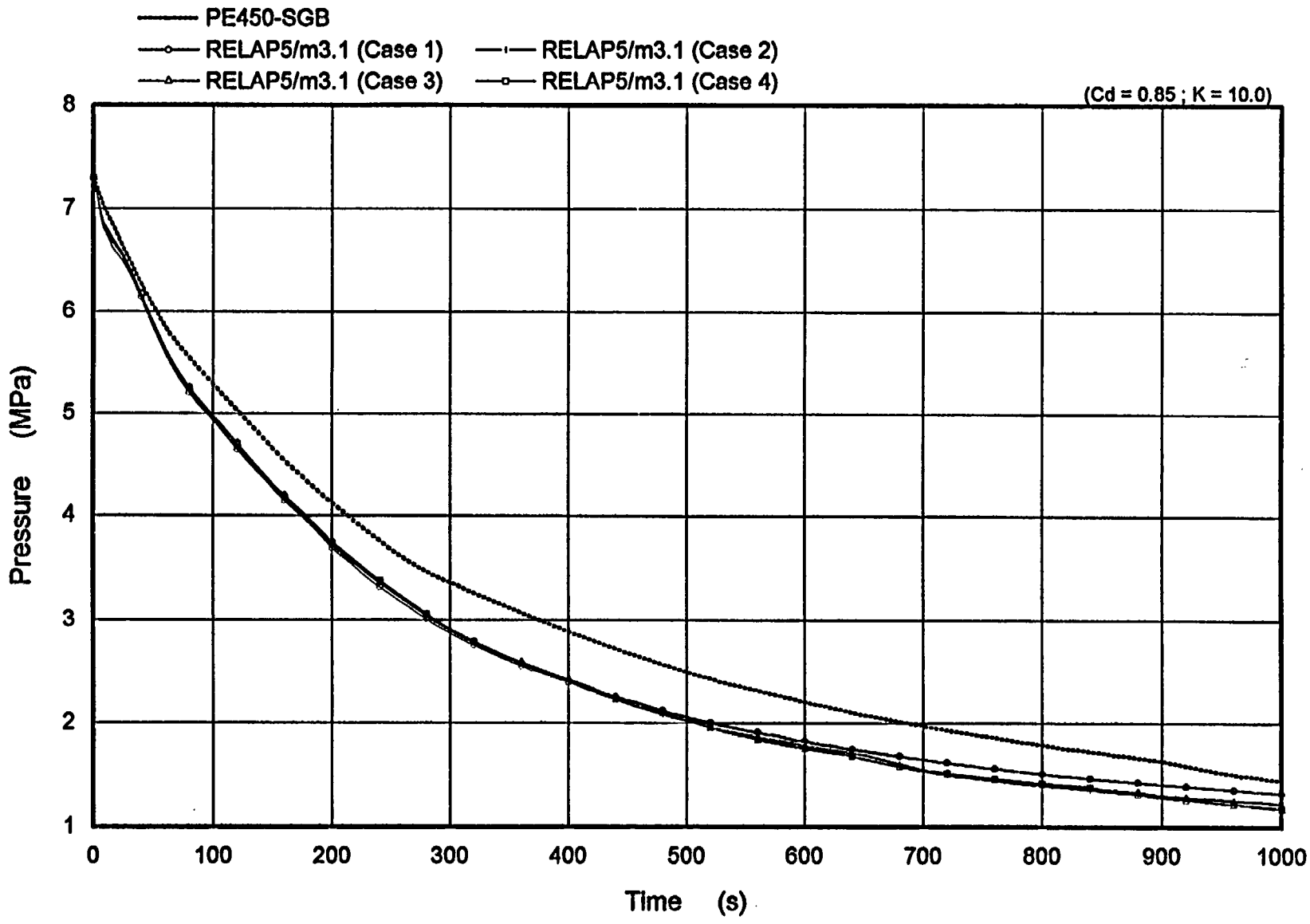

Figure 7.23 Comparison of Secondary Pressure of Broken Loop (S/G Nodes Sensitivity)

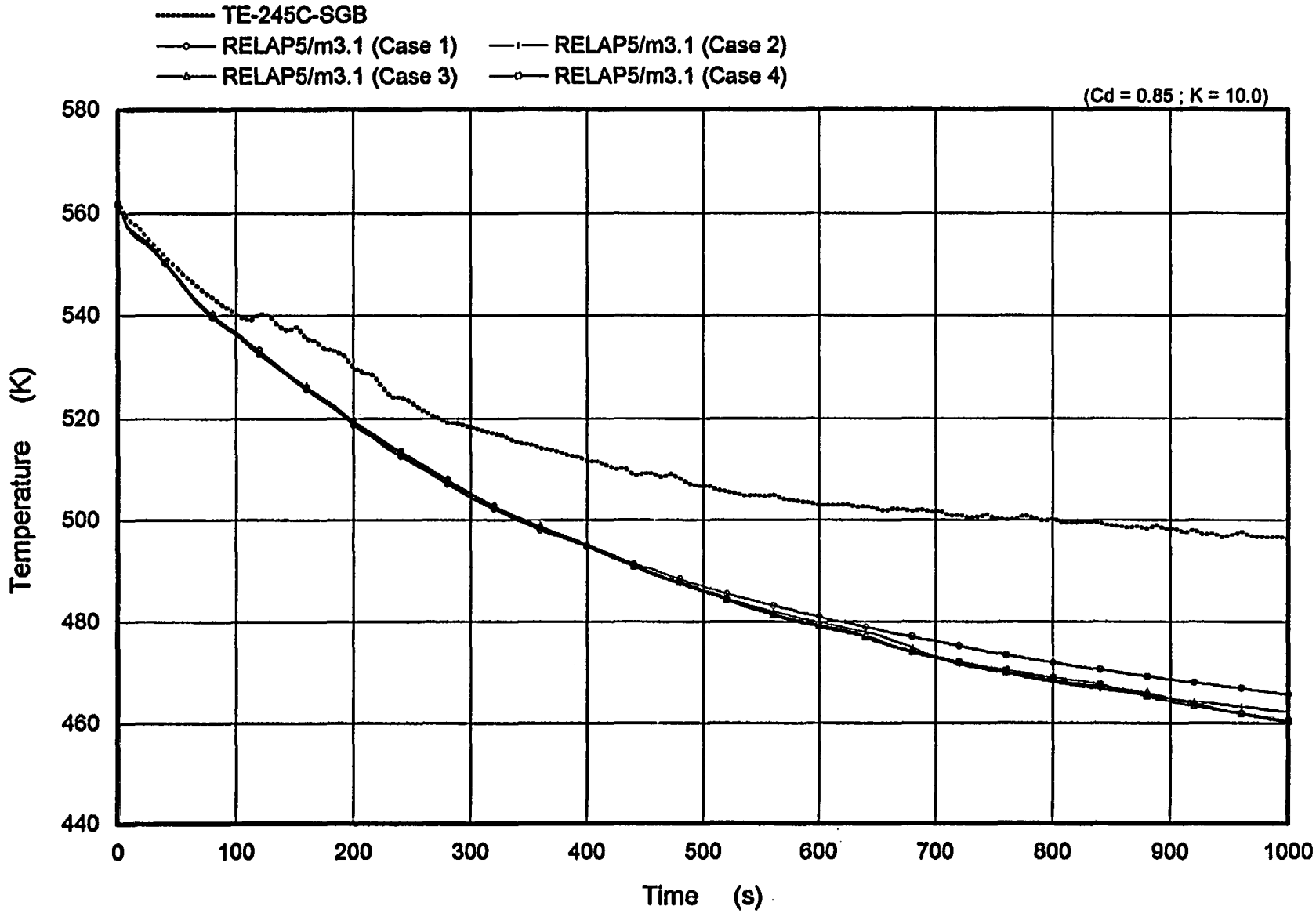

Figure 7.24 Comparison of Secondary Temperature of Broken Loop (S/G Nodes Sensitivity)

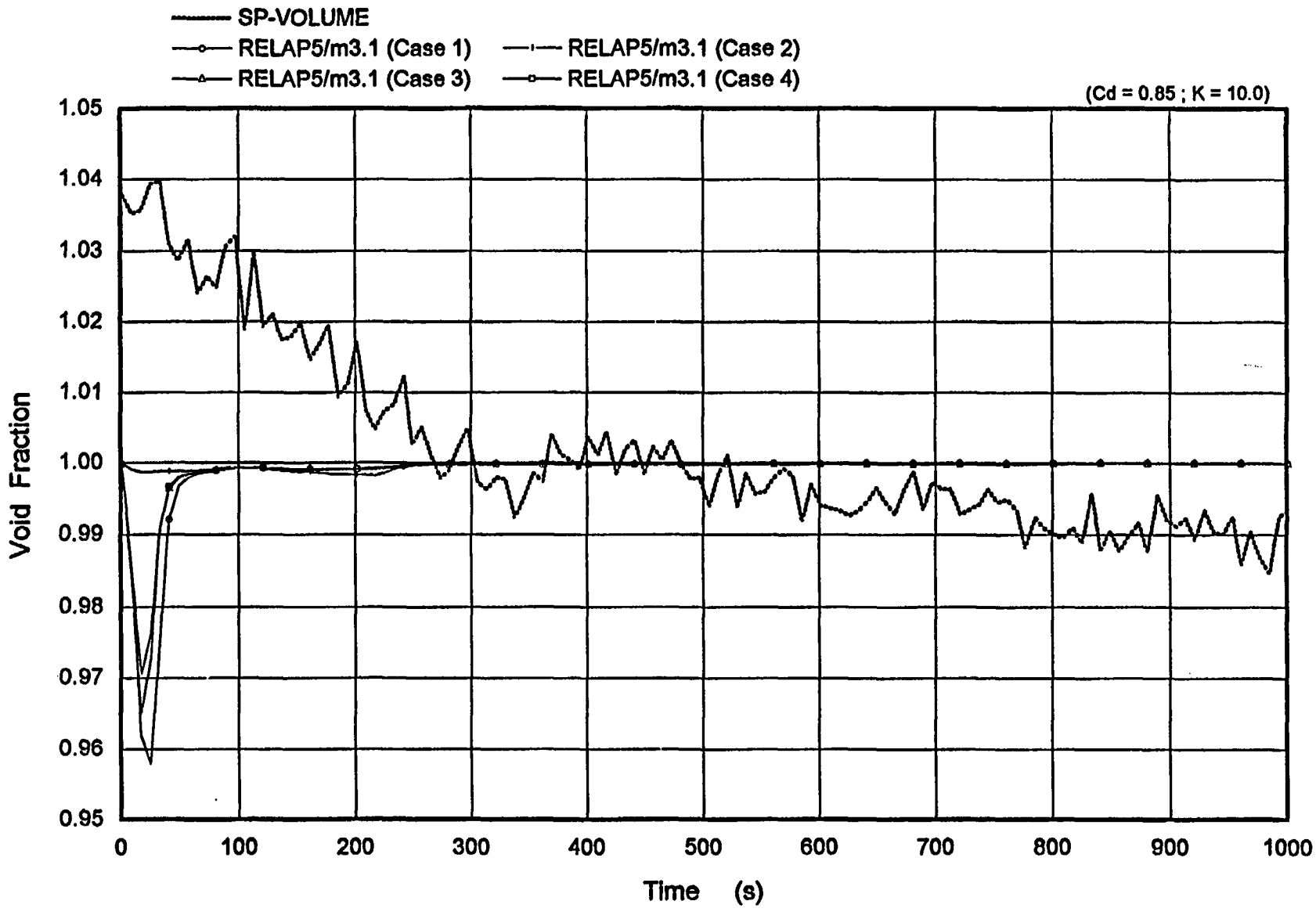

Figure 7.25 Comparison of Break Void Fraction (S/G Nodes Sensitivity)

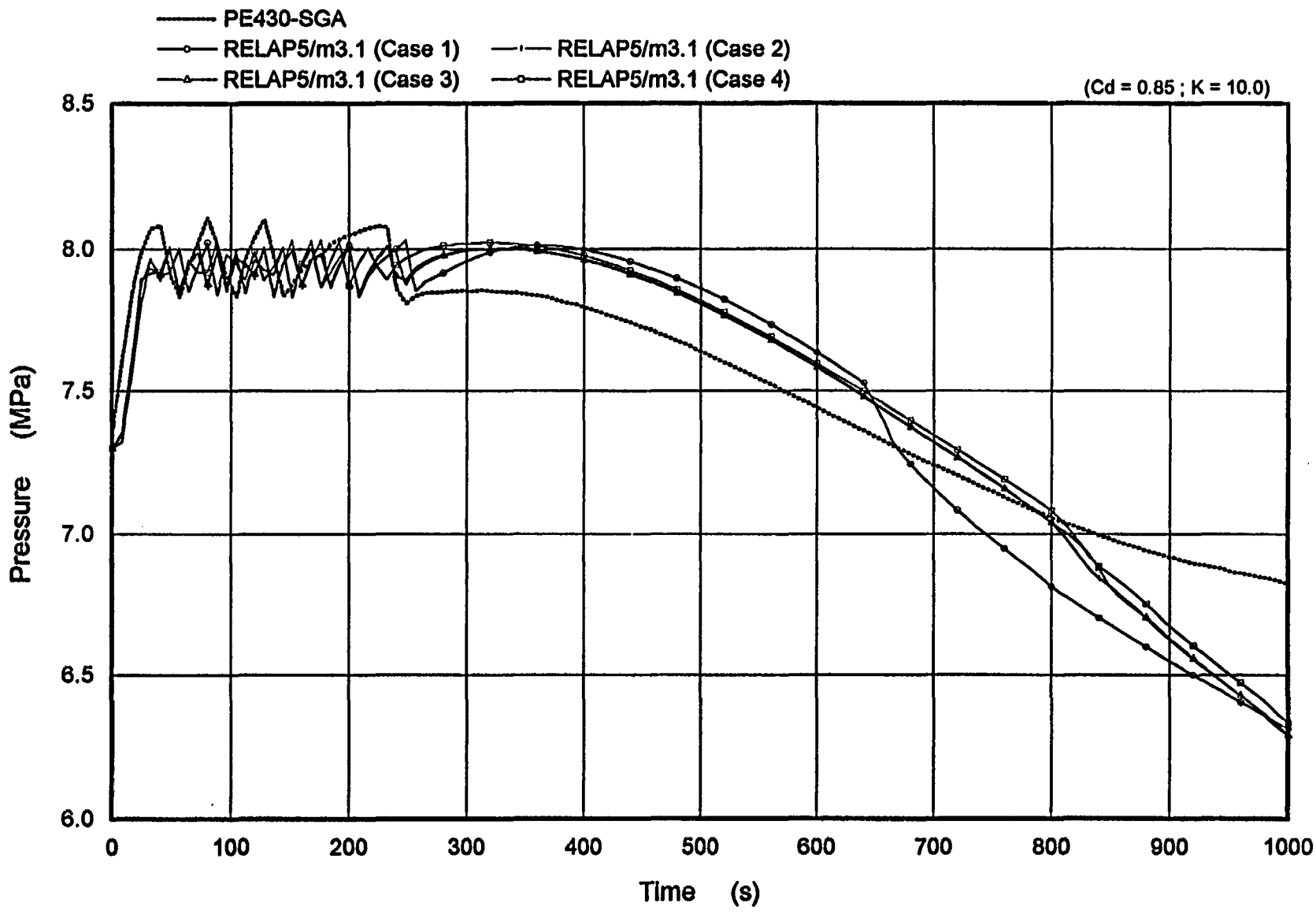

Figure 7.26 Comparison of Secondary Pressure of Intact Loop (S/G Nodes Sensitivity)

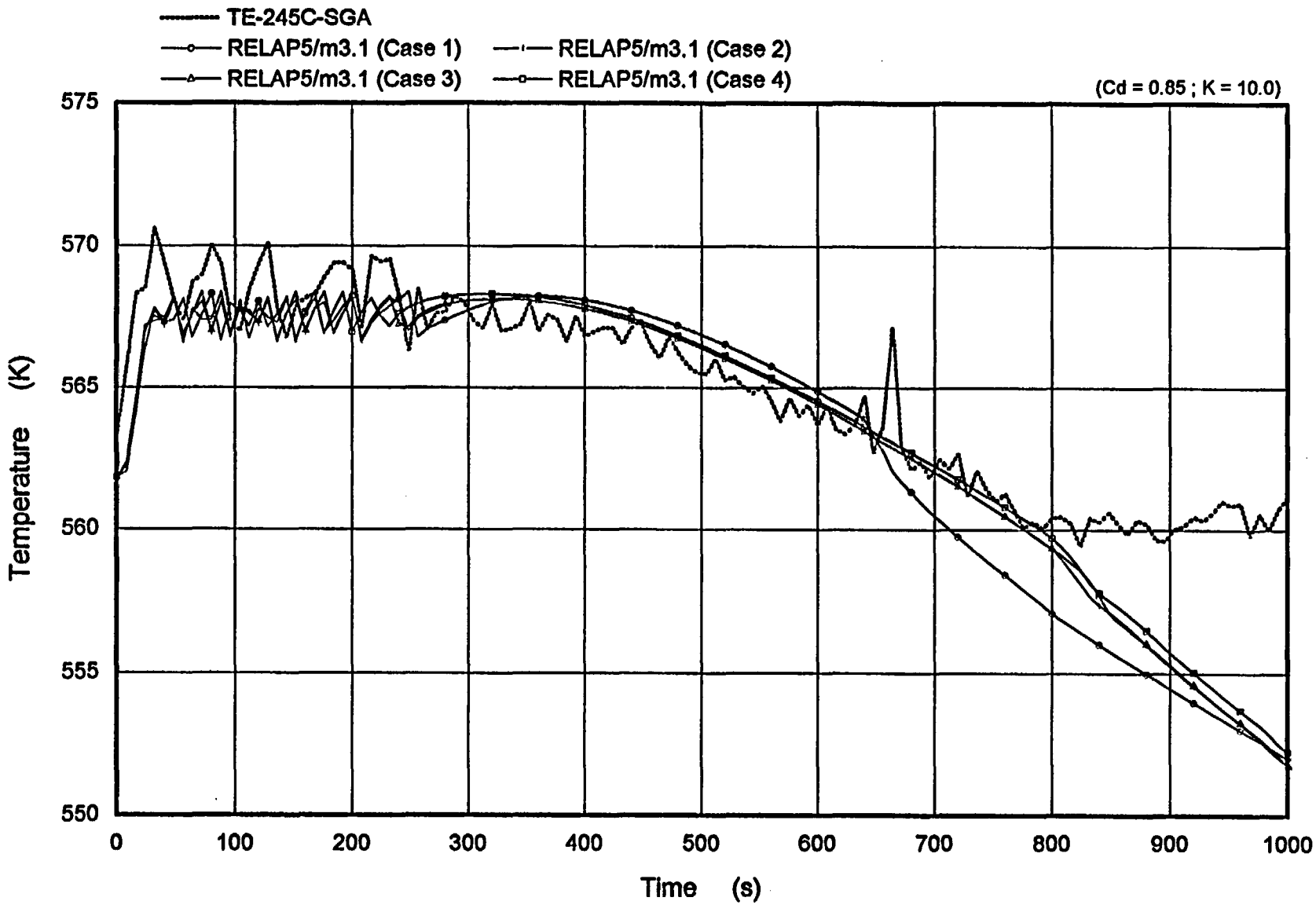

Figure 7.27 Comparison of Secondary Temperature of Intact Loop (S/G Nodes Sensitivity)

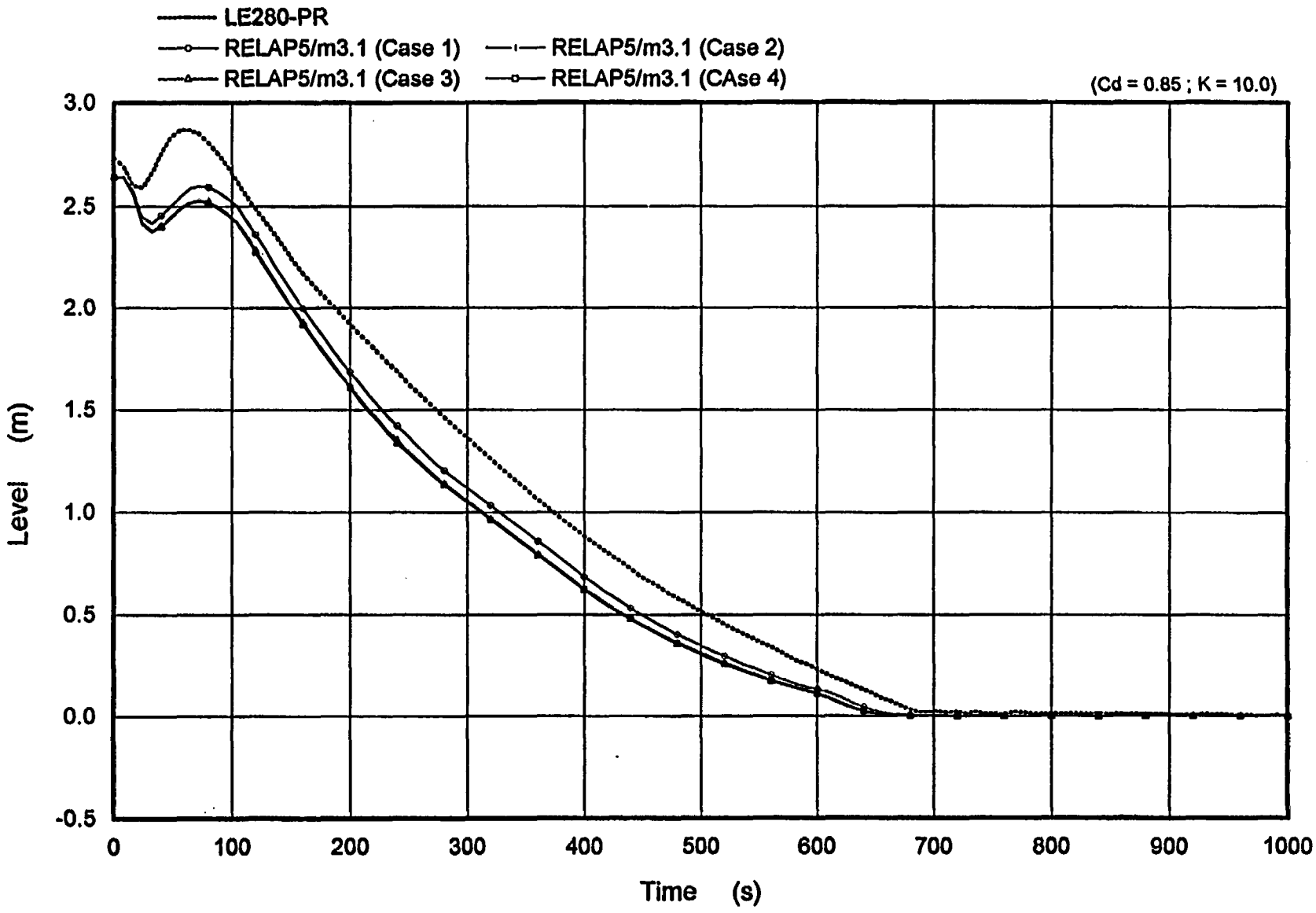

Figure 7.28 Collapsed Liquid Level of Pressurizer (S/G Nodes Sensitivity)

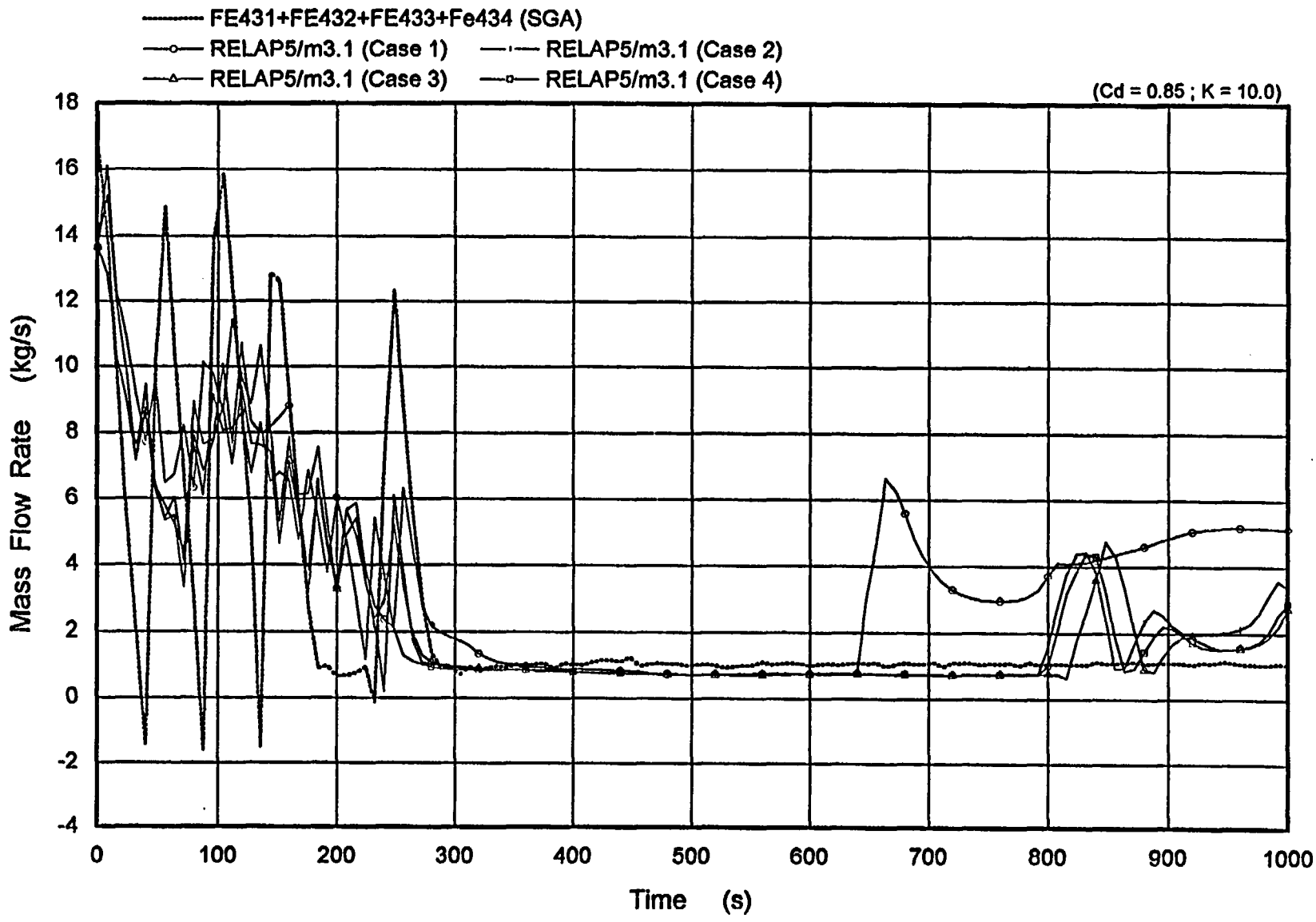

Figure 7.29 Downcomer Flow Rate of Intact Loop (S/G Nodes Sensitivity)

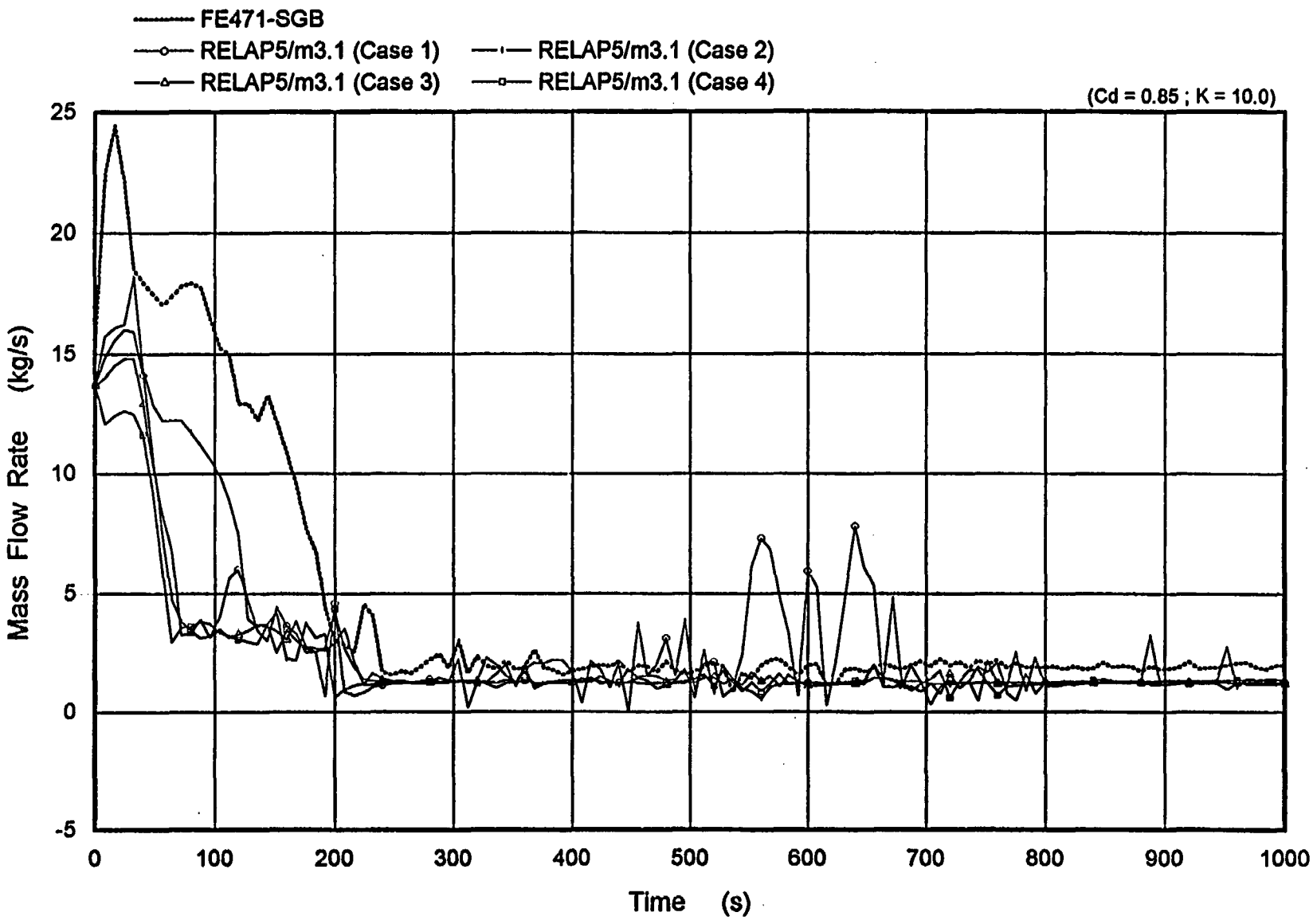

Figure 7.30 Downcomer Flow Rate of Broken Loop (S/G Nodes Sensitivity)

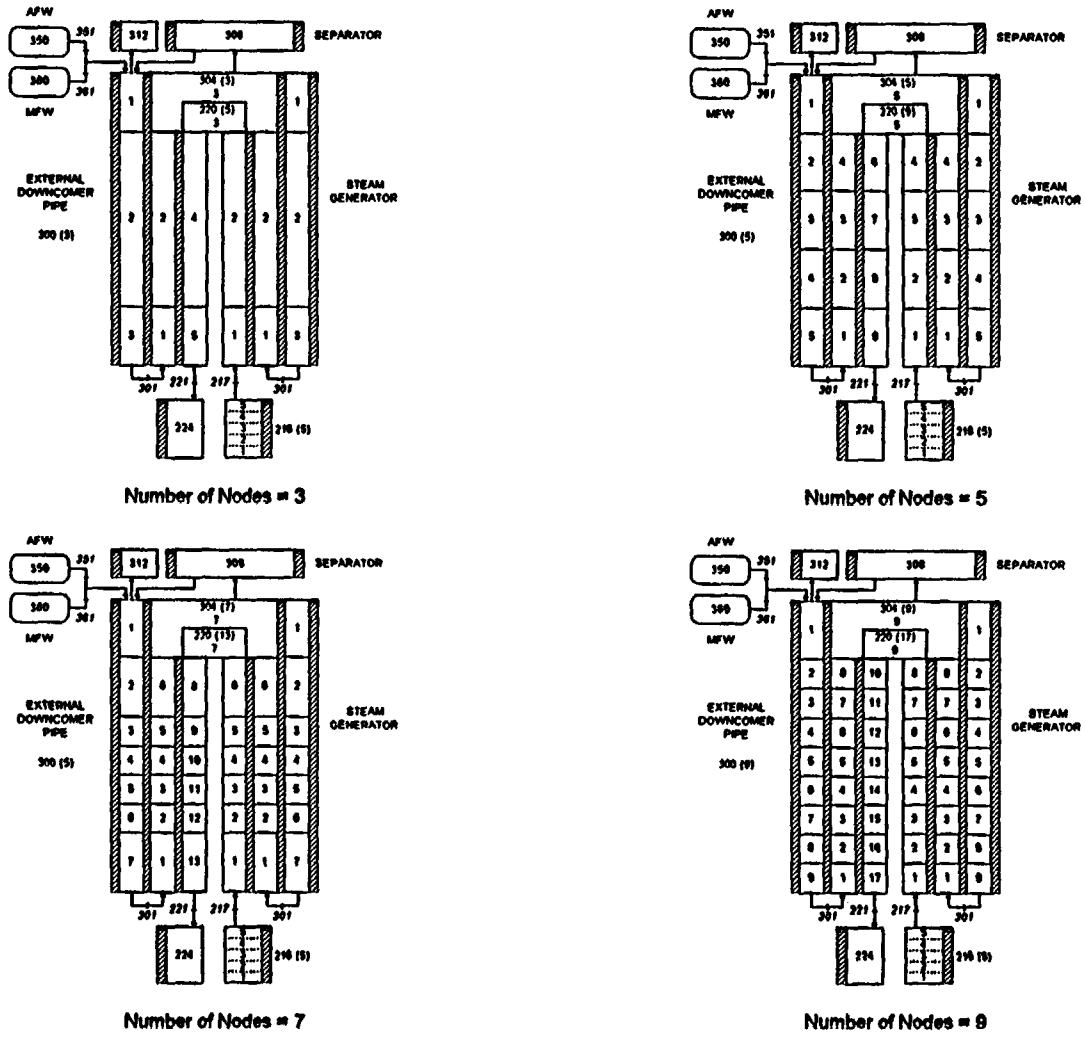

Figure 7.31 Steam Generator Nodalization Diagram for The Nodes Sensitivity Study

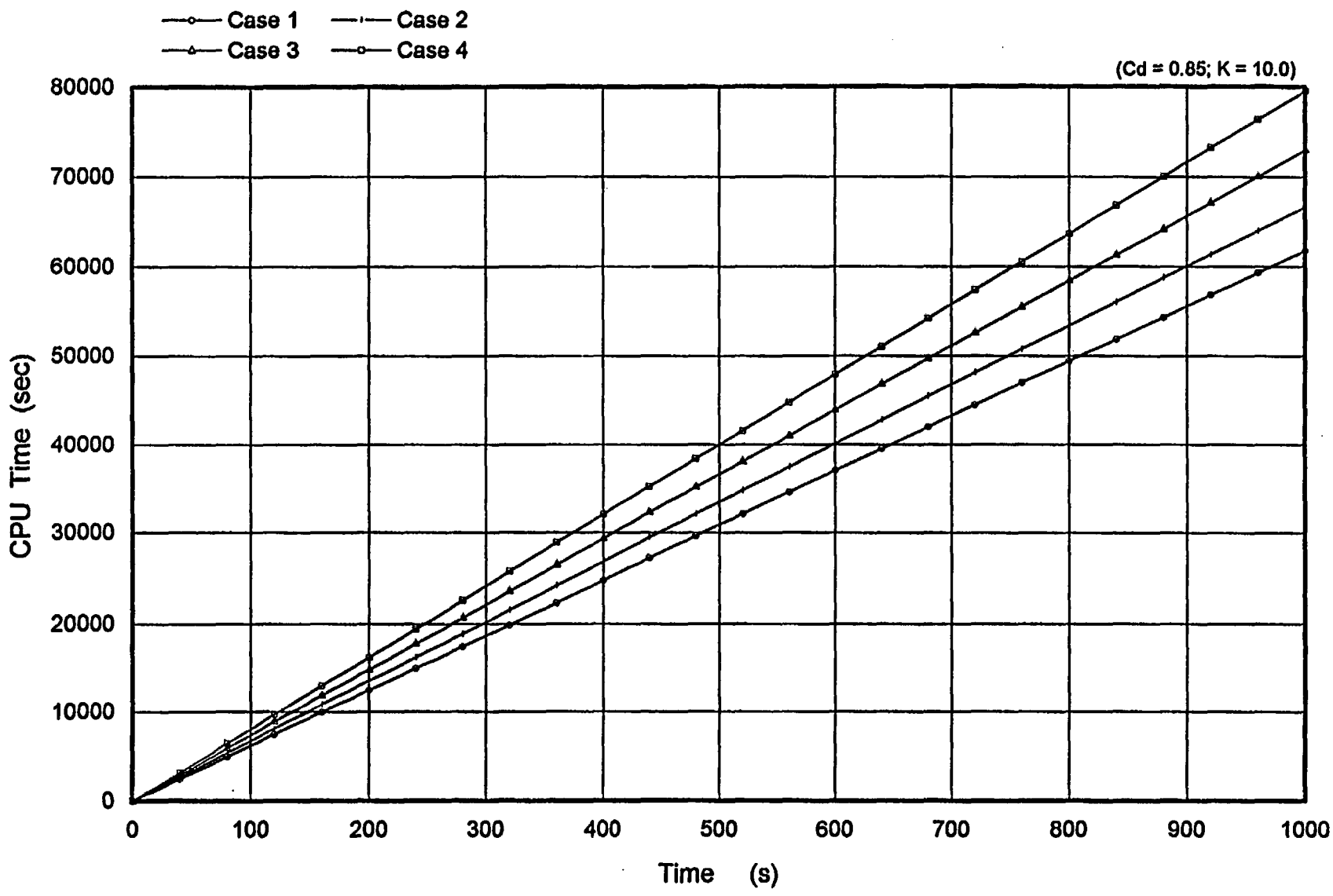

Figure 7.32 The Required CPU Time for Calculations (S/G Nodes Sensitivity)

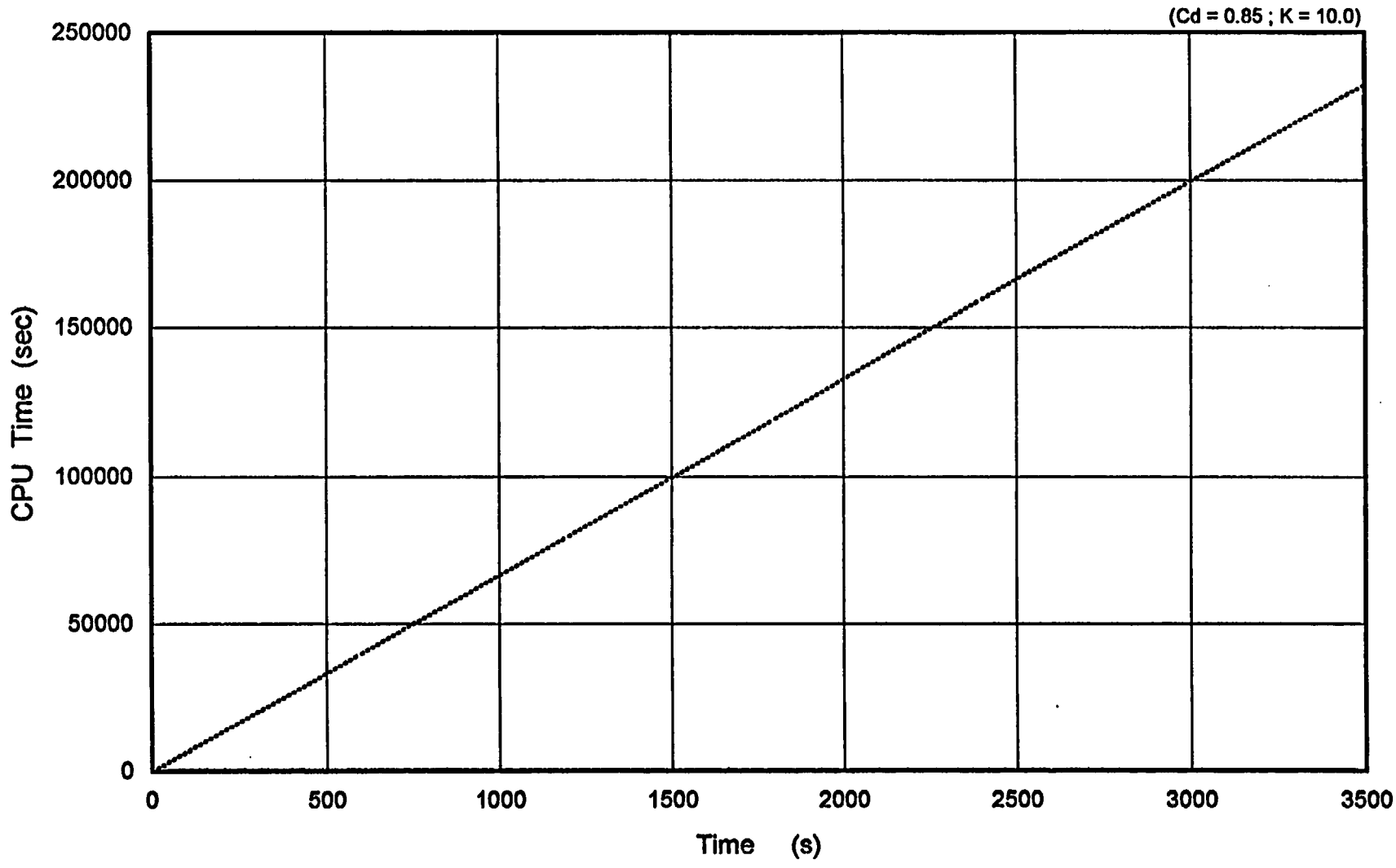

Figure 8.1 The Required CPU Time in the Base Calculation

NRC FORM 335 (2-89) NRCM 1102, 3201, 3202

U.S. NUCLEAR REGULATORY COMMISSION

BIBLIOGRAPHIC DATA SHEET

(See instructions on the reverse)

1. REPORT NUMBER (Assigned by NRC, Add Vol., Supp., Rev., and Addendum Numbers, if any.)

NUREG/IA-0148

2. TITLE AND SUBTITLE

Assessment of RELAP5/MOD3.1 Using LSTF Ten-Percent Main Steam-Line-Break Test Run SB-SL-01

3. DATE REPORT PUBLISHED

MONTH	YEAR
September	1998

4. FIN OR GRANT NUMBER

D6227

5. AUTHOR(S)

J. G. Oh, H. D. Lee, K. K. Jee, S. K. Kang/KOPEC
Y. S. Bang, K. W. Seul,/KINS
H. Kumamaru, Y. Anoda/JAERI

6. TYPE OF REPORT

7. PERIOD COVERED *(Inclusive Dates)*

8. PERFORMING ORGANIZATION - NAME AND ADDRESS *(If NRC, provide Division, Office or Region, U.S. Nuclear Regulatory Commission, and mailing address; if contractor, provide name and mailing address.)*

Korea Power Engineering Company
150 Duckjin-Dong, Yusong- Ku
Taejon, Korea 305-353

Korea Institute of Nuclear Safety
P.O. Box 114
Yusong, Taejon
Korea 305-600

Japan Atomic Energy Research Institute
Tokai-Mura, Naka-Gun
Ibaraki-Ken 319-1195, Japan

9. SPONSORING ORGANIZATION - NAME AND ADDRESS *(If NRC, type "Same as above"; if contractor, provide NRC Division, Office or Region, U.S. Nuclear Regulatory Commission, and mailing address.)*

Division of Systems Technology
Office of Nuclear Regulatory Research
U.S. Nuclear Regulatory Commission
Washington, DC 20555-0001

10. SUPPLEMENTARY NOTES

G. Rhee, NRC Project Manager

11. ABSTRACT *(200 words or less)*

Results produced by the RELAP5/MOD3.1 computer code were compared with the experimental data from JAERI's LSTF Test Run SB-SL-01 for a 10% main steam line break transient in a pressurized water reactor. The code simulation for the base case included a total of 189 fluid control volumes and 199 flow junctions to model the transient two-phase phenomena. Also, a total of 180 heat slabs were used to model the system heat transfer. The code predictions of the experimental results are generally satisfactory for the trends of key parameters.

Sensitivity studies performed for the break discharge coefficient, the separator drain line loss coefficient, and the number of steam generator nodes did not reveal any strong dependencies. Neverthless, optimal values of these parameters that led to the lowest overall statistical error were obtained, and these values were subsequently used in the "Base Case" analysis.

12. KEY WORDS/DESCRIPTORS *(List words or phrases that will assist researchers in locating the report.)*

RELAP5/MOD3.1
JAERI LSTF
main steam line break test
assessment
small-break LOCA (loss-of-coolant-accident)
pressurized water reactor

13. AVAILABILITY STATEMENT

unlimited

14. SECURITY CLASSIFICATION

(This Page)

unclassified

(This Report)

unclassified

15. NUMBER OF PAGES

16. PRICE

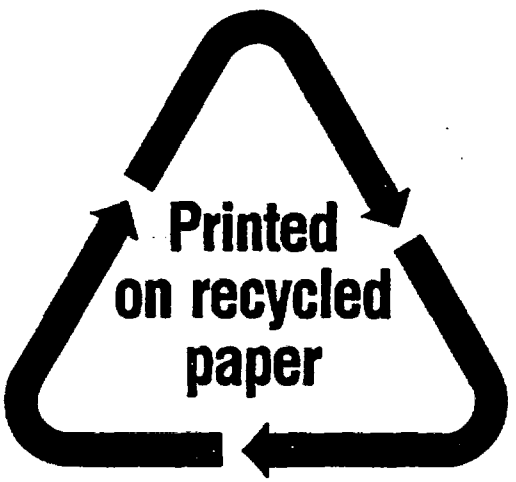

Federal Recycling Program

UNITED STATES
NUCLEAR REGULATORY COMMISSION
WASHINGTON, DC 20555-0001

OFFICIAL BUSINESS
PENALTY FOR PRIVATE USE, $300

SPECIAL STANDARD MAIL
POSTAGE AND FEES PAID
USNRC
PERMIT NO. G-67